Summer 2020

Stream Bank and Bar Erosion Contributions and Land Use Influence on Suspended Sediment Loads in Two Ozark Watersheds, Southeast Missouri

Kayla Ann Coonen
Missouri State University, Coonen09@live.missouristate.edu

STREAM BANK AND BAR EROSION CONTRIBUTIONS AND LAND USE INFLUENCE ON SUSPENDED SEDIMENT LOADS IN TWO OZARK WATERSHEDS, SOUTHEAST MISSOURI

A Master's Thesis

Presented to

The Graduate College of

Missouri State University

In Partial Fulfillment

Of the Requirements for the Degree

Master of Science, Geospatial Sciences in Geography

By

Kayla Ann Coonen

August 2020

STREAM BANK AND BAR EROSION CONTRIBUTIONS AND LAND USE INFLUENCE ON SUSPENDED SEDIMENT LOADS IN TWO OZARK WATERSHEDS, SOUTHEAST MISSOURI

Department of Geography, Geology and Planning

Missouri State University, August 2020

Master of Science

Kayla Coonen

ABSTRACT

In-channel sources and storages of fine-sediment such as in banks and bars can influence sediment loads and overall geomorphic activity in stream systems. However, in-channel processes and effects on sediment load are rarely quantified in geomorphic or water quality studies. This study uses a sediment budget approach to assess the influence of bank erosion and bar deposition on fine sediment loads in Mineral Fork (491 km^2) and Mill Creek (133 km^2) watersheds located in the Ozark Highlands in Washington County, Missouri. These watersheds were disturbed by historical lead and barite mining which included the construction of large tailings dams across headwater valleys. USEPA's Spreadsheet Tool for Estimating Pollutant Loads (STEPL) was used to quantify suspended sediment delivery from upland areas and assess land use-load relationships. Aerial photographs from 1995 and 2015 were used to identify spatial patterns of erosion and deposition in bank and bar forms. LiDAR was used to characterize the channel network and determine bank and bar heights. Field measurements were used to ground-truth bank and bar heights and fine-sediment composition of alluvial deposits. Historical tailings dams capture runoff from 27% of Mineral Fork and 28% of Mill Creek drainage areas, trapping 38% and 26% of the suspended sediment load annually, respectively. The total annual sediment yield for Mineral Fork watershed was 92 $Mg/km^2/yr$ with 55% released by bank erosion and <1% reduced by bar storage. The sediment yield for Mill Creek was 99 $Mg/km^2/yr$ with 33% released by bank erosion and 24% reduced by bar storage. These results indicate that in-channel processes are important contributors to sediment yields in these watersheds.

KEYWORDS: Bank Erosion, Mining, Sediment Budgets, STEPL, Nonpoint Source Pollution, Ozark Highlands, Missouri

STREAM BANK AND BAR EROSION CONTRIBUTIONS AND LAND USE INFLUENCE ON SUSPENDED SEDIMENT LOADS IN TWO OZARK WATERSHEDS, SOUTHEAST MISSOURI

By

Kayla Ann Coonen

A Master's Thesis
Submitted to the Graduate College
Of Missouri State University
In Partial Fulfillment of the Requirements
For the Degree of Master of Science, Geospatial Sciences in Geography

August 2020

Approved:

Robert T. Pavlowsky, Ph.D., Thesis Committee Chair

Toby J. Dogwiler, Ph.D., Committee Member

Marc R. Owen, MS, Committee Member

Julie Masterson, Ph.D., Dean of the Graduate College

ACKNOWLEDGEMENTS

I thank my advisor Dr. Robert Pavlowsky for his expertise, advising, and providing me with so many great opportunities during my time at Missouri State University. Throughout the course of this research and my graduate studies. Thank my committee member Marc Owen for his continued mentoring, knowledge, and support throughout the course of my graduate assistantship. I also thank my committee member Dr. Toby Dogwiler for his support, editorial assistance, and technological knowledge as I switched to complete my thesis online.

I thank all of the Ozarks Environmental and Water Resources Institute (OEWRI) staff (Tyler Pursley, Triston Rice, Josh Hess, Michael Ferguson, Max Hillermann, Jean Fehr, Hannah Eades, Sarah LeTarte, Hannah Adams, Katy Reminga, and Kelly Rose) for helping me make this research possible with field and laboratory work, and for all the support during my graduate studies. I also want to thank the OEWRI staff for the amazing memories at MSU, from the unproductive lunch hour to the 2:30 coffee breaks. And a special thanks to Sierra Casagrand for the help in the field, hours of helping me sieve samples, and most importantly the constant edits and emotional support you provided towards the end of my studies.

I am tremendously grateful to my parents (Julie Wild and Chris Coonen) and step-parents (Larry Wild and Teresa Coonen) who have given me endless support through all of my years of schooling. I appreciated the care packages, all the phones calls that ended in “I’m Proud of You,” and continued assistance for special trips home. Additionally, I thank my brother, Matthew Coonen, for helping me, even when I was hours away. I could not have gotten to this point in my academic career without all of you keeping my spirits high while I was away from home.

Lastly, I thank the OEWRI for my graduate assistantship, partial funding for this research through funding by USEPA Cooperative agreement number V97751001 Big River Riffle-Basin Monitoring Project for the Big River Superfund Site, and funding for my graduate assistantship through the USDA-NRCS Missouri Agricultural Watersheds Assessment Project award number R186424XXXXC030.

TABLE OF CONTENTS

LIST OF TABLES

LIST OF FIGURES

INTRODUCTION

Eroding stream banks can be significant sources of fine sediment to streams that increase water quality concerns, typically supplying 20% to 80% of the total suspended sediment load at the watershed outlet (Harden et al., 2009; De Rose and Basher, 2011; Kessler et al., 2013; Spiekermann et al., 2017). Bank erosion can occur gradually as the channel migrates back and forth across the valley floor over relatively long periods of time (Figure 1) (Trimble, 1983; Kondolf, 1997; De Rose and Basher, 2011). In many streams, it is a natural process for point bar and floodplain deposition to be on the opposite side of cut-bank erosion in order to maintain a constant channel width and shape (Kondolf, 1997). However, watershed-scale disturbances can increase flood discharge, bank failures, or sediment loads, which can accelerate bank erosion rates greater than 2 m/yr in smaller streams (Harden et al., 2009; Rhoades et al., 2009; De Rose and Basher, 2011; Martin and Pavlowsky, 2011; Kessler et al., 2013; Janes et al., 2017; Spiekermann et al., 2017).

Once eroded sediment is in transport, it is usually deposited relatively soon on channel beds, bars, and floodplains. Bank and floodplain sediment can remain in storage for a year to centuries before being remobilized again (Meade, 1982). Bank erosion can also exacerbate channel instability by causing channel instability through channel widening, flow turbulence along bends, and release of coarse sediment (Ferguson et al., 2003; Michalkova et al., 2011). The additional coarse sediment load can accelerate bar deposition and create flow deflection and more erosive currents in the channel (Jacobson and Primm, 1997; Blanckaert, 2011; Martin and Pavlowsky, 2011). Therefore, bank erosion processes can be both a cause and effect of the geomorphic and sediment characteristics of a stream channel.

The flood regime of a stream system will tend to control its shape and erosional potential (Rosgen, 1994). High rates of bank erosion are commonly caused by high-magnitude, low-frequency floods. However, flood effects on sand and gravel bars in rivers are not as well understood (Hagstrom et al., 2018). Nevertheless, assessments of bank erosion rates and their causal factors have been described in the literature (e.g., De Rose and Basher, 2011; Kessler et al., 2013; Janes et al., 2017; and Spiekermann et al., 2017). Many studies of bank and bar behavior have been completed for individual stream reaches. However, there have been fewer attempts to quantify the spatial distribution of bank erosion inputs from different locations within the channel network in relation to bank deposition and other in-channel sediment storages such as bench and bar deposits (Panfil and Jacobson, 2001; Martin and Pavlowsky, 2011; Owen et al., 2011).

Channel geomorphology influence on sediment loads

Sediment is recognized as the number one nonpoint source pollutant in the United States, with 70% of fine sediment in impaired streams coming from past and present human activities (Brown and Froemke, 2012; USEPA, 2018a). However, the important role of stream geomorphology as a natural control on suspended loads, such as adjustments in channel form and sediment storage, is commonly overlooked in nonpoint source (NPS) pollution models that assess water quality trends in watersheds (Nejadhashemi et al., 2011; Fox et al., 2016; Beck et al., 2018). Geomorphic processes involving the formation and adjustments of fluvial landforms by sediment erosion and deposition can significantly change stream sediment loads at timescales from years to decades (Jacobson and Gran, 1999; Knighton, 1998; Hession et al., 2003). Increased runoff and bed instability can cause channel enlargement and the release of sediment to the watershed, while impoundments and floodplain deposition can trap sediments (Ward and Elliot, 1995; Knighton, 1998; James, 2013). Additionally, floodplains can be a major sink for fine sediment with annual sedimentation rates typically ranging from 0.1 to 15 cm/yr (Table 1). In some watersheds, the sediment delivery rates to streams have decreased significantly since the period of highest land use disturbances that occurred almost a century ago due to improved land management practices, bank stability structures, and the regrowth of vegetation (Trimble, 1983,1999; Troeh et al., 2004). Conversely, bank erosion inputs and channel deposition can increase after a period of channel recovery or the implementation of stabilization practices in some cases (Trimble, 1999; Schenk and Hupp, 2009; Gillespie et al., 2018). Sediment budgets measure the amount of sediment eroded and stored in different sections of a watershed (i.e. uplands, headwaters, floodplains, and in-channel processes) (Trimble, 1999; Lauer et al., 2017). Sediment budgets are important assessment tools used to evaluate sediment fluxes and storage in a watershed by quantifying the amounts of sediment being stored in and eroded from different landform components (Phillips, 1991; Beach, 1994; Trimble, 2009).

An important contribution to a sediment budget can be the release of excess sediment previously deposited on floodplains. Historical land use practices associated with widespread agricultural settlement including the clearing of forests, soil disturbance by cultivation, and construction of road networks released large volumes of fine sediment from hillslopes for deposition on floodplains in the Midwest USA (Knox, 1972; Trimble, 1983). These "legacy" sediment deposits were stored in floodplains and other valley floor locations at depths up to several meters (Knox, 1972; Lecce, 1997; Wilkinson and McElroy B.J, 2007; Owen et al., 2011; James, 2013; Donovan et al., 2015; Pavlowsky et al., 2017). Flow obstructions, such as mill dams, increased the rate of legacy sediment deposition in some regions (Trimble and Lund, 1982; Walter and Merritts, 2008; Schenk and Hupp, 2009). In tributaries, the higher banks formed by legacy deposits produced deeper flows that were able to generate higher stream powers and increase bank erosion rates for more than 50 years (Knox, 1987; Lecce, 1997; Ward et al., 2016). In mining districts, where relatively large volumes of tailings were introduced to nearby rivers, legacy floodplain deposits were able to store metal-contaminated sediment from 100 to 1,000 years until remobilized by bank erosion (Marron, 1992; Rhoades et al., 2009; Lecce and Pavlowsky, 2014). Even after conservation practices were implemented to reduce soil erosion, legacy sediment stored in valleys was still being remobilized by bank erosion (Trimble, 1999; Troeh et al., 2004).

Typically, hydrologic watershed models are used to determine suspended sediment loads from predicted upland soil erosion yields with the relative contribution to stream loads that are decreasing with downstream distance (Brierley et al., 2006; Baartman et al., 2013; James, 2013). In general, suspended sediment loads tend to increase with rainfall amount, intensity, and land use characteristics that increase storm water routing, runoff rates and erosion (Lawler, 1993; Brown and Froemke, 2010, 2012; Emili and Greene, 2013; USEPA, 2018b). Trimble (1983) assessed sediment contributions to the Coon Creek watershed, Wisconsin from upland erosion, main valleys, and tributaries. The sheet and rill erosion of uplands in Coon Creek were estimated using the universal soil loss equation (USLE) in the form: A = RKLSCP, where A is equal to the amount of soil loss in tons per acre per year, R is the rainfall factor, K_f is the soil erodibility factor, L is the slope-length factor, S is the slope-gradient factor (S), C is the land use and land management factor, and P is the erosion control practice factor (Trimble and Lund, 1982; Troeh et al., 2004). Today, models like the Spreadsheet Tool for Estimating Pollutant Loads (STEPL) incorporate the USLE into calculations of sediment load outputs from watersheds with variable land uses and soil cover (Nejadhashemi et al., 2011; Park et al., 2014; WiDNR, 2014; Liu et al., 2017). However, stream bed and bank erosion inputs are rarely evaluated directly in watershed models and are only used to balance variations in modeled tributary inputs and assumed channel conditions (Trimble, 1999; Bracken et al., 2015). The literature reported that streambank erosion and other in-channel contributions such as bed material accounted for 7-92% of the annual suspended sediment load in a watershed (Table 2) (Fox et al., 2016).

Bank erosion assessments

Over the past several decades, the methods for measuring bank erosion rates have advanced from field work to GIS methods (Lawler, 1993). Field methods have long been employed to study bank erosion (Leopold, 1973). Cross-sectional surveys can be used to measure active channel widths and areas (Xia et al., 2014). Additionally, repeat cross-sectional surveys over time can be used to assess bank erosion rates between floods (Julian and Torres, 2006). Erosion pins are deployed to estimate bank erosion rates where rebar pins are inserted into the bank, leaving a known length exposed to provide a ‘benchmark’ against which bank erosion can be measured as they become more exposed (Couper et al., 2002; Harden et al., 2009; Foucher et al., 2017; Beck et al., 2018). Problems can arise with the use of erosion pins to evaluate short-term (months to years) bank erosion rates since negative values can result from the deposition of sediment during high flows, upper bank failures covering lower bank pins, and human interference (Couper et al., 2002). More frequent observations can reduce erosion pin error, but also add more cost and effort for the project (Couper et al., 2002; Xia et al., 2014).

Historical aerial photography is more commonly used now to track bank locations over time to determine streambank erosion rates (Rhoades et al., 2009; Martin and Pavlowsky, 2011).

Typically, bank line locations are digitized and compared between two dates of aerial photographs (Mount and Louis, 2005; De Rose and Basher, 2011; Spiekermann et al., 2017). However, digitizing needs to be completed at a relatively large and consistent scale of 1:1,000 or 1:600 to reduce worker and photograph errors during manual digitizing (Rhoades et al., 2009; Spiekermann et al., 2017). When planform surveys for different years are combined to identify areas of erosion and deposition in the channel, tiny polygon "slivers" may occur and these are likely insignificant for use as a survey result. Those areas can be identified by spatial error analysis and ignored for use in erosion inventories (De Rose and Basher, 2011). In general, while digitizing errors do occur, they are assumed to be random and cancel one another out (Mount and Louis, 2005; De Rose and Basher, 2011; Spiekermann et al., 2017). However, during georeferencing the root-mean-square error (RMSE) is calculated for distances between ground-points compared between two photographs to evaluate spatial errors for feature measurements (Mount and Louis, 2005; Janes et al., 2017). The typical range for RMSE errors in these studies was two to five meters for the georeferenced aerial photographs.

The use of aerial photographs limits assessment of the channel migration process to a two-dimensional result. By incorporating a high resolution light detection and ranging (LiDAR) derived digital elevation model (DEM), bank heights can be estimated and used to calculate a volume for the eroded banks (Rhoades et al., 2009; Kessler et al., 2013). The main problem associated with incorporating LiDAR to the aerial photography is having data sets from the same time periods. The collection data for the photographs and LiDAR are usually months or years apart, potentially altering the actual geomorphic characteristics of the period being measured to some degree (Kessler et al., 2012; Spiekermann et al., 2017). LiDAR also has errors depending on how the dataset was mosaiced from different flight series and the degree to which water surface reflections can give false heights on streambanks. Water reflection can be corrected in streams by using an assumed channel geometry or field data to correct the bank heights (Kessler et al., 2012; Podhoranyi and Fedorcak, 2014).

Channel sediment concerns in the Ozark Highlands

Historical farm and logging land clearing by European settlers caused increased soil erosion on uplands and in tributary valleys increasing fine and coarse sediment loads in streams of the Ozark Highlands of Missouri (Jacobson, 1995; Jacobson and Gran, 1999; Panfil and Jacobson, 2001; Owen et al., 2011; Reminga, 2019). These disturbances were magnified by prevailing topographic conditions including rolling hills with steep slopes, narrow valleys, and streams with gravel bed loads (Nigh and Schroeder, 2002). Over several meters of silty sediment were deposited on floodplains along some rivers that drained agricultural areas in the Ozark Highlands (Owen et al., 2011; Pavlowsky et al., 2017). However, these land use changes also increased the deposition rate and supply of coarser sand and gravel main channels and their tributaries (Jacobson and Primm, 1997; Jacobson and Gran, 1999; Martin and Pavlowsky, 2011). The coarse sediment deposits were located in the channel within persistent disturbance zones that were reactivated by large floods (Panfil and Jacobson, 2001; Lauer et al., 2017). Present-day gravel storages in the channel relate more to the influence of historical disturbances rather than recent land use impacts (Panfil and Jacobson, 2001). Nevertheless, both legacy sediment and recent gravel bars can increase channel instability in disturbance zones. These geomorphic conditions can increase bank erosion rates or the storage rate of fine sediment on bars or benches along the river channel (Martin and Pavlowsky, 2011; Lauer et al., 2017). Therefore, fine-grained sediment storage and remobilization rates should be included to calculate accurate sediment loads and sediment budgets in Ozark watersheds.

In the Ozark Highlands, there are no published studies that attempt to link the sediment being stored and transported through a stream network to stream loads. One related example would be the role that mining sediment storage plays in controlling sediment contamination trends in the Big River, southeast Missouri which was contaminated by large-scale lead mining from 1895 to 1972 (Pavlowsky et al., 2010, 2017). Another related example used the floodplain core records to understand how legacy sediment deposition rates related to historical land use changes along the James River, southwest Missouri (Owen et al., 2011). While there are several studies that provide some information about suspended sediment yields from Missouri watersheds, none describe how sediment is being routed through the channel system (Table 3). In addition, there is a gap in knowledge in our understanding of how channel processes, sediment storage, and land use factors control suspended sediment loads and associated pollutants. Further, watershed managers in southeast Missouri are concerned about channel instability, bank erosion, and sediment contamination by lead from mining operations since the 1700s in rural watersheds with a long history of soil disturbance (MDNR, 2006, 2008, 2014; Mugel, 2017)

Purpose and objectives

The purpose of this study is to assess and evaluate the contributions of bank and bar erosion to annual sediment loads of Mineral Fork (491 km^2) and Mill Creek (133 km^2) watersheds in the Ozark Highlands, Missouri. Since there are no published studies available for the Ozarks, this study will fill this gap and offer a methodology for assessing the watershed trends in channel erosion where management efforts are needed to reduce bank erosion inputs.

Bank erosion rates were determined using historical aerial photography and LiDAR data to evaluate to sediment loads derived from a simple NPS watershed model, the Spreadsheet Tool for Estimating Pollutant Loads (STEPL) (Tetra Tech, 2018; USEPA, 2019). These watersheds have been experiencing a decrease in water quality due to runoff and soil disturbances from historical land-clearing and lead and barite mining, and cattle grazing agriculture (Jacobson and Primm, 1997; Mugel, 2017; Schumacher and Smith, 2018; USEPA, 2018a). Environmental managers are concerned about excess sedimentation in Ozark streams from bank, sheet, and rill erosion (Adamski et al., 1995; MDNR, 2014, 2016, 2018).

The study watersheds are representative of landscape characteristics and stream network conditions of the Salem Plateau, the largest sub-region of the Ozark Highlands (Nigh and Schroeder, 2002; USDA-NRCS, 2006). They are affected by rural conditions including low income, failure of septic systems, and grazing agriculture on slopes and within riparian corridors (Jacobson and Primm, 1997; MDNR, 2014; USDA, 2017). Large barite tailings ponds and dams built between 1935-1991 to trap mine tailings and eroding soil are distributed throughout the middle and lower portions of these watersheds (Mugel, 2017; MSDIS, 2019). Over 27% of Mineral Fork and 28% of Mill Creek watersheds are composed of obstructed drainage areas by tailings dams up to 31 m high (MSDIS, 2019). Given that these dams trap 100% of the sediment and water from above drainage areas, they may affect sediment loads downstream. Moreover, mining disturbed lands can cause stream channel instability with excessive erosion and sedimentation (Mugel, 2017).

Like most of the Ozark Highlands, Mineral Fork and Mill Creek transport a bedload of sand and gravel that form bar complexes associated with local channel aggradation and high rates of bank erosion and channel widening (Martin and Pavlowsky, 2011). These geomorphic characteristics suggest that bank erosion and bar sedimentation may play an important role in fine sediment supply in these watersheds. The specific objectives of this study are:

1) Assess geomorphic characteristics of Ozark streams using LiDAR, aerial photography, and some ground-truthing involved bank measurements in the field;
2) Determine the spatial distribution and mass of fine sediment of channel erosion and deposition within watersheds; and
3) Develop a sediment budget for each watershed that accounts for the contributions of channel processes including bank and bar erosion and sedimentation to sediment loads.

Benefits of this study

Sediment transport and storage can have long-term implications for geomorphic activity and water quality in streams. This study will contribute to a better understanding of sediment sources and loads in southeastern Missouri watersheds and aid in evaluating the effects of historical mining disturbances on channel stability, bank erosion, and sediment loads in Barite Mining District. Channel processes are often excluded from sediment loads in NPS assessments. The methodology and results presented in this study will advance our understanding for using sediment budget analysis to improve NPS assessments in small- to medium-sized watersheds in the Ozarks. Moreover, it will use fluvial geomorphology concepts to link land use changes to channel behavior and sediment sources throughout the drainage network. This will provide a better understanding of the long-term recovery of stream channels from past land disturbances and anthropogenic sediment inputs.

Table 1. Floodplain deposition rates in the Ozark Highlands and Midwest Driftless Area.

Stream	Drainage Area (km^2)	Overbank Deposition Rates (cm/yr)	Reference
SW Ozark Highlands			
Honey Creek, MO	174	0.6-0.8	Carlson, 1999
James River, MO	637	0.5	Owen et al., 2011
SE Ozark Highlands			
Big River, MO	2,500	0.7-1.0	Pavlowsky, 2013
Big River, MO	2,500	0.2-3.4	Keppel et al., 2015
Big River, MO	2,500	0.1-1.0	Pavlowsky and Owen, 2015
Big River, MO	626-2,500	1.3-3.0	Pavlowsky et al., 2017
Big River, MO	2,500	0.8	Jordan, 2019
Big Barren Creek, MO	191	0.2-0.6	Reminga, 2019
Midwest Driftless Area			
Kickapoo Valley, WI	1,989	1.52	Happ, 1944
Coon Creek, WI	350	1.5-15.0	Trimble and Lund, 1982
Galena River, WI, IL	340-400	0.8-1.9	Magilligan, 1985
Shullsburg Branch, WI, IL	26	0.3-1.3	Knox, 1987
Galena River, WI, IL	700-170,000	0.5-3.4	Knox, 2006

Table 2. Bank erosion contributions to suspended sediment loads from watersheds in the U.S.

Watershed	Drainage Area (km^2)	Suspended sediment load from streambanks (%)	Reference
Delaware Estuary, PA	35,066	39	Meade, 1982
Sacramento River, CA	7,100	59	USACE, 1983
Obion Forked Deer River, TN	2,000	81	Simon and Hupp, 1986
East Nishnabotna River, IA	2,300	30-40	Odgaard, 1987
Des Moines River, IA	41,000	30-40	Odgaard, 1987
Blue Earth River, MN	1,550	31-44	Sekely et al., 2002
James River, MS	74	78	Simon et al., 2002
Yalobusha River, MS	4,000	90	Simon and Thomas, 2002
Shades Creek, AL	190	71-82	Simon et al., 2004
Blue Earth River, MN	1,550	23-56	Thoma et al., 2005
Le Sueur River, MN	2,880	11-14	Gran et al., 2009
Lower Hinkson Creek, MO	231	67	Huang, 2012
Walnut Creek, IA	52	23-53	Palmer et al., 2014
Piedmont Streams, Baltimore County, MD	155	70	Donovan et al., 2015

Table 3. Suspended sediment yields from selected watersheds in the U.S.

Stream	Drainage Area (km^2)	Sediment Yield ($Mg/km^2/yr$)	Floodplain Storage (%)	Reference
Waterfall Creek, TN	2	13	N/A	Hart and Schurger, 2005
Terry Creek, TN	3	8	N/A	Hart and Schurger, 2005
Upper Pigeon Roost Creek, TN	9	111	N/A	Hart and Schurger, 2005
Wilson's Creek, MO	46	30	N/A	Hutchison, 2010
Pearson Creek, MO	54	18	N/A	Hutchison, 2010
Upper James River, MO	637	39	N/A	Hutchison, 2010
Finley Creek, MO	676	9	N/A	Hutchison, 2010
Middle James River, MO	1,197	87	N/A	Hutchison, 2010
Le Suer River, MN	2,880	47	N/A	Day et al., 2013
Lower Mississippi River, LA	276,460	218	N/A	Turner and Rabalais, 2004
Missouri River	1,300,000	48	N/A	Turner and Rabalais, 2004
Indian Creek, MN	17	118	65	Beach, 1994
Hay Creek, MN	127	258	87	Beach, 1994
Beaver Creek, MN	144	365	64	Beach, 1994
Coon Creek, WI	360	103	37	Trimble, 1999
Upper Tar, Piedmont, NC	1,119	48	92	Phillips, 1991
Upper Neuse, Piedmont, NC	1,997	64	84	Phillips, 1991
Deep River, Piedmont, NC	3,748	60	91	Phillips, 1991
Haw River, Piedmont, NC	4,217	46	93	Phillips, 1991
Minnesota River, MN	45,000	17	25-50	Lauer et al., 2017

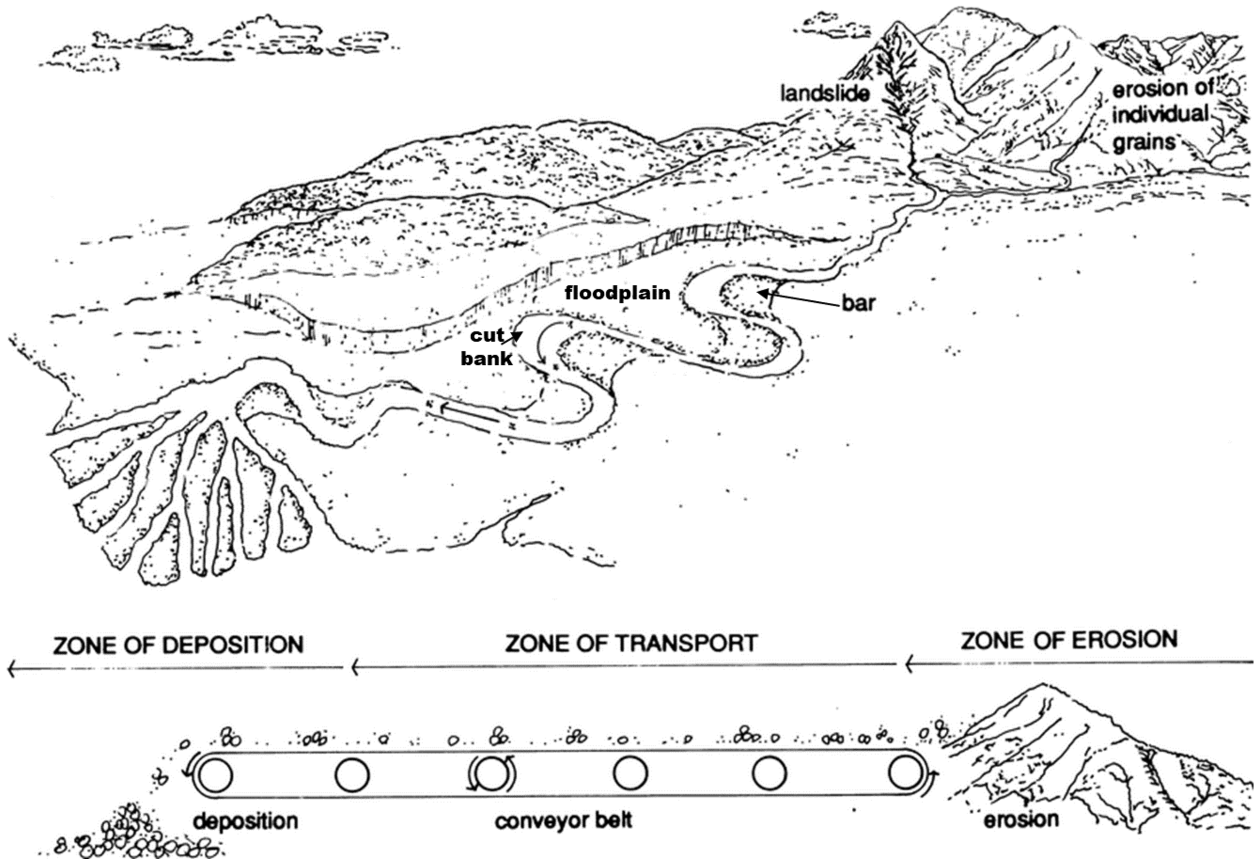

Figure 1. Model of sediment storage and remobilization within the channel (Kondolf, 1997).

STUDY AREA

Location

The Mineral Fork Watershed (HUC-10# 0714010402) and Mill Creek Watershed (HUC-12# 071401040301) are located in Washington County, Missouri within the Big River basin (HUC-8# 07140104) (Figure 2) (USGS, 2018a). In addition to the Mill Creek watershed, Mineral Fork contains six 12-Digit Hydrologic Unit Code (HUC) watersheds within its boundaries (Table 4). All together these two watersheds contain seven 12-Digit HUC subwatersheds in the study area as follows: Mineral Fork (MF), Clear Creek-Mineral Fork (CCMF), Old Mines Creek (OMC), Mine a Breton Creek (MBC), Fourche a Renault (FR), Sunnen Lake-Fourche a Renault (SLFR), and Mill Creek (MC). The whole Mineral Fork watershed has a drainage area of 491 km^2, total channel length of 433 km, and drainage density of 0.88 km/km^2. The Mill Creek watershed has a drainage area of 133 km^2, total channel length of 198 km, and drainage density of 1.49 km/km^2. These watersheds drain in the Meramec River Hills Subsection of the of the Salem Plateau Division of the Ozark Highland Province (Nigh and Schroeder, 2002). Maximum elevation of headwaters is about 430 masl with base-level elevations near 150 masl at the confluence of Big River. The local relief in the study area is typically greater than 45 m and rises to more than 76 m along the major valleys of Mineral Fork (Nigh and Schroeder, 2002). Streams within this region have incised through horizontally-bedded sedimentary strata, mainly composed of dolomite and limestone with some shale and sandstone (Panfil and Jacobson, 2001; Schumacher and Smith, 2018). In general, main channels and major tributaries of both watersheds flow in deep and narrow valleys, with relatively high gradients, and in bedrock-influenced riffle-pool streams with gravelly beds (Jacobson, 1995; Jacobson and Primm, 1997; Skaer and Cook, 2005).

Geology and soils

Both watersheds drain in the Salem Plateau of the Ozark Highlands, which contain Cambrian and Ordovician sedimentary rocks composed primarily of dolomites, chert, and sandstones (Figure 3) (Adamski et al., 1995; USDA-NRCS, 2006). The Cambrian Eminence and Potosi dolomites make up 74% of the surficial bedrock in Mineral Fork and Mill Creek watersheds (Table 5). This formation was mineralized by hydrothermal fluid interaction along orogenic belts during the Cambrian period and has been mined for shallow deposits of galena, smithsonite (zinc carbonate ore), and barite (barium sulfate ore) since at least the early 1800s in the Southeast Missouri Barite District in Washington County (Gregg and Shelton, 1989; Mugel, 2017).

Upland soils in Washington County, Missouri are generally formed in parent materials consisting of a thin layer of silty Pleistocene loess over cherty clay residuum formed from the weathering of the dolomites and limestones in the region (Skaer and Cook, 2005). The residuum in the Ozarks is about 3 to 12 m thick, although locally it can be greater than 60 m (Seeger, 2006). Most of the uplands soils occur on gently-sloping to moderately-steep slopes with a fragipan and gently-sloping to very-steep slopes containing chert fragments (Nigh and Schroeder, 2002). In total, these watersheds contain 50.1 km^2 of floodplain and alluvial terrace soils with the Cedargap series occupying 70% of the floodplain soil area (Table 6). The Haymond and Kaintuck series occur on larger floodplains, where the Cedargap and Bloomsdale soils are commonly found on the valley floor of the narrow upstream reaches (Skaer and Cook, 2005). Upper stream bank deposits were formed by overbank deposition and are composed of silt loam to fine sandy loam with >90% <2 mm sediment particles (Skaer and Cook, 2005). Lower bank units were typically formed by bar and bench deposition (now stratigraphically buried by overbank floodplain deposits) that are composed of coarser materials with loam to sandy loam textures with <80% <2 mm including gravel- and cobble-sized fragments (Skaer and Cook, 2005).

Climate and hydrology

Southeastern Missouri has a moist continental climate region (Peel et al., 2007; Skaer and Cook, 2005). From 1990-2019, the mean monthly rainfall in Southeast Missouri ranged from 6.5- 13.7 cm with an average of 9.7 cm per month. The highest monthly rainfall totals (>10 cm) occur in May, with typically less monthly precipitation (<9 cm) during the winter in December, January, and February (MRCC, 2018). Snowfall occurs from November to March with totals depths from 1.8 to 8.1 cm per month, with an average of 5.1 cm/month during the winter. Between 1990 and 2019, the average annual temperature ranged from 12-15°C with an average of 13°C. Over that period, average monthly temperatures range from -0.6°C in January to 25°C in July (MRCC, 2018). Over the last 30 years, overall precipitation and temperature trends show consistent, slightly increasing temperatures and overall rainfall since 1990 (MRCC, 2018).

Streamflow typically peaks in spring and rapidly declines through the summer. There are no USGS gages located in the two watersheds. The mean annual discharge is 5.7 m^3/s for Mineral Fork and 1.6 m^3/s for Mill Creek based on regional drainage area-discharge regression equations developed from available USGS gaging data (Appendix A). The estimated maximum annual discharge is 488 m^3/s for Mineral Fork and 137 m^3/s for Mill Creek. The uplands contain karst features, and most low order stream channels are ephemeral or perennial “losing” streams (USDA-NRCS, 2006). There are no natural lakes or ponds in the study area, however many ponds have been constructed to trap mine tailings, support recreation, or supply water for livestock purposes (Nigh and Schroeder, 2002).

Settlement and land use history

Historical land use. Oak-woodlands was the primary vegetation cover type in the pre-settlement period in the study area with denser deciduous and pine forests occupying steep valley slopes and bottoms (Nigh and Schroeder, 2002). These forests were logged and cleared to varying extent across the Ozarks to support the settlement and economic growth of the region. The second-growth forest was denser and with different composition compared to pre-settlement conditions and was first harvested in the 1950s (Jacobson and Primm, 1997; Nigh and Schroeder, 2002).

The first phase of European settlement in the study area was by French miners in the early to middle 1700s who worked shallow lead pits for galena around the towns of Potosi and Old Lead Mines located in the Mineral Fork watershed (Mugel, 2017). The French mining operations were abandoned after several years leaving only relatively small farming villages. The second phase of European settlers began clearing the flatter uplands and valley floors for pasture or row-crop agriculture around the 1840s (Jacobson and Primm, 1997). However, when the Civil War ended and railroads extended lines into the region, farming activity increased after 1865 including more farm acreage, clearing and cultivation of hillslopes, and stripping the land for mining purposes (Nigh and Schroeder, 2002). The resulting vegetation and soil disturbances increased runoff and soil erosion rates significantly in many Ozark watersheds causing soil loss and fertility problems, headwater stream incision, and accelerated delivery of gravel sediment to main channels (Jacobson, 1995; Jacobson and Gran, 1999).

Many farmers would work or lease out shallow pit mines on their land during the winter for galena and barite (locally known as “tiff”) in the 1800s. Then, more modern mining operations moved into the district beginning in the early 1930s (Mugel, 2017). Surface soils contained barite as residual deposits which were separated from the clayey host material by processing in grinding and washer plants near Mineral Point (on Mill Creek) and northeast of Potosi (along tributaries of Mineral Fork) (Mugel, 2017). The mining wastes were diverted into tailings ponds within Mineral Fork and Mill Creek watersheds (Smith and Schumacher, 1993). There are over 60 abandoned tailings ponds in the Barite District today storing a total of 39 million tons of tailings wastes (Mugel, 2017). Large tailings ponds and dams built between 1935-1991 to trap mine tailings and eroding soil are distributed throughout the middle and lower portions of these watersheds (Figure 4) (Mugel, 2017; MSDIS, 2019). There are 5.2 km^2 of ponds and a combination of 40 active wet and dry dams between the two watersheds. These tailings dams range from 4 m to 31 m high with drainage areas ranging from 0.1 to 68.8 km^2 (MSDIS, 2019). One of the largest ponds with a dam in the study area is Sunnen Lake in Mineral Fork watershed which was developed for recreation and traps about one-half of the inflowing sediment load (USGS, 2018a). Over 27% of the combined drainage area of the study watersheds is located behind large tailings dams that are assumed to retain most of the runoff and trap all the sediment flowing to them. Historically, there were probably more operating dams, but many have filled in with sediment or were breached in recent time (MSDIS, 2019). Overall, about 12% (80 km^2) of the land area for these two watersheds was disturbed by surface barite mining including pits, ponds and tailings dams (Schumacher and Smith, 2018). Approximately 1.8

million tons of barite were produced in the district until the last mine closed in 1998 (Schumacher and Smith, 2018).

Legacy over-bank deposits most likely occur along the floodplains of Mineral Fork and Mill Creek below areas disturbed by cultivation, mining, and roadways. Field observations made during this study indicate that buried A-horizons can be found up to one meter deep in the cut-bank profiles suggesting that eroded soil was deposited on older floodplains since settlement (Pavlowsky et al., 2017; Jordan, 2019). Tailings dams can create flow obstructions which can trap sediment and increase the rate of legacy sediment deposition along streams (Trimble and Lund, 1982; Walter and Merritts, 2008; Schenk and Hupp, 2009). For streams in smaller watersheds, the higher banks formed by legacy deposits may produce deeper flows that can generate higher stream powers and increase bank erosion rates (i.e. Knox, 1987; Lecce, 1997; Ward et al., 2016).

Land use and land cover. Forestland is the major land use within these watersheds based on the 2010-2017 National Agricultural Statistics Service (NASS) Crop Database (Table 7). Deciduous forest covered 79.3% of the watershed in 2017 (Figure 5). Today, wider valley bottoms are usually cleared for agriculture (Nigh and Schroeder, 2002). Agricultural land occupies 9.3% of the land area in the study, with pastureland covering 9% and 0.3% as cropland. Cattle and poultry are the main types of livestock produced in Washington County (USDA, 2017). Cropland which includes row crops, double crops, small grains, and fallow ground only covers about 0.1% of the area and alfalfa and other hay crops about 0.2% of the watershed (USDA-NASS, 2018). The remainder of the watershed area is developed land (5.4%) or in wetlands and open water (0.6%). Most of the urban area is formed in Potosi, Missouri (population of 2,626 in 2017) which drain into both Mineral Fork and Mill Creek watersheds and

Mineral Point, Missouri (population of 354 in 2017) located east of Potosi, which drain into Mill Creek (Figure 5) (US Census Bureau, 2017).

Table 4. 12-Digit HUC watersheds within Mineral Fork and Mill Creek.

Watersheds	Abbreviations	Watershed Type	Ad* (km^2)	Ad Below Dams (km^2)	% Ad behind Dams	Land use (%) Urban	Agriculture	Forest	Mined
Mill Creek	MC	12-Digit HUC	132.6	96.2	28	7	6	72	15
Mineral Fork	MF	12-Digit HUC	51.5	42.3	18	3	3	90	4
Clear Creek-Mineral Fork	CCMF	12-Digit HUC	98.8	75.6	24	3	4	92	2
Old Mines Creek	OMC	12-Digit HUC	48.1	39.4	17	7	6	75	11
Mine a Breton Creek	MBC	12-Digit HUC	123.6	105.4	15	8	15	73	4
Fourche a Renault	FR	12-Digit HUC	100.7	96.8	4	4	17	80	0
Sunnen Lake-Fourche a Renault	SLFR	12-Digit HUC	68.8	68.8	100	4	7	88	0
Mineral Fork (Whole)	MF-Whole	10-Digit HUC	490.5	428.6	27	5	10	82	3

*A_d = drainage area

Table 5. Descriptions of bedrock geology in Mineral Fork and Mill Creek watersheds.

Unit Name	Symbol	Geologic Age	Primary Rock Type	Secondary Rock Type	% Area
Eminence and Potosi dolomite	Cep	Cambrian	Dolomite	Chert	74
Gasconade dolomite	Og	Ordovician	Dolomite	Sandstone	21
Roubidoux sandstone and dolomite	Or	Ordovician	Sandstone	Chert, Dolomite	4
Elvins Bonne Terre Dolomite	Ceb	Cambrian	Dolomite	Conglomerate	1

Table 6. Alluvial soils within Mineral Fork and Mill Creek watersheds.

Soil Series	Texture	Landform	Flood Frequency	Soil Order	Area (km^2)	% of Area
Cedargap	gravelly silt loam	Floodplain	Frequently Flooded	Mollisols	34.83	69.7
Racket	loam	Floodplain	Frequently Flooded	Mollisols	4.28	8.6
Razort	silt loam	Floodplain	Occasionally Flooded	Alfisols	3.82	7.6
Bloomsdale	silt loam	Floodplain	Frequently Flooded	Alfisols	2.88	5.8
Haymond	silt loam	Floodplain	Frequently Flooded	Inceptisols	1.77	3.5
Higdon	silt loam	Stream terrace	Occasionally Flooded	Alfisols	0.64	1.3
Sturkie	silt loam	Floodplain	Occasionally Flooded	Mollisols	0.61	1.2
Kaintuck-Relfe complex	sandy loam	Floodplain	Frequently Flooded	Entisols	0.62	1.2
Horsecreek	silt loam	Stream terrace	Occasionally Flooded	Alfisols	0.26	0.5
Racoon-Freeburg complex	silt loam	Stream terrace	Occasionally Flooded	Alfisols	0.21	0.4
Deible	silt loam	Stream terrace	Rarely Flooded	Alfisols	0.09	0.2

Table 7. Change in land cover from 2010 to 2017 without mined land.

% of Land Cover	2010	2017	% Change
Forest	84.1	84.7	0.0
Pastureland	10.3	9.0	-12.3
Urban	5.0	5.4	4.3
Cropland	0.0	0.3	29.7
Water/Wetlands	0.7	0.6	-9.3

*(USDA-NASS, 2018)

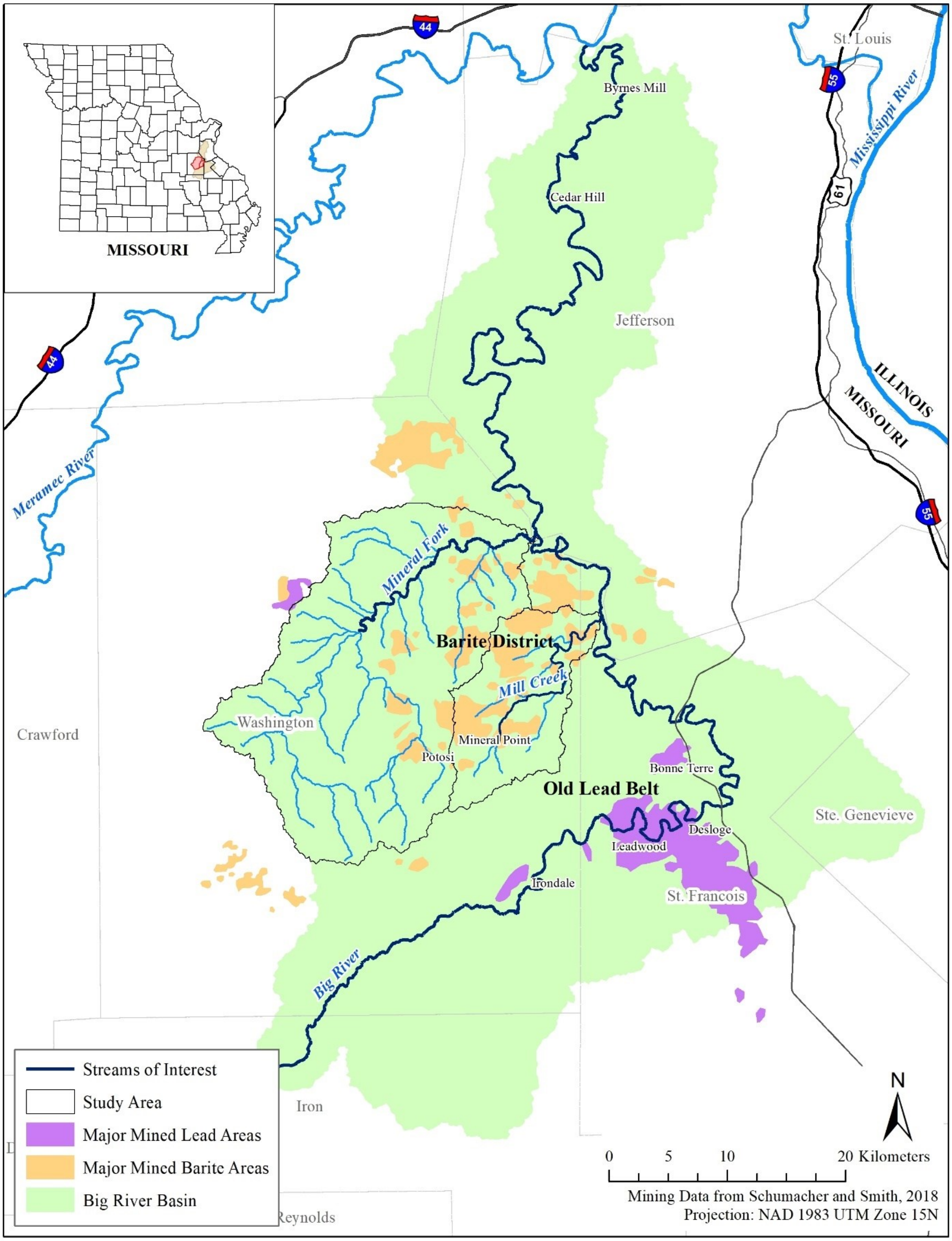

Figure 2. Mineral Fork and Mill Creek watersheds within the Big River in relation to the Old Lead Belt and the Barite Mining District.

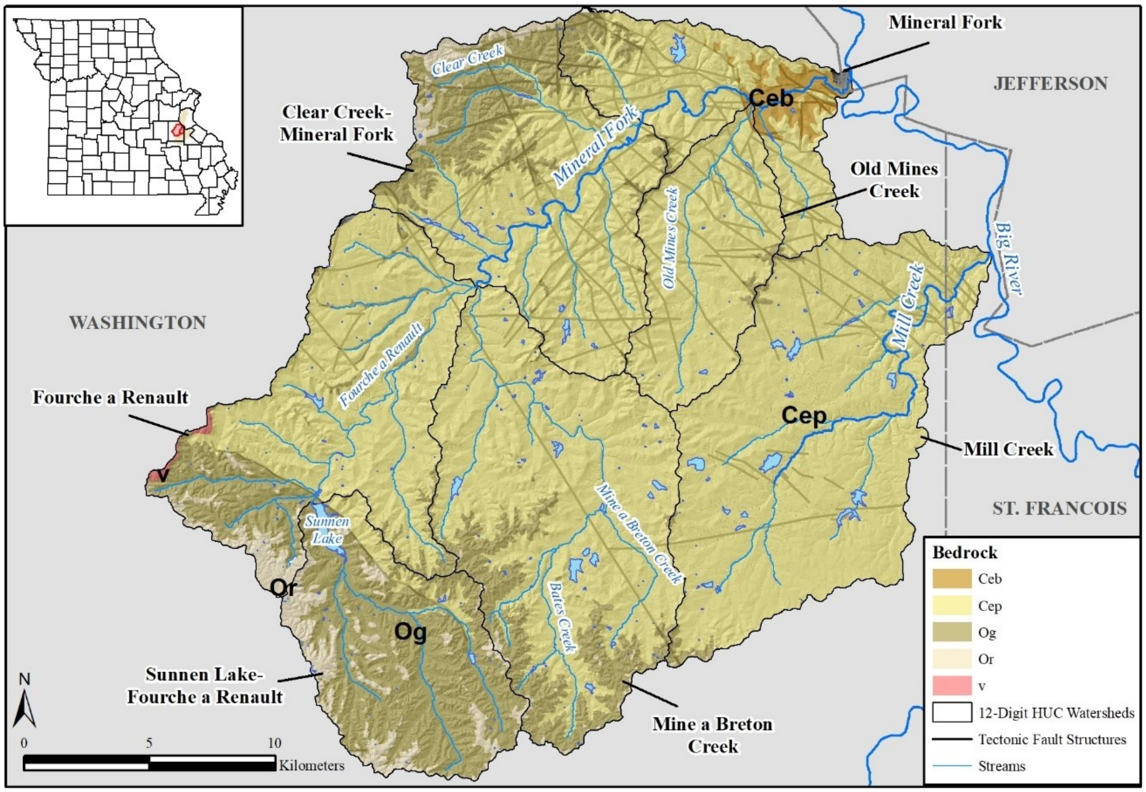

Figure 3. Geology of Mineral Fork and Mill Creek.

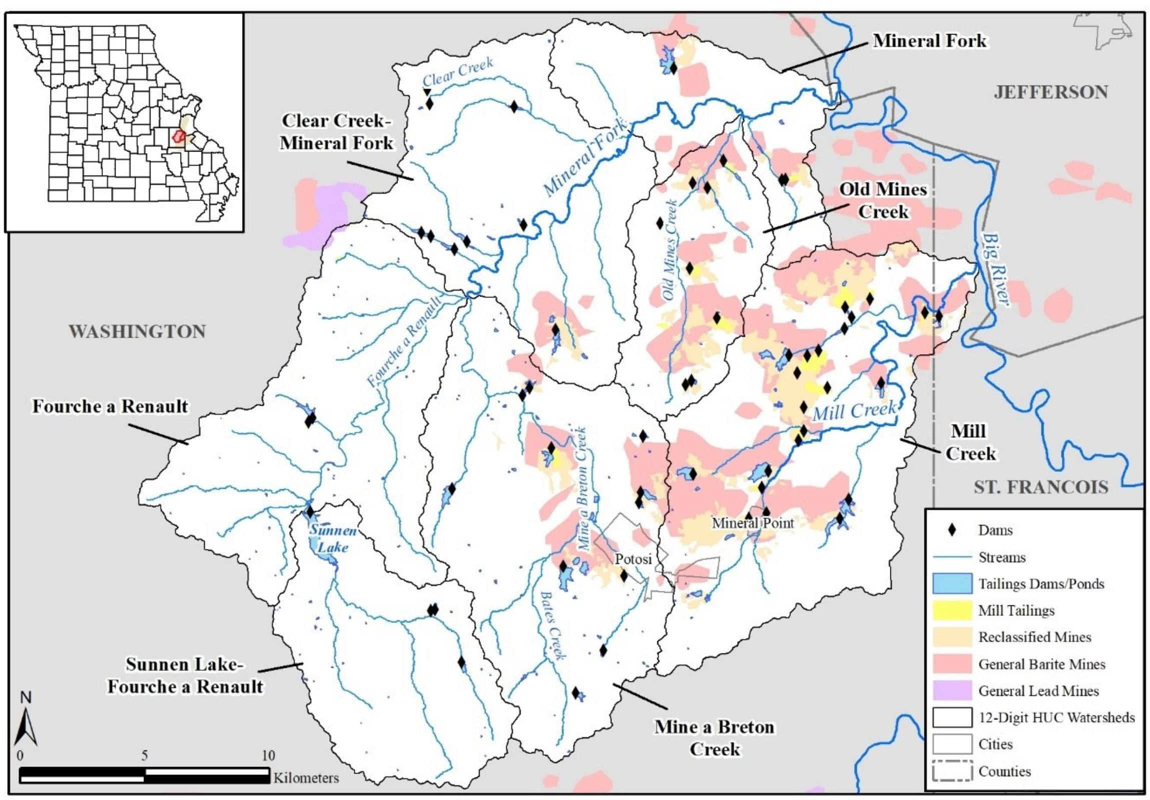

Figure 4. Major mined areas in Mineral Fork and Mill Creek watersheds.

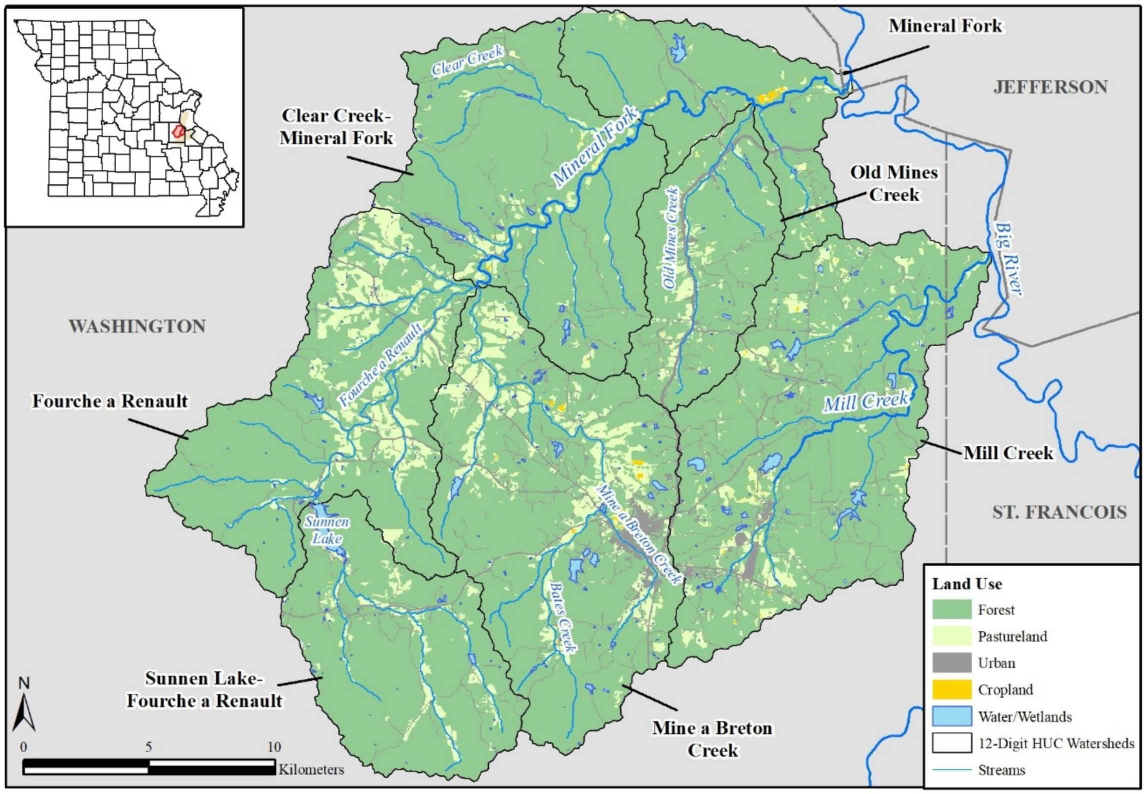

Figure 5. Land Use classification from USDA-NASS 2017 for Mineral Fork and Mill Creek watersheds.

METHODS

This study assessed the volumetric changes of bank and bar landforms between 1995 and 2015 and then converted the volumes into masses of eroded and deposited fine sediment. The masses of in-channel fine sediment erosion and storage were then compared with sediment supplied by upland erosion and stream loads derived from STEPL modeling to develop a sediment budget for the Mineral Fork and Mill Creek watersheds. The sediment budget was used to assess the importance of bank and bar sediment processes and fine sediment load contributions compared to total sediment transport for the watershed. The methods of the study are described below including channel bank and bar assessment, spatial data sets and analysis, geomorphic spatial analysis, STEPL sediment load modeling, and sediment budget framework.

Channel bank and bar assessment

Ozark streambanks are typically formed in floodplain deposits composed of two sedimentary units, a finer-grained silty unit overlying a coarser-grained loamy unit containing gravel (Panfil and Jacobson, 2001; Skaer and Cook, 2005; Owen et al., 2011). The upper unit was formed by overbank flood deposition of suspended sediment composed of silt and clay with lesser amounts of sand. The lower unit was formed by the deposition of bed-load along the channel bed with finer sediments filling pore spaces (Panfil and Jacobson, 2001; Owen et al., 2011). Profile descriptions of floodplain parent materials with varying texture in the study area include Cedargap (gravelly), Kaintuck (sandy), and Haymond (silty) soil series (Skaer and Cook, 2005). In contrast, bar deposits are coarser than adjacent bank deposits and are generally composed of sand and gravel (2-64 mm) with some cobble-sized clasts (64-256 mm) and finer materials (<63 um) (Panfil and Jacobson, 2001; Pavlowsky et al., 2017). Bar forms are deposited on the channel bed in zones of flow separation (e.g., point and delta bars) or where sediment transport capacity is low relatively to sediment supply (e.g., center and side bars) (Rosgen, 1994). The profile characteristics of the Relfe soils generally describe the sedimentology of bar features in the study area (Skaer and Cook, 2005).

As defined here, fine sediment is the material fraction of a bank or bar deposit less than two millimeter in diameter including sand, silt, and clay particles. This fraction includes sediment transported both in suspension (suspended load) and saltation or traction (bed-load). Suspended sediment particles are assumed to be composed mostly of silt and clay particles (<63 µm) with some finer sand particles (<250 µm) (Rosgen, 1994). For example, sand percentages (63-2,000 µm) in suspended sediment loads averaged from 6 to 39% in five southeastern Minnesota rivers (Groten et al., 2016) and from 2 to 25% in Big River which receives flow from both Mineral Fork and Mill Creek (Barr, 2016). In comparison, the sand content in floodplain deposits in the study area varies from less than 20% in upper units to 10 to 40% in lower/coarser units (Skaer and Cook, 2005). Thus, the fine sediment fraction evaluated for this study is assumed to be similar in texture to that expected in the suspended load of these streams. The percent fines were calculated by subtracting the % of coarse sediment (>2 mm) from 100%.

Channel and sediment assessment procedures. Field surveys of bank and bar location, height, and stratigraphy were completed at 20 sites to provide data needed to verify bank height measurements using LiDAR and estimate bank unit thickness based on local influences of stream order and bank height (Appendix B). Sampling sites were distributed throughout the study watersheds along tributaries and main channel at accessible locations not affected by road crossings or local disturbances (Figure 6). GPS location and several photographs were collected at each site. A stadia rod or folding ruler was used to measure bank height from the bank top (i.e., near bank-full stage) to the bank toe. The bank toe was typically below the waterline at the break in slope and texture, which was where the base of the floodplain bank meets the flatter channel bed. Water depths were measured at the bank toe and channel thalweg (deepest point). The cut-bank was scraped clean to identify stratigraphy including unit boundaries, sand or gravel lenses, and buried soils.

Fourteen sediment samples were collected from upper bank (7) and lower bank (7) sedimentary units at seven sites in Mineral Fork watershed to quantify the percentage of fine sediment in the deposits (Figure 6; Appendix C). Composite samples from 0.2 to 0.5 m thick were collected from cut-bank exposures by vertical scraping at a uniform depth. All sediment samples were bagged and labeled in the field and returned to the laboratory at Missouri State University for size analysis. The field samples were dried at 60°C in an oven, disaggregated with a mortar and pestle, and passed through a 2 mm sieve. The fine sediment fraction reported as the <2 mm mass divided by the total sample mass. The total field sample sometimes included coarser clasts up to 64 mm in diameter.

Bank deposit and unit characteristics. Estimates of the thickness and fine sediment content of upper and lower bank units were needed to apportion fine sediment fractions for budget calculations. Analysis of stratigraphic measurements indicated that coarse unit thickness averages about 55% of total bank height (as measured from the thalweg) across the range of different bank heights evaluated for this study (Figure 7).

Field data and published information were used to develop relationships to predict the fine sediment content of bank deposits. No trend in texture of the upper bank unit was indicated for either bank height or stream order. Therefore, a constant value of a 90% fine sediment fraction by volume (and 10% >2 mm) was assumed for all upper banks mapped as the Cedargap soil series which included 70% of the floodplain soils in the study area (Skaer and Cook, 2005; Figure 8; Appendix C). Floodplain banks associated with other soil series tend to have finer upper units and were assumed to contain 100% fine sediment (Skaer and Cook, 2005). Sediment samples from five of the seven sites plot along the 10% >2 mm line (90% fine sediment). Further, this value also approximates the average composition of the upper A and B horizons of the Cedargap soil series which represents the majority of sampled floodplains and previously mapped soils along these streams (Skaer and Cook, 2005; Appendix B).

In contrast to the upper unit, the lower bank unit tends to become finer with increasing bank height (Figure 8). Again, no trend was found with stream order, however, the sample size was small. In the study area, banks with lower heights tend to be formed in geomorphic settings associated with coarser sediment: (i) gravelly bench deposits where fine sediment is beginning to bury coarse bar deposits to form young floodplains as shown by the Relfe soil series; and (ii) gravelly floodplain deposits located along smaller and steeper channels where coarse sediment transport and deposition is more frequent as shown by the Cedargap and Bloomsdale soils series (Skaer and Cook, 2005). In contrast, higher banks tend occur in geomorphic settings associated with finer-grained deposits: (i) floodplains along larger streams with lower slopes and wider valley floors that deposit more silt and sand as shown by the Kaintuck and Haymond soil series; and (ii) higher terraces along smaller streams as shown by the Higdon soil series (Skaer and Cook, 2005). A linear regression equation was not appropriate for predicting textural characteristics of lower bank units since deposits with similar textures were clustered according to geomorphic features with discrete characteristics, not those grading into one another. Thus, a step-function was used to classify lower unit texture according natural breaks with bank height as follows: 40% fine sediment for <1.1 m height; 60% fine sediment for 1.1 m to 1.4 m height; and 70% fine sediment for >1.4 m height (Figure 8).

Bar Deposit Characteristics. No bar sediment samples were evaluated for this study. Published values indicate that total pore or void space in gravel deposits generally averages about 40%, thus comparing well with samples from the lower bank units composed of older buried bar deposits (i.e., <40% fines by volume for low banks, Figure 8). However, fine sediment does not typically fill in all the open spaces in recent or well-sorted gravel deposits. Therefore, fine sediment content is typically less than the total open space might allow in bar deposits ranging from 20 to 25% for silt and clay and up to 35% for sand (StormTech, 2012; Dunning, 2017). Moreover, textural analyses of subsurface samples from the profile of the Relfe soil series which occurs on larger bench and bar surfaces along Mineral Fork contains 20 to 30% fine sediment (Skaer and Cook, 2005). Based on the evaluation above, it was assumed that all bar deposits contained 25% fine sediment by volume for this study.

Bulk Density. Assumed bulk density values were used to convert volumetric measurements into mass units for the sediment budget. For bank deposits, a bulk density of 1.4 Mg/m^3 was used for fine sediment and 2.2 Mg/m^3 for coarse material >2 mm (Bunte and Abt, 2001; Skaer and Cook, 2005). For bar deposits, a bulk density of 1.9 Mg/m^3 was used for fine sediment and 2.2 Mg/m^3 for coarse sediment (Manger, 1963; Bunte and Abt, 2001; Pavlowsky et al., 2017).

Spatial Datasets

Aerial photograph analysis. Historical aerial photographs from 1995 and 2015 were used to assess channel width, bank location, and bar area to evaluate changes over a 20-year period (Table 8). Pre-georeferenced USGS Digital Orthophoto Quarter Quads (DOQQ) were retrieved from the Missouri Spatial Data Information Service for 1995 and 2015 (MSDIS, 2017). The 1995 aerial photos have a spatial resolution of 1 m and were flown between March 1, 1995 and April 6, 1995. The 2015 aerial photos have a 0.15 m spatial resolution and were flown between March 15, 2015 and April 17, 2015.

To account for rectification differences between the two sets of aerial photos, a mean point-to-point error was calculated (Hughes et al., 2006). The point-to-point error is the measured distance between known points on the two sets of photographs (Table 8). For this study, 30 hard points were chosen in the study area, typically at building corners, and the 2015 color leaf-off was used as the reference photo (Table 8). Other studies have used between six and 30 points depending on the size of the watershed (Mount and Louis, 2005; Hughes et al., 2006; Martin and Pavlowsky, 2011). UTM coordinates were assigned to each of the 1995 and 2015 points in ESRI's ArcMap 10.7 and the distance between each set of points was calculated using the distance formula. The distance between each set of points ranged from 0.98 m to 7.69 m with a mean point-to-point distance of 2.76 m (n=30). This mean point-to-point error was later incorporated into the next step of assessing erosion and deposition polygons to eliminate the area inside the detection limit of error.

<u>Erosion and deposition polygons</u>. Both the wetted channel bank lines and bar features were digitized from the 1995 and 2015 aerial photograph sets at a 1:1,000 scale in ArcGIS (Figure 9a, b) (De Rose and Basher, 2011; Spiekermann et al., 2017). The aerial photographs were used to digitize the active channel with the protocol to identify the stream banks until they were not visible. Bar features were distinguished using the wetted channel boundaries as a guide

and an active channel layer was created by combining the two sets of features. These features were converted to polygons and classified as either wetted channel or a bar in the attribute table.

Areas of bank erosion and deposition were identified by overlay analysis of the 1995 and 2015 active channel polygon layers. Bank erosion areas were identified by areas of the 2015 active channel beyond the 1995 active channel polygon using the erase tool in ArcGIS. Deposition areas were identified as areas of the 1995 active channel outside of the 2015 active channel polygon using the same tool. The same procedure was used to identify areas of erosion and deposition of bar areas. Finally, the areas of all erosion and deposition polygons were calculated in ArcGIS. In all, there were a four different polygon features produced from this analysis: 1) bank erosion; 2) bank deposition; 3) bar erosion; and 4) bar deposition.

Error analysis. To account for the error associated with georeferencing, the mean point-to-point error was incorporated into the erosion and deposition polygon analysis. A buffer using half of the mean point-to-point error distance (1.38 m) was placed around the erosion and deposition polygons (Figure 9c, d) (Mount and Louis, 2005; Hughes et al., 2006; Owen et al., 2011). Areas from the bank erosion and deposition that overlapped the error buffer were removed from the original polygons, creating erosion and deposition areas that were beyond the error buffer accounting for rectification differences between the photo years (Figure 9c, d) (Rhoades et al., 2009; Martin and Pavlowsky, 2011).

LiDAR analysis. A LiDAR derived DEM with one-meter horizontal and 0.185 m vertical resolution was used to assign bank and bar heights to polygons and create a stream network. The LiDAR derived DEM was obtained from MSDIS for Washington County and parts of St. Francois County was flown June 30, 2011 (Table 8) (MSDIS, 2017). The LiDAR DEM was used to delineate a stream network using the Strahler Stream Order method within each watershed using the hydrology toolbox in ArcGIS (Strahler, 1957). The DEM was used to create a flow accumulation and flow direction raster to establish a stream network with the stream link tool. A threshold of 100,000 pixels (0.1 km^2) was used for stream order classification. There was a total of six stream orders created from using the Strahler method (Figure 10). The first and second stream orders were not easy to identify because of low visibility in these heavily forested watersheds. Therefore, only 3% of the first order and 24% of the second order streams were digitized and later were not considered as part of the erosion and deposition analysis. However, 77% of third order streams were fully digitized. Third order streams remained in the cell analysis, but the 23% unassessed stream length was addressed separately to determine the mass.

The LiDAR DEM was also used to assign landform heights to each polygon classified as erosion or deposition for both the bars and banks (Notebaert et al., 2009; Rhoades et al., 2009; De Rose and Basher, 2011; Kessler et al., 2012; Spiekermann et al., 2017). Because the aerial photographs dates were different than the LiDAR flight date, banks and bars heights were sampled using the LiDAR where both erosion and deposition occurred. Heights were only sampled on erosion and deposition polygons below dams and on the third, fourth, fifth, and sixth order streams. Polygons in third and fourth order streams were sampled every two kilometers, and fifth and sixth order streams were sampled every 1 km because the stream length is smaller. Of the 152 sites sampled, 10 (7%) had depositional bank heights larger than erosional bank height. It was assumed that the cut-bank side of the channel should occur in the older part of the floodplain which is higher due to a longer period of deposition. Therefore, the depositional bank heights for these sites were corrected to equal those of the erosional bank heights. Of the 157 sites sampled, 21 (13%) had depositional bar heights larger than erosional bar heights.

To account for the elevation inaccuracies from water reflection in the LiDAR, the assigned bank and bar heights were corrected to include water depths using field-based channel topographic surveys. Bank height and water depth measurements were collected during rapid field assessments that were completed throughout the watershed (Appendix B). The relationship between bank heights recorded in the field and LiDAR banks heights shows an R^2 value of 0.904, with the trend plotting just below the 1:1 as expected (Figure 11). This equation was used to correct LiDAR height to actual field measured heights. In general, water depth added 0.07 to 0.14 m to LiDAR DEM derived bank heights. Average bank and bar heights were calculated for each stream order in each 12-Digit HUC watershed.

Geomorphic spatial analysis at the reach-scale

Grid cell analysis. A longitudinal series of grid cells were overlain on digitized channel centerlines to create a uniform reach scale for landform change analysis. Reach-scale studies of stream geomorphology typically assess stream channel lengths that are 20-100 widths long (Rosgen, 1994). For this study, active channel widths typically ranged from 10 m to 45 m. Therefore, a cell length of 500 m was chosen for this study that is in the range of other studies of Ozarks streams (Jacobson and Gran, 1999; Panfil and Jacobson, 2001; Pavlowsky et al., 2017). These cells were created by placing a 100-meter buffer around the centerline derived from the digitized stream network below dams that were then cut every 500 meters to create a total of 430 cells each 500 m long for the two study watersheds (Figure 12).

Cell analysis. The bank and bar erosion and deposition polygons were analyzed by the cell unit as part of the reach-scale analysis in the third, fourth, fifth, and sixth order streams. In ArcGIS, the “Intersect” tool is used to assign bank erosion, bank deposition, bar erosion, and bar deposition polygons to each 500 m channel cell and the area of each was recalculated. If a polygon was overlapping two cells, it would be divided into two polygons, one in each cell. Finally, the average bank and bar heights for each of the cells were attributed by values from each 12-Digit HUC watershed to each stream order. The bank and bar heights were multiplied by the area to calculate the overall volume of sediment for each of the four different features. These sediment volumes will ultimately be used in the sediment budget. (Table 9; Figure 13; Appendix D-E). Results of cell locations and analyses are stored on the Ozarks Environmental and Water Resources Institute (OEWRI) server. Lastly, unmeasured lengths, mainly in the third order streams, were added to the masses from the cell analysis to the determine the volume of the missing stream length in subwatershed. The volume of erosion/deposition for bank/bars in the unassessed stream length was determined by taking the average volume of third order cells in per 12-Digit HUC subwatershed. The average cell volume (mass/0.5 km) was multiplied by the length of unassessed stream order length below the dams to get the complete in-channel sediment budget. The calculation and analysis of these values will be presented later in the results chapter.

Sediment budget development

The sediment budget approach applied in this study generally followed Trimble (1983) and Trimble and Lund (1982). Sediment budgets measure the amount of sediment eroded and stored in different landform units of a watershed (i.e. uplands, headwaters, floodplains, and in-channel processes) over a period of time (Phillips, 1991; Beach, 1994; Trimble, 1999). To create detailed sediment budgets, both sediment storage zones and active erosion zones need to be added together to determine the output of sediment within a watershed (Davis, 2009). For example, storage can occur in uplands at the base of slopes, on floodplains, in gravel bars, or in impoundments (i.e. reservoirs, dams, lakes, ponds) (Trimble and Lund, 1982; Renwick et al., 2005; Joyce et al., 2018). Additionally, sediment can be lost through sheet and rill erosion in the uplands, re-mobilization of stored in-channel sediment (bars), or bank erosion (Trimble, 1999; Davis, 2009; Lauer et al., 2017). Each of these factors will be incorporated into a sediment budget using in-channel masses from this study, predicted sheet and rill erosion from uplands and sediment loads from streams by STEPL modeling, and floodplain deposition rates based on previous studies (Table 10).

STEPL Modeling. By using algorithms, Spreadsheet Tool for Estimating Pollutant Loads (STEPL) calculates the nonpoint source loads, including fine sediment, nutrients, and runoff, from the uplands of a watershed for predefined land use categories (urban, cropland, pastureland, forest, and user-defined) (Tetra Tech, 2018). STEPL is a downloadable Microsoft Excel spreadsheet that includes default parameters and options for users to customize and modify inputs (WiDNR, 2014). The inputs for STEPL include: (1) land use area, (2) precipitation, (3) agricultural animal numbers, (4) Universal Soil Loss Equation (USLE) output based on variable K_f- and LS-factors, and (5) hydrologic soil group (Appendix F-G) (Tetra Tech, 2018). Much of this data was obtained from the Soil Survey Geographic Database (SSURGO) and land-use data from USDA-NASS (USDA-NRCS, 2017; USDA-NASS, 2018).

The User-Defined land use category was manipulated to represent areas within the watershed that were mined. The 2017 land use data often classified the areas influenced by lead or barite surface mining as forested (Figure 14). Forested lands typically have lower runoff and sediment loads than agricultural land. Also, the mined lands within the watershed were more representative of old construction sites that typically do not have as much vegetative cover and bare ground is subject to increased runoff and soil erosion. Mined lands include features such as surface mining pits and tailings piles, ponds/dams, and areas of soil disturbance that are becoming forest covered. The area of mined land was mapped using the 2015 aerial photos and 2011 LiDAR dataset and used to reclassify the land use in Mineral Fork and Mill Creek (Figure 4, 14). The area of the watershed classified as mined lands was included in the User-Defined category in STEPL.

The suspended sediment load in STEPL is computed based on the USLE and the sediment delivery ratio (Park et al., 2014; 2015). STEPL is not a spatial model and it calculates sediment loading for the watershed using default or generalized variables. Therefore, for this study, STEPL was manipulated into being more spatially weighted by using specific soil series data to derive area weighted K-, LS-, and C-Factors for each of the different land uses (Appendix G) (USDA-NRCS, 2017). Finally, the total suspended sediment load is calculated by multiplying soil erosion by the sediment delivery ratio, which is a rough estimate of sediment deposition and storage within the watershed (Tetra Tech, 2018). The sediment delivery ratio (SDR) is calculated based on the watershed area where a lower percentage of eroded soil is exported out of the watershed as the drainage area increases (NRCS, 1983; James, 2013). Therefore, the sediment load from STEPL represents the total mass of sediment leaving the watershed from sheet and rill erosion annually after the SDR is applied to the upland erosion mass.

Tailings dam influences. Mineral Fork and Mill Creek watersheds contain 40 large tailings dams and recreational lake dams along tributary and headwater streams according to the records in the Missouri 2019 Dams shapefile (MSDIS, 2019) (Appendix H). The largest dams that were capable of trapping 100% of the fine sediment loads were identified from published locations and dam heights (MSDIS, 2019) and observations of disconnected drainage systems from LiDAR (collected 2011) and aerial photography (collected 2015). A secondary "below dam" drainage divide was delineated through the location points of most downstream large dams along the tributary network to delineate the effective sediment-contributing drainage area for each watershed. The following "below dam" drainage area was reduced by 27% for Mineral Fork and 28% for Mill Creek (Figure 12). It was assumed for sediment load modeling purposes that all the tailings dams trapped 100% of the sediment. However, based on trap-efficiency equations, the Sunnen Lake dam passes about 50% of the suspended sediment load it receives annually (St. Louis District Corps of Engineers, 1970; Ward et al., 2016).

STEPL was used to calculate the percent of the sediment load that was reduced due to runoff retention and sediment deposition in the old tailing's ponds and Sunnen Lake. First, STEPL was used to estimate the upland erosion and stream loads for the entire watershed area including the drainage areas behind the dams. Next, STEPL was applied only to the land areas below the most downstream dam on a tributary, not including land areas above the dam. The total load and below dam load were compared to determine the percent reduction in the overall sediment load from the effects of dams. The drainage area above Sunnen Lake dam was assessed separately to estimate suspended sediment load at the dam and then reduce by a best management practice (BMP) efficiency setting of 50%. The reduced stream load from the Sunnen Lake outlet was added to the upland erosion load for the "below dam" drainage area for sediment budget calculations for the whole Mineral Fork watershed.

Overbank floodplain deposition. Overbank sedimentation storage was estimated using deposition rates from research near Mineral Fork and Mill Creek and a review of published results (Table 1). Based on the soil maps, Mineral Fork has 25.1 km^2 of frequently flooded soils and 3.9 km^2 of occasionally flooded soils. Mill Creek has a total area of 5.4 km^2 of frequently flooded soils and 0.7 km^2 of occasionally flooded soils mapped in the watershed (Skaer and

Cook, 2005). A review of floodplain sedimentation rates derived from Big River floodplain core profiles using Cs-137 to identify the 1963 bomb testing peak showed that while higher deposition rates >10 mm/yr occur on lower “in-channel” floodplain and bench surfaces, more moderate rates from 6 and 10 mm/yr occur on floodplain surfaces at/near bank-full stage. However, lower rates from 1-3 mm/yr occur on higher floodplains in wider valleys in stable riparian zones (Pavlowsky, 2013; Keppel et al., 2015; Pavlowsky and Owen, 2015; Jordan, 2019). In a review of the literature, streams with drainage areas and soil conditions similar to the study area tend to have lower floodplain sedimentation rates (1-10 mm/yr) (Owen et al., 2011; Keppel et al., 2015; Pavlowsky and Owen, 2015). From the review and field observations, it was assumed that soils frequently flooded had a deposition rate of 3 mm/yr and occasionally flooded soils had a rate of 0.5 mm/yr In order to calculate mass, the total deposition volume (area times deposition rate) was multiplied by 1.4 Mg/m^3 (Manger, 1963; Pavlowsky et al., 2017).

Table 8. Aerial photograph characteristics.

Year	Source	Flight Date	Type	Resolution (m)	Point to Point Range (m)	Mean Point to Point Error (m)	Buffer (m)
2015	MSDIS	3/15/2015	True color leaf-off DOQQ	0.15	Reference Image		
1995	MSDIS	4/6/1995	Black and White DOQQ	1	0.98 - 7.69	2.76	1.38
2011	MSDIS	6/30/2011	LiDAR DEM	1	N/A	N/A	N/A

Table 9. Definition of variables for deposit volume and mass calculations.

Variable	Equation
Bank Erosion and Deposition Cells	
Average Width (m)	*Area (m^2) / *Length (m)
Lateral Change Rate (m/yr)	Average Width (m) / 20 (yr)
Total Volume (m^3)	*Area (m^2) * *Bank Height (m)
Lower Unit Volume (m^3)	(Total Volume * 0.55) * Fraction of Fines (0.4 - 0.7)
Upper Unit Volume (m^3)	(Total Volume * 0.45) * Fraction of Fines (0.9 -1.0)
Total Volume of Fines (m^3)	Lower Unit Volume (m^3) + Upper Unit Volume (m^3)
Mass (Mg)	Total Volume of Fines (m^3) * bulk density (1.4 Mg/m^3)
Bar Erosion and Deposition Cells	
Average Width (m)	*Area (m^2) / *Length (m)
Total Volume (m^3)	*Area (m^2) * *Bar Height (m)
Total Volume of Fines (m^3)	Total Volume (m^3) * Fraction of Fines (0.25)
Mass (Mg)	Total Volume of Fines (m^3) * bulk density (1.9 Mg/m^3)

*Values from sampled LiDAR heights by subwatershed/stream order

Table 10. Description of sediment budget terms.

Component*#	Description
Upland Erosion	Overall soil erosion rates predicted by STEPL using variables in appendix (Tetra Tech, 2018).
Floodplain Storage	Estimated mass of sediment deposited into long-term storage on frequently (3 mm/yr) and occasionally (0.5 mm/yr) flooded soil series (Skaer and Cook, 2005). Annual deposition rates were based on assumptions from literature review and limited regional data (Table 1).
Other Storage	Upland Erosion rate (#1) minus floodplain (#2), bank, and bar depositional storage rate and export load.
Bank Erosion (net)	Sum of annual bank erosion and bank deposition rates (Figure 25). Positive value indicates a net supply or release to the channel and negative value indicates a net sink or storage from channel transport. Part of the in-channel derived load (Table 25).
Bar Erosion (net)	Sum of annual bar erosion and bar deposition rates (Figure 25). Positive value indicates a net supply or release to the channel and negative value indicates a net sink or storage from channel transport. Part of the in-channel derived load (Table 25).
Upland Load	Output of stream sediment from the watershed predicted by STEPL from upland erosion (#1) after application of sediment delivery ratio (Tetra Tech, 2018).
In-channel load	Output of stream sediment from the watershed calculated by this study by assessment of annual erosion and deposition rates of bank and bar deposits (Table 25).
Export Load	Total sediment load exported from the watershed outlet as the sum of both upland (#6) and in-channel (#7) loads. The export load from the Mineral Fork and Mill Creek watersheds would be assumed to enter Big River (Table 27).
Sediment Yield	Export load reported as a per unit area (km^2) rate that indicates the intensity of sediment production from the watershed (Table 27).

*all units in Mg/yr except for sediment yield which is $Mg/km^2/yr$

#Positive (+) mass values denote erosion or the release of sediment to the channel, while negative (-) values denote deposition or storage of sediment in colluvial or alluvial deposit

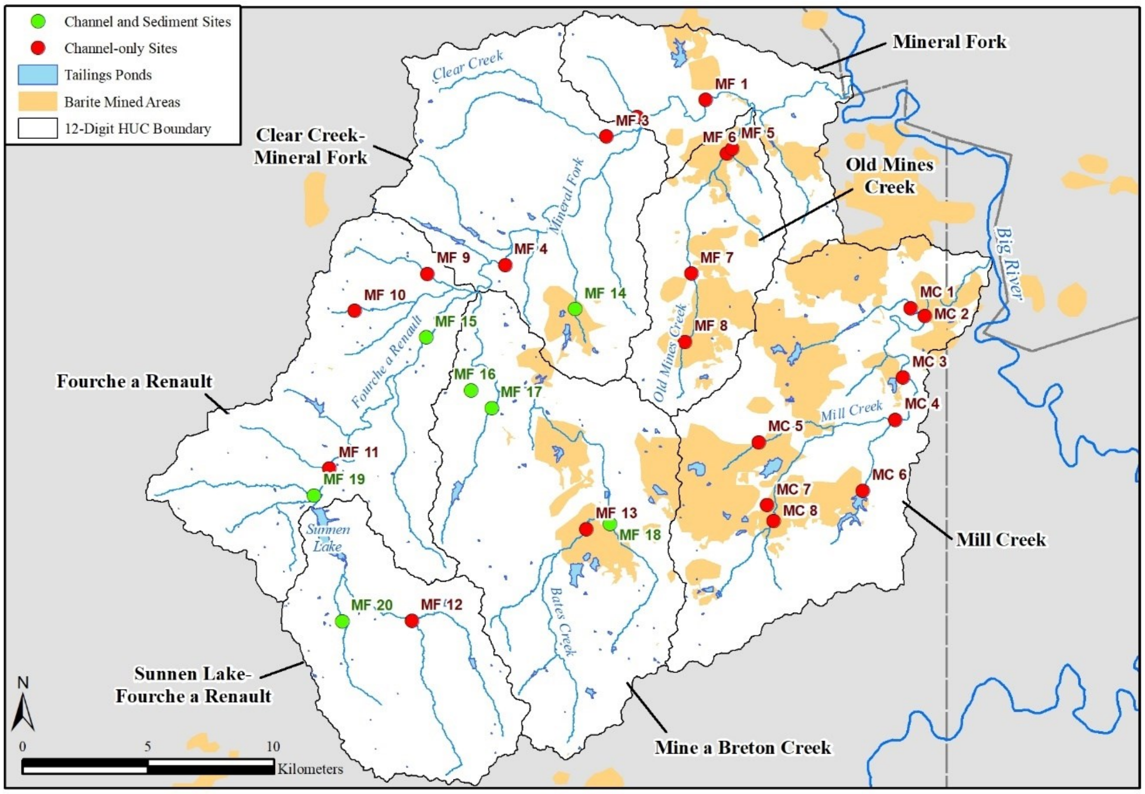

Figure 6. Location of field assessment sites.

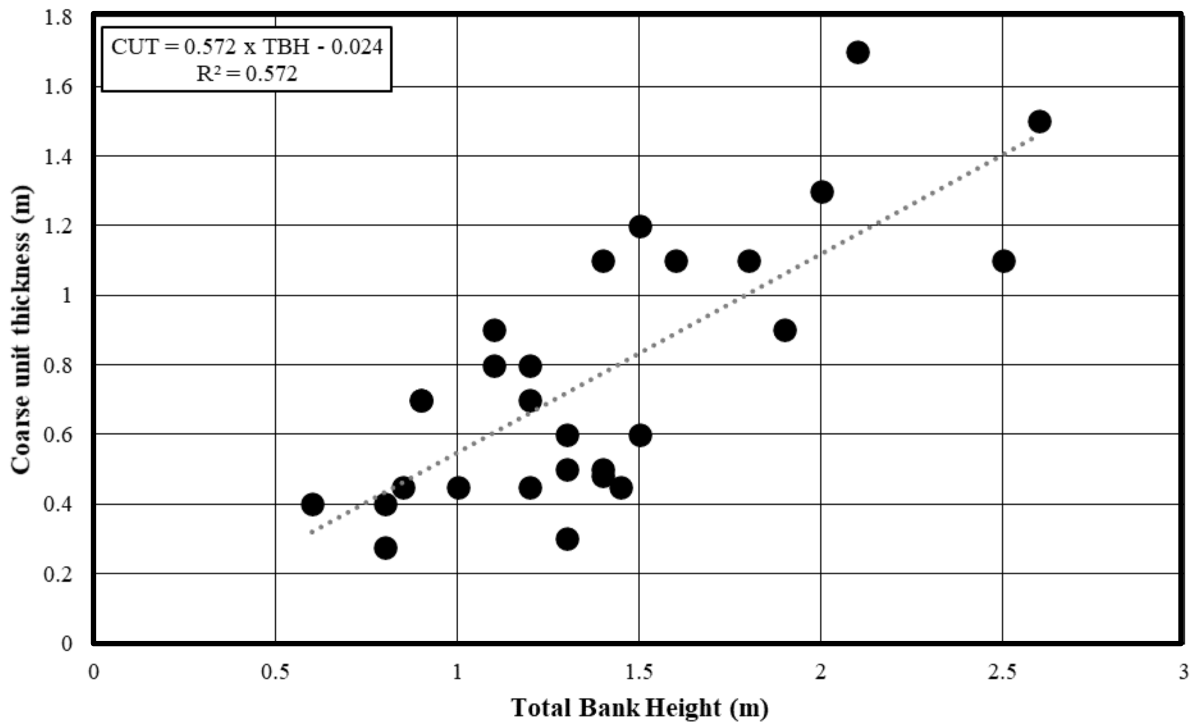

Figure 7. Coarse unit thickness in bank deposits.

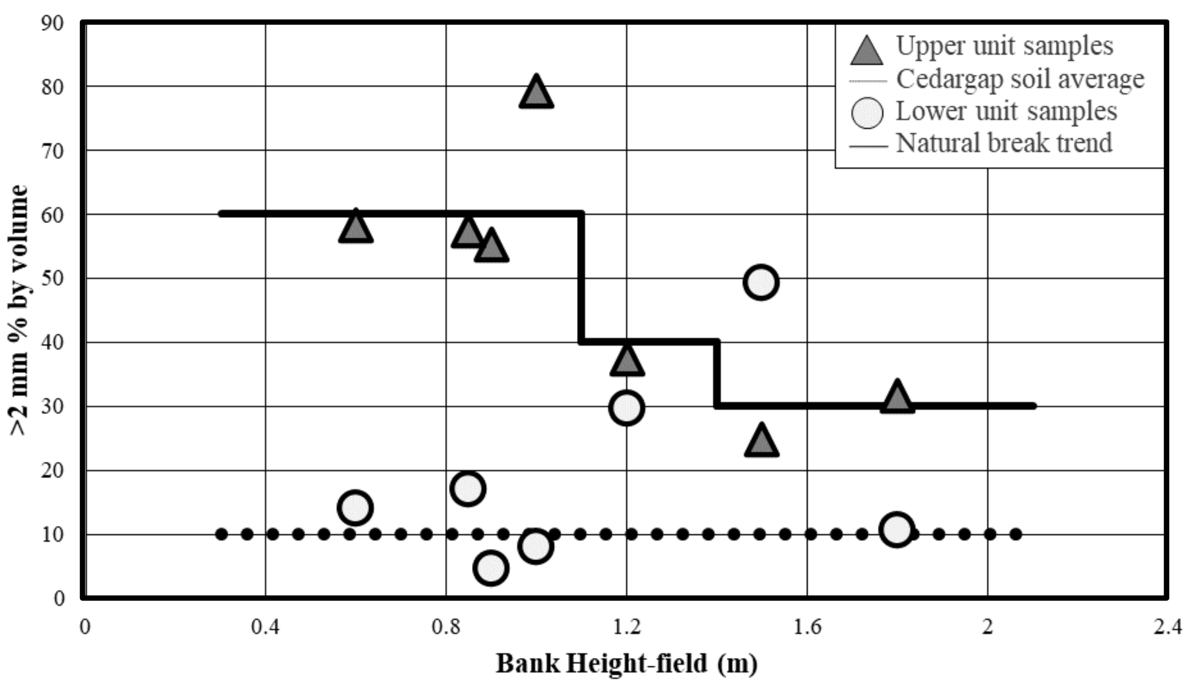

Figure 8. Texture of bank deposits.

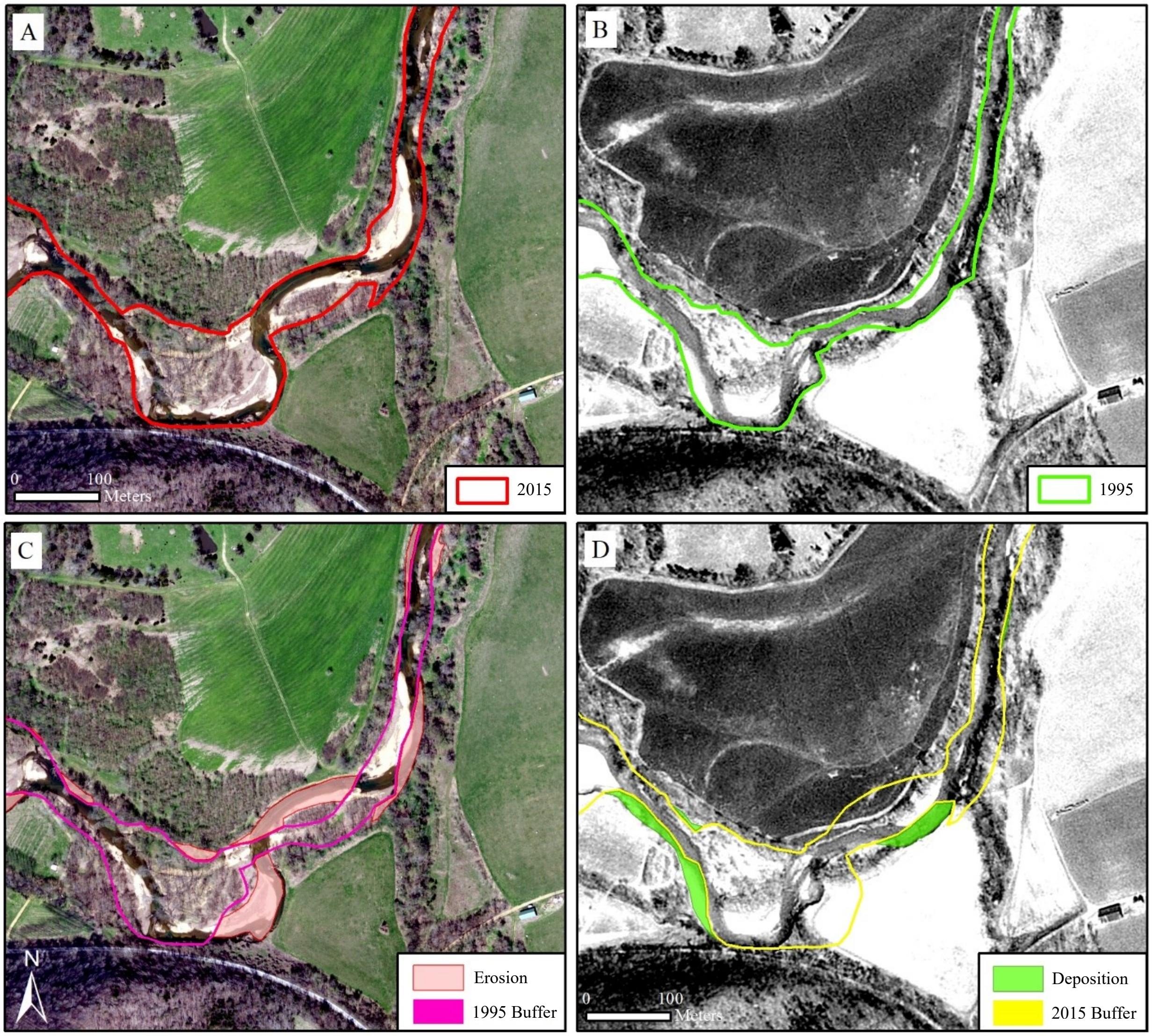

Figure 9. Application of error to active channel features. (A) 2015 digitized active channel compared to the (B) 1995 digitized active channel from the aerial photographs. (C) Areas of erosion where parts of the active channel that do not overlap the 1995 active channel buffer (1.4 m). (D) Areas of deposition where parts of the active channel that do not overlap the 2015 active channel buffer (1.4 m).

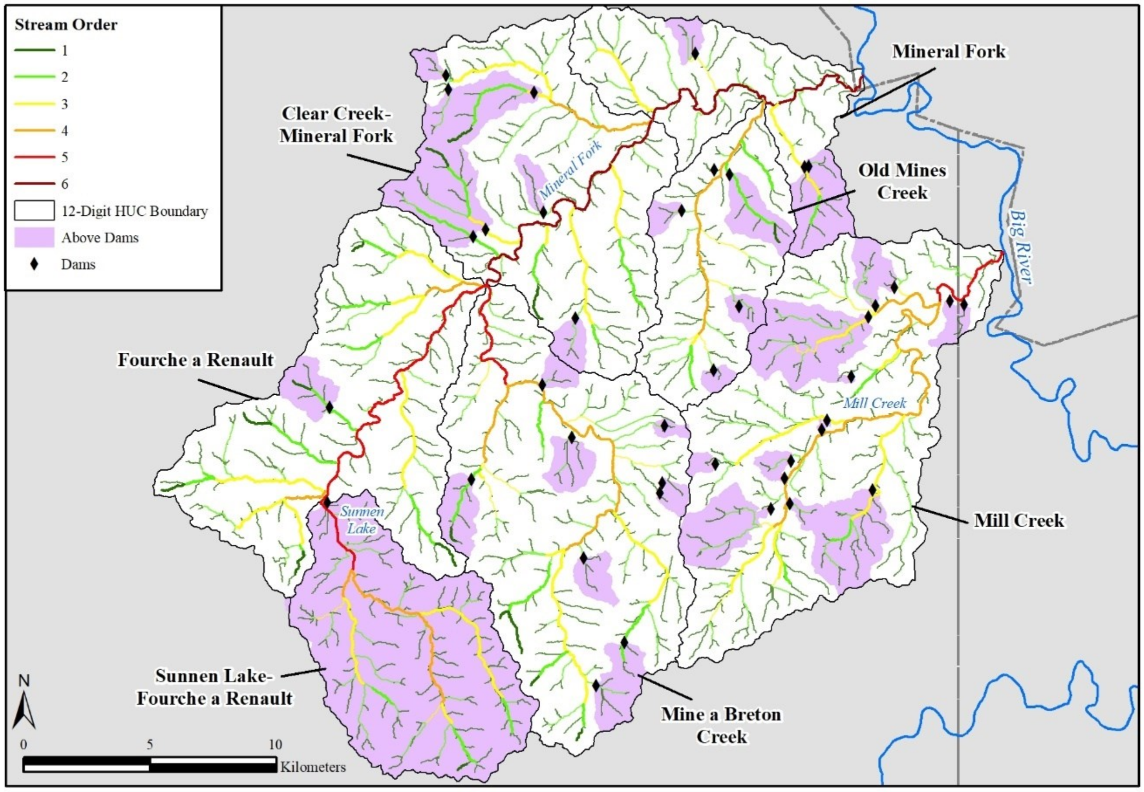

Figure 10. Digitized and delineated stream network

.

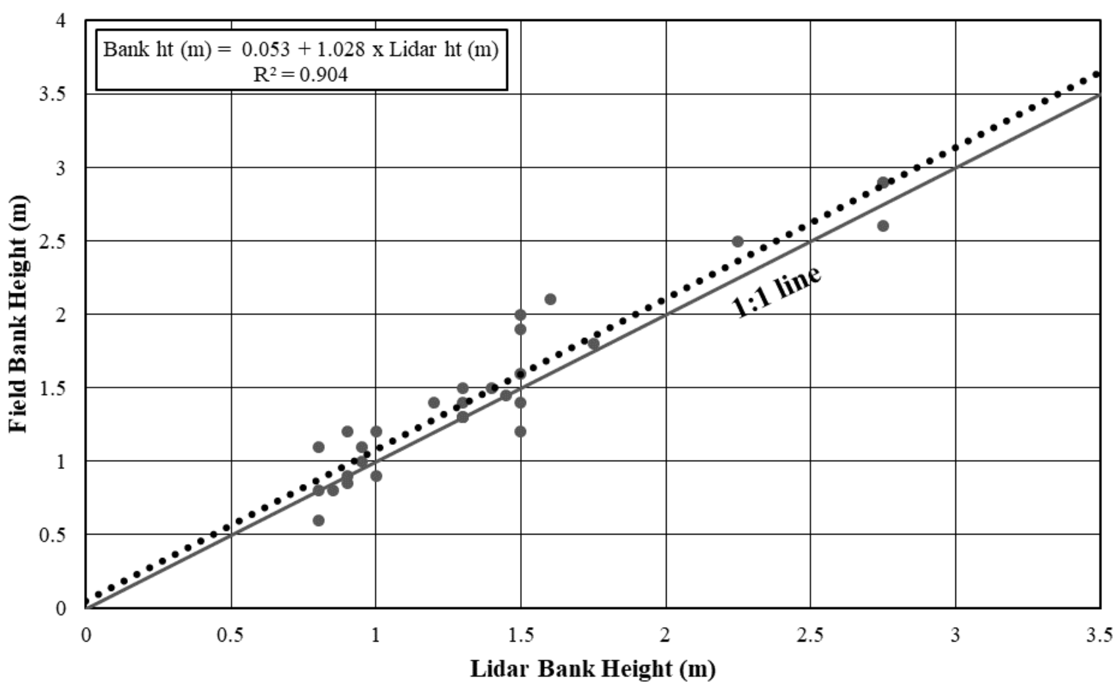

Figure 11. Comparison of LiDAR bank height to field bank height.

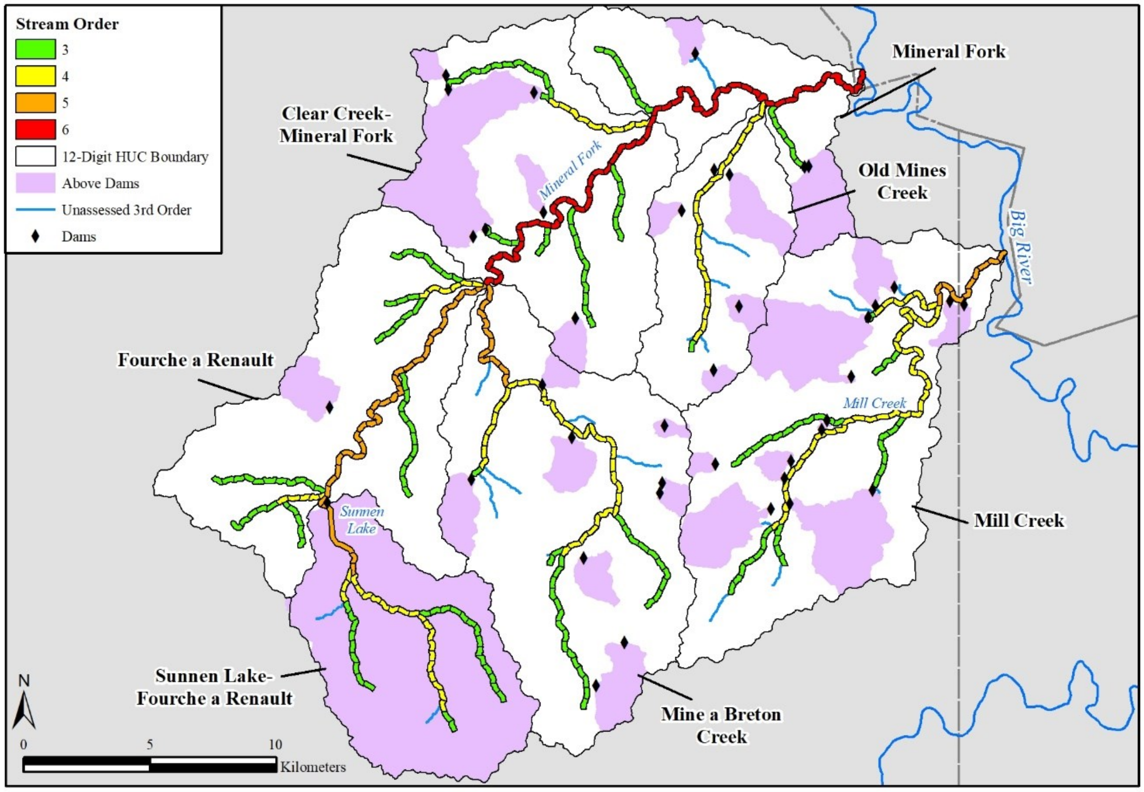

Figure 12. Cell distribution below dams by stream order.

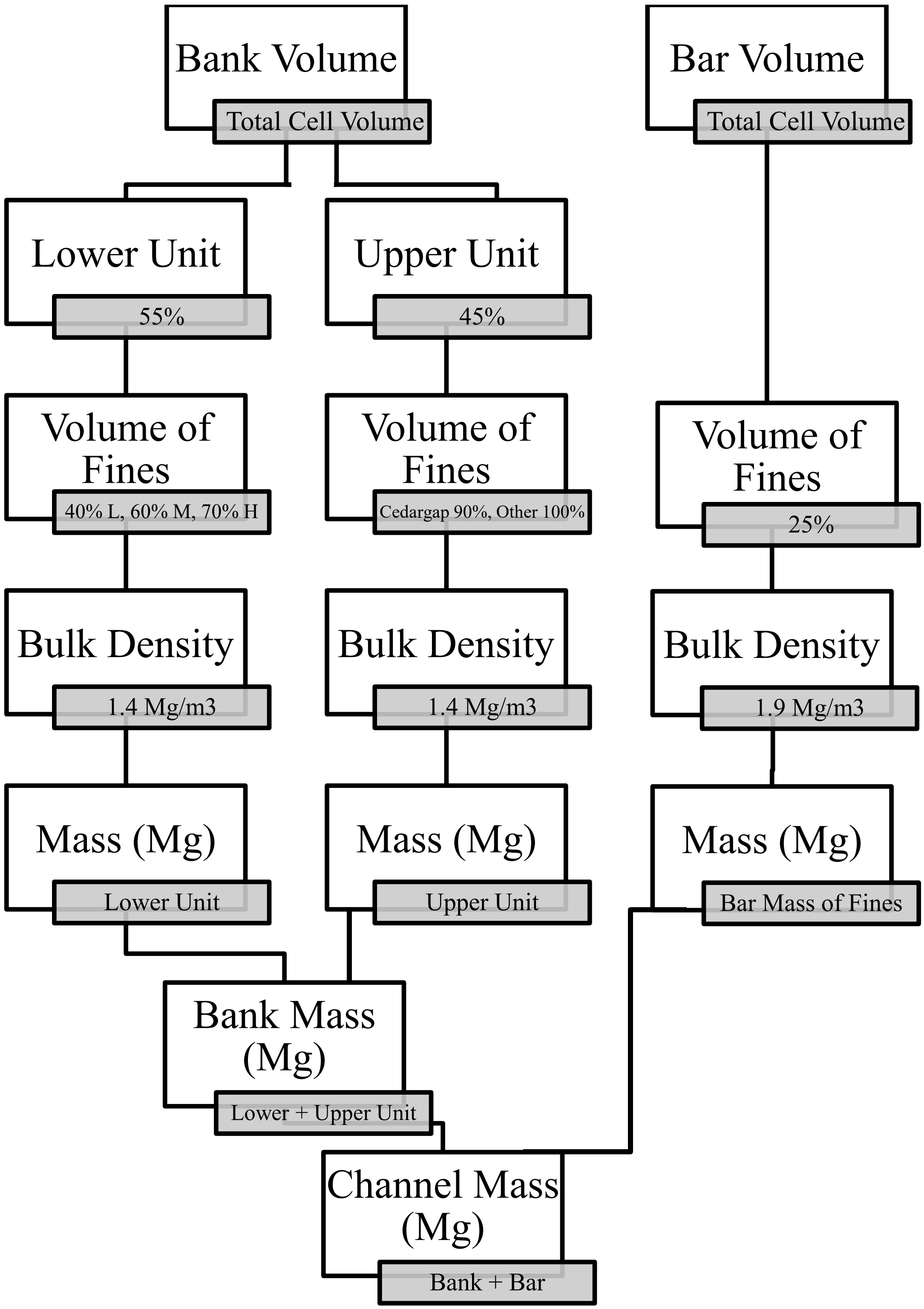

Figure 13. Deposit volume to fine sediment mass conversion by cell.

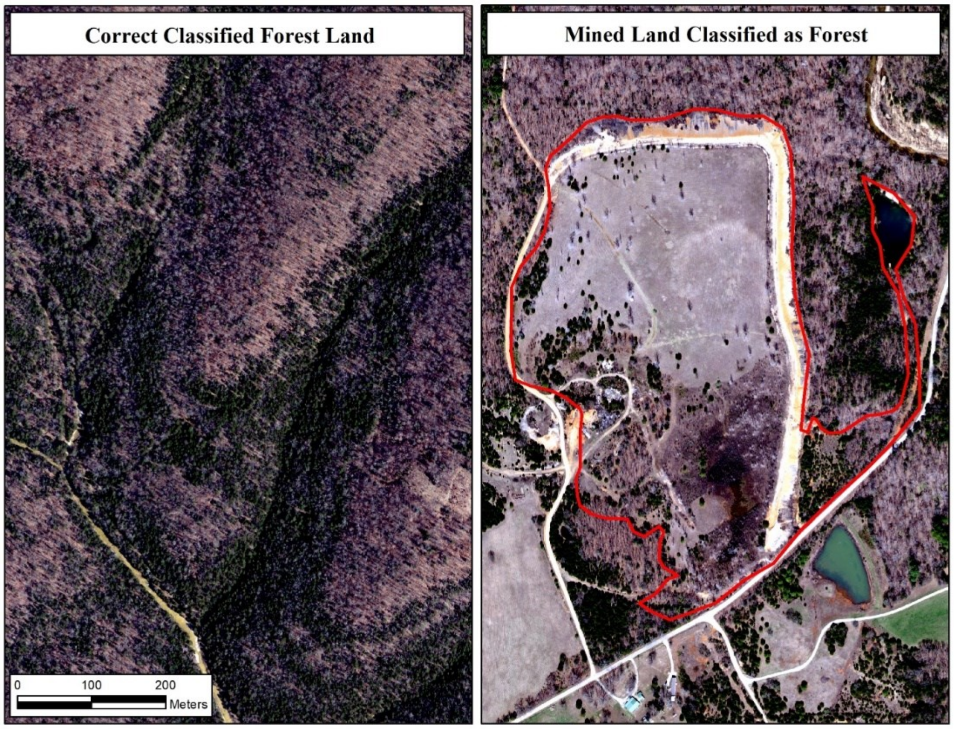

Figure 14. Mining areas classified as forest from the 2015 DOQQ aerial photo.

RESULTS AND DISCUSSION

Channel delineation and network analysis

Stream network and orders. The stream networks were delineated for each watershed from the LiDAR data using the Strahler Order method. The total channel length by stream order for Mineral Fork was as follows: 486 km, first; 224 km, second; 104 km, third; 51 km, fourth; 25 km, fifth; and 28 km, sixth (Table 11). Not all segments of the channel network could be digitized into channel and bar features on the aerial photographs due to the resolution errors and obstruction by trees and shadows. Only 4% of the first order and 29% of the second order streams were digitized in the Mineral Fork watershed. Therefore, only the third, fourth, fifth, and sixth stream orders were evaluated in this study. In Mineral Fork, 100% of the fourth, fifth, and sixth order and 78% of the third order delineated streams were digitized (Table 11). Of the total assessed stream length (188 km), 16% of the network length was above dams as follows: 18%, third; 21%, fourth; 13%, fifth; and 0%, sixth. Since it was assumed that 100% of sediment load was trapped behind the large tailing's dams, the stream lengths above dams were not included in the channel assessment, with the exception of Sunnen Lake dam with its 50% trap efficiency for sediment. Therefore, the total assessed length by stream order in Mineral Fork was as follows: 86 km, third; 40 km, fourth; 22 km, fifth; and 28 km, sixth (Table 11).

The total channel length by stream order for Mill Creek was as follows: 139 km, first; 70 km, second; 31 km, third; 24 km, fourth; and 5 km, fifth (Table 12). The first order streams were not visible and only 4% of the second order streams were digitized. Therefore, similar to Mineral Fork, the in-channel analysis only included third, fourth, and fifth order streams in the Mill Creek watershed. The digitized stream network included 100% of the fourth and fifth order and 73% of the third order stream lengths in the Mill Creek watershed. Dams were only located on third order streams, leaving 20% of the stream length above dams. Therefore, the total assessed length by stream order in Mill Creek was as follows: 25 km, third; 24 km, fourth; 5 km, fifth (Table 12).

Cell distribution. The channel morphology in each watershed below dams was compared between the two aerial photograph years to support the analysis of in-channel contributions to sediment budgets. The digitized stream network was divided into 500-m long channel cells to quantify the spatial patterns of bank and bar erosion and deposition areas in stream order segments (Jacobson and Gran, 1999; Panfil and Jacobson, 2001). Mineral Fork had 344 cells within its watershed below dams. The cells in Mineral Fork were grouped by stream order as follows: 44%, third; 28%, fourth; 13%, fifth; and 16%, sixth (Figure 15). Mill Creek had 86 cells. The cells in Mill Creek were distributed by order as follows: 38%, third; 50%, fourth; and 12%, fifth (Figure 15). The 430 cells were used as the unit of assessment to sum net erosion or deposition in the channel erosion and deposition areas and were multiplied by average landform height values for each stream order in each 12-Digit HUC subwatersheds. Volume of bank and bar landform changes were then summed to assess sediment erosion and deposition of both the cell and stream order scales.

Bank and bar deposit assessment

The total gravel bar area was digitized in the 1995 and 2015 aerial photographs, while the active channel was used to determine if the active channel was widening or laterally moving in a cut-bank point to bar formation (Kondolf, 1997). Examples of the spatial distribution of erosion and deposition using polygons are shown in Figures 16 and 17. Typically, both erosion and deposition for banks and bars were observed in spatially similar locations (Joyce et al., 2018).

More specifically, where bank erosion occurred deposition impacts were adjacent to it. Figures 16 and 17 also showed a detailed map of multiple cells/reaches where there were erosion zones that contributed the most to the sediment load. Similarly, gravel bars were present in all of the reaches (cells) in the figures for 1995 and 2015 (Figures 16, 17). Additionally, the reaches were used to determine if there was movement of the gravel bars downstream (Panfil and Jacobson, 2001).

After identifying all of the erosion and deposition polygons, it was determined how much of the stream length was disturbed. The total length of bank erosion (i.e. cut-banks) in Mineral Fork was 87.0 km in the third through sixth order streams, or 21% of the digitized stream length. The total length of polygons defined as bank deposition in Mineral Fork was 78.6 km, or 19% of the active channel length evaluated for this study. Similarly, in Mill Creek, the total length of cut-banks was 23.6 km, or 24% of the digitized stream length. The total length of bank deposition was 9.7 km or 10% of the digitized stream length. The frequencies of eroding channel lengths observed in Mineral Fork and Mill Creek are similar to other Ozark streams where 20 to 40% of channel lengths are in disturbed active zones along the main channel segments (Martin and Pavlowsky, 2011; Owen et al., 2011).

Variable discharge effects on planform analysis. Studies have shown that there are errors associated with using aerial photographs to determine channel morphology (Mount and Louis, 2005; De Rose and Basher, 2011). One of the disadvantages are rectification procedures and the ability to consistently locate bank features between dates of photography such as cases where the resolution of the image is low or the study area is in a dense woody riparian cover (De Rose and Basher, 2011; Spiekermann et al., 2017). However, mean point-to-point errors and other polynomial transformations from georeferencing can reduce inaccuracies by applying buffers to remove areas that are inside of the limit of error (2 m to 5 m) (Mount and Louis, 2005; Hughes et al., 2006; De Rose and Basher, 2011). This study used a mean point-to-point error of 2.8 m, and applied half of the error on each side of the stream creating a buffer of 1.4 m.

Another problem with using the aerial photographs was the need to check if the discharge during the photograph dates were similar thus allowing channel morphology, and not water depth, to describe wetted width dimensions. This is usually addressed by finding the flow measurements from historical USGS gage records among photograph dates (Barr, 2016). However, these small watersheds do not contain gaging stations. Further, the photographs used from MSDIS did not have exact flight dates of when the photographs were taken, only a range of dates. The closest gages to Mineral Fork and Mill Creek were south (upstream) of the watersheds on the Big River at Richwoods (#7018100) and north (downstream) of the watersheds on the Meramec River near Sullivan (#7014500) (USGS, 2018b). The antecedent flooding was compared by assessing the peak annual flood discharge in the 5-year period before each aerial photograph year (Figure 18). The period from 1990 to 1994 had higher annual floods compared to 2010-2014 (Table 13). The average of the annual flood peak record was the mean annual flood with a recurrence interval of 2.33 years. The average flood peak in the five years before aerial photographs were collected was 1.5-1.7 times larger in 1995 compared to 2015. Therefore, the flood power could have had an influence on the wider channel in 1995 and photograph series taken after the period of more floods might yield sharper and wider banks and brighter and easier to delineate bars.

Water surface width on the day of the aerial photographs were taken varied with baseflow or recent runoff. In order to detect if there was an impact of channel flooding and water levels on the active channel width, 14 different 500 m reaches in the third through sixth stream orders were compared to determine if there was a significant difference in the active channel width between the photograph years (Table 14). Based on a 1:1 line for the 1995 active channel widths to the 2015 widths, there was an R^2 value of 0.84 (Figure 19). Trends showed that when the active channel width increased, 1995 had a wider channel than 2015. Alternatively, when the active channel width decreased, 2015 had a wider channel than 1995 (Figure 19). Therefore, the 1:1 showed that there was not a significant difference between the different years. The average difference in channel width (1.1 m) was less than half of the mean point-to-point error (2.8 m). Further, there was relatively little scatter among the site pairs suggesting that the discharge and depth/width relation was similar for both years and that bank and bar lines would not vary significantly due to water depth errors.

Bank and bar heights as a factor for volume. Because the aerial photos dates were different than the LiDAR flight date, a subsample of bank (n = 152) and bar (n=157) heights were collected in stream orders (3rd – 6th) below the dams. The water reflection from the LiDAR was corrected on these heights to include water depths using field-based channel topographic surveys. Of the 152 bank sites sampled, 10 (7%) had depositional bank heights larger than erosional bank height. It was assumed that the cut-bank side of the channel should typically erode into the older formation of floodplain deposits (i.e. low terrace or historical floodplain), which are assumed to be higher due to a longer period of deposition. Therefore, the depositional bank heights for these sites were corrected to equal those of the erosional bank height. Similarly, of the 157 bar sites sampled, only 21 (13%) had depositional bar heights larger than erosional bar heights. An average height was calculated for each stream order for bank and bar erosion and deposition for each 12-Digit HUC watershed (Table 15-18). The average bank and bar heights were assigned to each cell based on stream order location and subwatershed. Lastly, unmeasured lengths of the third order streams were added in the analysis to estimate the volumes of the missing stream length for each subwatershed. The volumes of erosion/deposition for bank/bars was determined by taking the average volume in third order cells in each subwatershed and multiplied that number by the length of unassessed stream order length below the dams.

Mass of bank and bar erosion and deposition of fine sediment

Geomorphic trends. As expected, average bank and bar heights increase from third to sixth order streams by 1.6 to 1.9 times for banks and 1.4 to 1.6 times for bars (Tables 15-18; Figure 20). Third order banks averaged from 1.6 to 2.0 m high and sixth order banks from 2.7 to 2.8 m (Table 15). Average depositional bank heights were about one-third lower than eroding banks (Table 6; Figure 20). Erosional and depositional bar heights tended to be within 10% of one another with eroding bars usually higher, ranging overall from 1 to 1.4 m in third order channels to 1.7 to 1.8 m in sixth order channels (Table 17-18; Figure 20). Except for sixth order streams, average bar heights tended to be slightly higher than depositional banks (Figure 20). While this trend may reflect variations in bank and bar heights downstream, and not within the same reach, it does suggest that in this study the depositional banks are forming on lower bar surfaces as young benches or shelves (Owen et al. 2011). Further, bar features in the Ozarks can accrete to relatively high elevations near bank-full stage in disturbance reaches (Panfil and Jacobson, 2001; Martin and Pavlowsky, 2011). Specifically, for the subwatersheds, both erosional and depositional bank heights, and bar heights to a lesser degree, tended to be higher in MC and MF subwatersheds which drained directly into the Big River (Figure 12). This trend is expected since longitudinal bank lines and channel beds would grade to meet those of the larger river with local base-level control and decreasing slopes increasing floodplain and channel deposition rates.

As expected, active channel width (including the wetted channel bed and gravel bars) increased downstream from about 8 to 10 m in third order streams to 40 to 55 m in sixth order streams (Figure 21). Average channel widths both increased and decreased among stream orders and subwatersheds over the 20-year study period (Figure 21). The largest increase by almost 40% occurred in third order streams in OMC subwatershed. This geomorphic response may have been caused by recent land disturbances that increase runoff rates into relatively unstable channels due to the presence of mobile gravel deposits possibly linked to the effects of settlement pressure and lead and barite mining since the mid-1700s (Adamski et al., 1995; Jacobson and Primm, 1997; Jacobson and Gran, 1999; Olson, 2017).

The largest decreases in width from 24 to 37% occurred in the SLFR subwatershed for third to fifth order streams (no sixth order streams were mapped in SLFR) (Figure 22a). It is possible that the drainage network was affected by the relatively larger floods prior to 1995 or that more conservation practices for riparian buffers were implemented there since 1995 compared to the other watersheds (Jacobson and Pugh, 1997; Zaimes and Schultz, 2015). Higher antecedent flood magnitudes preceding the collection of the 1995 photographs would suggest that channel widths would at least be temporarily wider than average width in 1995 since bank scour and vegetation removal would be expected to occur during larger floods (Table 13) (Hagstrom et al., 2018). If this was the case, then channels would be expected to recover and be less scoured during 2015. Thus, a tendency for decreased channel widths in 2015 might be assumed given no other changes in land use or flood climatology. However, average width differences were less than 10-20% with nine subwatershed-order classes indicating increases in width and ten classes showing decreases in width over the 20-year period (Figure 22a). The average annual erosion rate for the all the subwatersheds combined was 0.15 m/yr. This 50:50 distribution of width change suggests the higher antecedent flood frequency and magnitude did not influence the results of the present study to a significant degree.

Bank erosion rates can be used to evaluate channel activity since relatively high rates indicate unstable planform conditions with poorly organized bar forms in Ozark streams (Jacobson, 1995; Jacobson and Primm, 1997; Martin and Pavlowsky, 2011). Bank erosion rates >1-2 m/yr in smaller streams like those in this study were considered excessive (Harden et al., 2009; Rhoades et al., 2009; De Rose and Basher, 2011; Kessler et al., 2013; Janes et al., 2017; Spiekermann et al., 2017). In this study, average bank erosion rates and their range among the subwatersheds increased with stream order as follows: third, 0.09 m/yr (0.04-0.10 m/yr); fourth, 0.13 m/yr (0.04-0.18 m/yr); fifth, 0.18 m/yr (0.05-0.28 m/yr); and sixth, 0.18 m/yr (0.27-0.43 m/yr). Average annual bank erosion rates as a percent of active channel width ranged from 0.2 to 1.2% from 1995 to 2015 for the seven subwatersheds evaluated for this study (Figure 22b). There was a tendency for relatively higher rates in third and fourth order streams (>0.9%) and lower rates in fifth and sixth order streams (<0.7%). Locally, one sixth order stream cell in MF had an average bank erosion rate of 0.43 m/yr which was 8% of the active channel width. Bank erosion rates for Mineral Fork and Mill Creek compare well with those reported for 40 stream segments draining the Mid-Atlantic Piedmont with average rates from 0.4-0.19 m/yr and relative rates averaging 2.5%, with a range of 0.9-4.4%, of the active channel width (Donovan et al. 2015).

Gravel bars are common in Ozarks streams and tend to cluster in disturbance zones separated by relatively stable segments (Jacobson and Primm, 1997; Martin and Pavlowsky, 2011; Olson, 2017). In the Mineral Fork watershed, 1.39 km^2 of bars were mapped in 1995 and 1.37 km^2 in 2015 (1.4% decrease). On average, gravel bars in third and fourth order streams in the Mineral Fork watershed covered 17 to 36% of the active channel area in 1995 and 31 to 43% in 2015. Bar area in fifth and sixth order streams covered 29% of the active channel during both 1995 and 2015. In the Mill Creek watershed, 0.25 km^2 of bars were mapped in 1995 and 0.27 km^2 in 2015 (8% increase). The Mill Creek watershed had relatively higher bar areas in the active channel compared to Mineral Fork overall with 29% in 1995 and 43% in 2015. Like the active width, average bar width also tends to increase downstream from less than 5 m in third order channels to 10-15 m in sixth order streams (Figure 23).

All stream order classes contained at least two subwatersheds where bar area in the active channel increased by > 40% from 1995 to 2015 (Figure 24). The greatest increases in bar area occurred in fifth order streams (up to 65% in FR). It is possible that some of the gravel sediment previously released by historical or more recent land use disturbances and channel incision was first deposited in in upstream reaches and then migrated downstream into higher order channels in a wave-like process (Jacobson and Primm, 1997; Jacobson and Gran, 1999). Bar areas decreased by 10-30% in third and fourth order channels in some subwatersheds perhaps as the result of erosion and downstream transport of gravel (Figure 24). Surprisingly, bar areas in sixth order streams of the lower Mineral Fork watershed did not change much between the two photograph years (<10% increase) (Figure 24). Valley confinement by higher bluffs and lower rates of lateral channel migration along the lower segments may have limited available bar accommodation space along the lower Mineral Fork Creek (Lecce, 1997; De Rose and Basher, 2011; Janes et al., 2017).

Patterns of bank and bar storage and erosion masses. The cell-level channel characteristics and sediment samples collected in the field were used to estimate the total mass of fines for bank and bar erosion and deposition. The alternation of depositing and eroding cells has persisted in many Ozark streams since at least since the early 1900s (Jacobson, 1995). This can also be an indication of a dynamic equilibrium condition among discharge, sediment supply, and topography (Martin and Pavlowsky, 2011). Therefore, patterns of the bank and bar storage and erosion were identified by subwatershed and stream order to determine the overall mass of storage and erosion per cell to make sure to include these reach-scale sediment variations. Sediment masses by cell were also used to determine areas where most of the bank erosion, bar erosion, and net erosion load were located to identify which cells combined to make up 25% of the overall load contribution of fine sediment.

Bank erosion. Of the 430, 500 m long cells assessed for this study, 98% produced bank erosion and 93% bank deposition. As expected, average eroded masses increased from third to sixth order streams by 11.8 to 15.5 times (Tables 19-20). Third order bank erosion masses per cell averaged from 24 to 55 Mg/yr and sixth order from 357 to 821 Mg/yr (Table 19). Average depositional bank masses were lower than eroding banks with rates from 11 to 40 Mg/yr in third order and 198 to 328 Mg/yr in sixth order (Table 20).

The Mill Creek watershed had a total of 8,334 Mg/yr of sediment from bank erosion and 2,114 Mg/yr from bank deposition with a net supply of sediment to the channel system by bank erosion of 6,190 Mg/yr (Table 21; Figure 25). Therefore, eroding banks were releasing nearly four times as much fine sediment as they were depositing during the formation of new bench and floodplain landforms. Only one of the 86 cells in Mill Creek did not contain bank erosion (Figure 26). Specifically, the locations in Mill Creek with the highest erosion (i.e. supplying 25% of the total bank erosion load, not including deposition) were in four cells along the main stem of Mill Creek with inputs ranging from 353 to 739 Mg/yr in the per cell (Figure 26).

The Mineral Fork watershed had a total of 48,382 Mg/yr of bank erosion and 26,593 Mg/yr from bank deposition yielding a net sediment output from bank erosion of 21,789 Mg/yr (Table 21). The subwatersheds within Mineral Fork indicated that MF and CCMF have the highest contributions of sediment from bank erosion and deposition (Figure 25). These watersheds contain the highest banks along main stem of Mineral Fork Creek which flows directly into Big River. Moreover, MF supplies 46% of the overall bank erosion load and 34% of the annual bank storage and CCMF contributes to 26% of bank erosion and 26% to bank deposition to the Mineral Fork watershed. OMC and SLFR (which had 50% sediment trap from Sunnen Lake) contain the smallest contributions to bank erosion and deposition loads. There was no bank erosion measured in only seven cells in the following watersheds: OMC (1 cell), MBC (3 cells), FR (2 cells), and SLFR (2 cells). Of the 344 cells in the whole Mineral Fork watershed, the largest contributors of bank eroded sediment include five cells in MF and two in CCMF (Figure 26). Ultimately, cells with the highest bank erosion rates were downstream from the barite mined areas (Schumacher and Smith, 2018). The cells that accounted for 25% of the bank erosion load ranged from 1,314 to 3,015 Mg/yr in the Mineral Fork watershed.

Bar erosion. Of the 430 cells, 90% included bar erosion and 91% bar deposition. Similar to banks, average bar masses increase from third to sixth order streams by about 9.5 to 19.4 times (Tables 22-23). Third order bar erosion masses per cell averaged from 11 to 82 Mg/yr and sixth order from 401 to 440 Mg/yr (Table 22). Average depositional bar sediment rates were lower than measured in eroding bars from 17 to 30 Mg/yr in third order streams but were higher than bar erosion rates in the sixth order streams ranging from 391 to 593 Mg/yr (Table 23).

The streams in Mill Creek and Mineral Fork watersheds flow through alluvial soils with gravelly silt loam and channels with coarse beds. As expected, bars had a significant influence on the fine sediment storage within each watershed. The Mill Creek watershed had a total of 5,546 Mg/yr of fine sediment released by bar erosion and 9,985 Mg/yr of storage by bar deposition (Table 21). This demonstrated that the bar storage was 1.8 times the load of fine sediment released by bar erosion. Even though bank erosion and deposition were a common process in the Mill Creek watershed, gravel bars had higher rates of both erosion and storage compared to banks (Figure 25). If bar erosion is the only factor being assessed (without bar storage), Mill Creek had two cells that make up the highest erosion and 13 cells with no measured bar erosion. The two cells that included 25% of the bar erosion load contributed 575 and 858 Mg/yr. The stream reaches affected by high erosion were again located on the main stem of Mill Creek, compared to the cells indicating no erosion that were located in the lower-order tributaries (Figure 27).

The Mineral Fork watershed had a total of 48,777 Mg/yr of bar erosion and 48,818 Mg/yr from bar deposition (Table 21). Bars in Mineral Fork stored nearly equal amounts of fine sediment by bar deposition as released by bar erosion (-41 Mg/yr of net storage). Recall that bar area only decreased by -1.4% since 1995. Of the subwatersheds in Mineral Fork, the largest influence of bar storage and bar erosion was in MF, CCMF, and MBC, with OMC and SLFR having the lowest contribution of bar sediment (Table 21). MF and FR were the only two subwatersheds that had more sediment put into bar storage than released by bar erosion (Figure 25). Subwatersheds CCMF, OMC, MBC, and SLFR had the highest annual bar erosion masses. With bar deposition was not considered, the highest sediment masses released to the channel from bar erosion were also located in MF (3 cells), CCMF (3 cells), and MBC (4 cells) (Figure

27). The cells that contributed to 25% of the bar erosion load ranged from 572 to 1,574 Mg/yr. Again, deposition cells were located near reaches with high bar erosion rates and occurred downstream from the barite mined areas (Figure 27). Of the 344 cells in the whole Mineral Fork watershed, there were only a few without measured bar erosion cells in all of the subwatersheds: MF (5 cells), CCMF (13 cells), OMC (4 cells), MBC (3 cells), FR (8 cells), and SLFR (2 cells).

Net Mass. When all factors were being included (bank and bar erosion and deposition), Mill Creek had a net in-channel load of 1,751 Mg/yr (Table 21). Mill Creek had 59% of its cells with a net erosion and 41% indicating either no erosion, in balance, or with a net storage. Therefore, if stabilization practices were being considered for the Mill Creek watershed, they would be most effective within the two high erosion cells near Fountain Farm Branch and in the mining disturbed areas (Figure 28). The two cells that contributed to 25% of the overall net erosion output yielded 519 and 841 Mg/yr of fine sediment. In Mill Creek there were more cells releasing fine sediment than there were cells storing fine sediment (Figure 28, 29). However, there was higher rates of net deposition occurred in the downstream segment of Mill Creek (Figure 29).

Bank and bar erosion and deposition in Mineral Fork yielded a net in-channel sediment load of 21,748 Mg/yr (Table 21). Moreover, 94% of the cells indicated net erosion, with 6% having no erosion or net storage. On average the net sediment masses released per cell increase from third to sixth order streams by about 19.1 times (Table 24). Third order net masses per cell averaged from 22 to 119 Mg/yr and sixth order masses from 957 to 1,526 Mg/yr (Table 24). Since bar erosion and bar deposition were balanced with similar masses, the bank erosion rates had a greater influence on the net sediment load in the Mineral Fork watershed. The fifth order streams in Mill Creek were the only places in the channel network that had a net storage of sediment. Bank erosion, bar erosion, and bar deposition all had similar annual masses in the overall in-channel sediment budget and were almost two times higher than the bank deposition mass (Figure 25). If bank stabilization practices were being considered for the whole Mineral Fork watershed, they would be most effective along the lower segment (sixth order stream) of Mineral Fork Creek within MF and CCMF (Figure 28). MF contained ten cells and CCMF had two cells that combine to make up 25% of the overall load contribution of fine sediment. More importantly, MF contributed 44% of the overall in-channel sediment load to Mineral Fork (Table 21). The cells that contributed to 25% of the overall net erosion output ranged from 1,819 to 5,659 Mg/yr of fine sediment from in-channel processes.

Ultimately, bar storage was a key factor in understanding the spatial variability of sediment storages and sinks within the two watersheds. The channel reaches where bar deposition was greater than bank erosion tended to be adjacent to land disturbed by historical mining activities which can cause channel instability (Gillespie et al., 2018). However, there were still more cells eroding than depositing in both watersheds. Cells with high erosion masses tended to be in the larger stream orders where banks were higher. This was also where there was much more gravel bar activity. The alternation of depositing and eroding cells, especially in Mill Creek, was consistent with channel responses and patterns of many Ozark streams (Figure 29) (Jacobson, 1995; Martin and Pavlowsky, 2011). Altogether, the collective length of all actively eroding and depositing reaches accounted for 34% of the stream length in Mill Creek and 40% in Mineral Fork.

In Mill Creek, the spacing or wavelength of erosion and deposition cycles was about 2 km in 3rd and upper 4th order channels and 2.5 to 4 km in lower 4th and 5th order channels which scales to 100 to 200 channel widths (Figure 29). The concept of alternating reaches is still being studied and could be similar to the concept of hierarchical patch dynamics from landscape ecology. At coarse spatial scales, this concept contains a longitudinal series of alternating stream segments with different geomorphological structures (Poole, 2002). Geomorphic variables that might be important in controlling the amounts of bank and bar erosion and deposition could be controlled by the locations and stability of the higher banks in the larger order streams and the width of the valley flood as confirmed by slopes and bluffs. Active reaches may also be controlled by low order tributary inputs or valley confinement trends (Jacobson and Gran, 1999; Martin and Pavlowsky, 2011). Jacobson and Gran (1999) reported that gravel bar accumulations along the Current River, Missouri were controlled by lagged sediment transport in wave-like patterns from the low-order tributaries to the main stems in a watershed. Geomorphic factors driving in-channel sediment cycling could also be linked to historical mining disturbances or legacy effects from the conversion of forest to agricultural land (Jacobson and Primm, 1997; Pavlowsky et al., 2017).

Sediment load contributions

Sediment budgets measure the amount of sediment eroded and stored in all sections of a watershed which include uplands, floodplains, and in-channel processes (Phillips, 1991; Beach, 1994; Trimble, 1999). Therefore, in order to create detailed sediment budgets for Mill Creek and Mineral Fork, sediment storage and erosion components were combined to determine the overall amount of sediment that makes it out of the basin (Table 10) (Davis, 2009). The sediment budget in this study specifically evaluated erosion in the uplands, over-bank floodplain deposition, bank erosion and deposition, gravel bar storage and erosion, and the influences of tailings dams on trapping sediment (Trimble and Lund, 1982; Trimble, 1999; Renwick et al., 2005; Davis, 2009; Schenk and Hupp, 2009; Lauer et al., 2017; Gillespie et al., 2018; Joyce et al., 2018).

STEPL. Before dams were considered as sediment traps that reduce the overall sediment load, the entire Mineral Fork watershed produced an upland sediment load of 24,132 Mg/yr from upland sources. STEPL estimated that upland erosion was about 292,522 Mg/yr before a sediment delivery ratio of 0.08 was applied to calculated the upland loads at the watershed outlet (Table 25). The entire Mill Creek watershed produced a sediment load of 12,554 Mg/yr, with the estimated upland erosion calculated by STEPL at 115,157 Mg/yr (Table 25). Because Mill Creek watershed had a smaller drainage area than the Mineral Fork watershed, the sediment delivery ratio was higher at 0.11.

Mineral Fork has 27% of its drainage areas above tailings dams and Mill Creek has 28%. The tailings dams were assumed to trap 100% of the sediment that entered the impoundment, except for Sunnen Lake that only trapped 50% of the sediment due to its size (Renwick et al., 2005; Trimble and Lund, 1982; Ward et al., 2016). The upland erosion load below dams in STEPL was 17,785 Mg/yr in Mineral Fork. Therefore, the total upland load was reduced by 26% with 6,348 Mg/yr of sediment behind the dams (Table 26). The Mill Creek watershed had an upland erosion load of 7,741 Mg/yr for the watershed area below the dams. The amount of sediment being stored above the tailings dams was 4,813 Mg/yr, which lead to a 38% reduction in the overall sediment load (Table 26).

Overbank floodplain storage. Historical floodplain sedimentation could have followed the introduction of mining and agricultural settlement as described by other studies around the Ozarks and the Midwest (Knox, 1972, 1987, 2006; Owen et al., 2011; Pavlowsky et al., 2017; Reminga, 2019). The floodplains soils within the cells were predominantly classified as frequently flooded (84%), with a few cells that that had soils that were identified as occasionally flooded (16%). The annual mass of overbank floodplain deposition was assumed using mapped alluvial soils from the Soil Survey and deposition rates calculated from other studies surrounding the study area (Skaer and Cook, 2005; USDA-NRCS, 2017). The soils that were frequently flooded had a deposition rate of 3 mm/yr applied to the area and occasionally flooded soils had a rate of 0.5 mm/yr (Table 1) (Pavlowsky and Owen, 2015). Therefore, Mineral Fork had an annual mass of 108,263 Mg/yr of sediment that was depositing on the floodplains, which provided 40% of the fine-sediment storage in Mineral Fork. Approximately, 23,269 Mg/yr of sediment contributed to the overbank floodplain storage in Mill Creek, providing 33% of the sediment storage was from overbank deposition. More specifically, other research has suggested that soil disturbance on hillslopes by mining activities might have been a major source of overbank floodplain sedimentation (Knox, 1987; Pavlowsky et al., 2017; Jordan, 2019).

Sediment budget evaluation. Sediment budgets are important for determining where sediment is coming from and going to within a watershed. However, it is important to assess the effects of specific land uses such as mining disturbed land cover to understand how they may increase or decrease the sediment yields from the uplands bank erosion (Xiao and Ji, 2007; James and Lecce, 2013). The upland loads below dams and in-channel sediment inputs were combined to complete a sediment budget for the Mineral Fork and Mill Creek watersheds.

<u>Sediment budget for Mineral Fork and Mill Creek watersheds.</u> With the land uses, floodplain deposition, and in-channel processes, Mineral Fork had a sediment yield of 92.2 $Mg/km^2/yr$ and Mill Creek had a yield of 98.6 $Mg/km^2/yr$ for the drainage area below dams (Table 27). The mass of sediment that was exported out of the basin from the upland sources was derived from the sediment delivery ratio and how much sediment was being stored in tailings

dams. Only 7% of the total upland erosion in Mineral Fork was estimated to make it out of the basin. Sheet and rill erosion from the uplands contribute to 45% of the total load with 17,785 Mg/yr. With the different land uses in the uplands, bank erosion, and bar storage, Mineral Fork was exporting 39,533 Mg/yr of sediment into Big River (Figure 30). About 8% of the soil eroded from the uplands in Mill Creek left the watershed. Upland erosion of 7,741 Mg/yr contributed to 42% of the total load. Ultimately, Mill Creek had a sediment export of 9,492 Mg/yr to Big River (Figure 31).

Significance of in-channel sediment processes. In addition to the upland erosion, bank erosion and deposition were also major contributors to the sediment budgets. Based on the differences between bank erosion and bank deposition in each cell, Mineral Fork had a net sediment load export of 21,789 Mg/yr (Table 27). The net load of bank erosion contributed to 55% of the load that made it to the outlet of the watershed. Mill Creek had a net sediment load of 6,190 Mg/yr from bank erosion (Table 27). The net bank erosion load contributed to 34% of the sediment load leaving the watershed. Bank erosion as a ratio of the upland load estimated in STEPL was 2.7 in Mineral Fork and 1.1 in Mill Creek (Figure 32a). Net bank erosion as a percent of the upland load was 1.2 in Mineral Fork and 0.8 in Mill Creek (Figure 32a). Therefore, overall bank erosion contributions, even after bank deposition was incorporated, were relatively higher compared to annual loads, especially in Mineral Fork.

Ozark streams have been known to have a large presence of gravel bars. After taking the difference in bars from 1995 to 2015, the Mineral Fork watershed was in balance. Specifically, there was only net load -41 Mg/yr of fine-grained sediment being deposited on the bars (Table 27). Ultimately, the net deposition in bars accounted for only 0.1% of the reduction of sediment to the watershed outlet. Comparatively, Mill Creek had a net storage of -4,439 Mg/yr along the bars in the watershed (Table 27). The bars had a pronounced influence on the sediment storage within each watershed. Mill Creek had a net deposition in bars accounted for 24% of the load reduction of sediment to the watershed outlet. Even when bar erosion was compared to the upland load estimated in STEPL, bar erosion had a ratio of 2.7 in Mineral Fork and 0.7 in Mill Creek (Figure 32b). Again, bar erosion contributions were relatively high compared when compared to annual loads. However, net bar erosion as a percent of the upland load was 0 in Mineral Fork and -0.6 in Mill Creek (Figure 32b). In the case of the Mineral Fork watershed the zero indicates that the bar erosion and deposition loads are in balance. The negative percent indicated that there was a net bar storage in Mill Creek. However, bar storage was important for Mill Creek by having a significant reduction in the overall export of sediment out of the watershed basin.

When combining the annual bank and bar erosion and deposition loads, the in-channel contributions released more sediment than it was storing in both watersheds. The in-channel load as a percent of the total load was 55% in Mineral Fork and 19% in Mill Creek (Figure 32c). Mineral Fork and Mill Creek had their sediment loads more influenced by in-channel processes than sediment eroding from the uplands. Generally, in-channel storage is not studied. Based on the in-channel contributions of Mineral Fork and Mill Creek watersheds, deposition process and bar forms should be included more often in bank erosion studies. In Mineral Fork, bank erosion loads as a percent of the upland load was reduced by half after bank deposition loads were incorporated. Similarly, sediment from bars was storing more than it was releasing in Mill Creek. Therefore, studies that have not incorporated storage factors in their bank erosion studies could be overestimating the amount of sediment being exported from a watershed.

Land use contributions. Each of the land use categories specified in STEPL were used to determine which land use had the largest sediment load contribution to Mineral Fork and Mill Creek. Even though mines in the study area have been closed since 1998, the land use category did not accurately represent the land use/land cover of the mining disturbed landscape. Therefore, for this study, STEPL was manipulated to have mined areas as a land use type in the user-defined category (Tetra Tech, 2018). The mined land was mapped based on location found on the landscape of the LiDAR derived DEM. Mineral Fork was a predominantly forested watershed with this land use covering 82% of the watershed. However, the main sources to sediment load in the uplands came from mining areas (31%), pastureland (27%), and forest (26%) (Table 28). Mining and pasture land covered 2% and 11%, respectively, of the drainage area in Mineral Fork. However, they represented the largest contributors to the upland erosion loads because mined land and pastureland had less cover and higher rates of erosion than forested land (Troeh et al., 2004; Park et al., 2014). The land use in Mill Creek was forest (78%), mines (8%), and pasture (7%). The largest sediment contributors were mining areas (58%) and forest (28%) (Table 28). The parameters from USLE and the increase in the percent of mined land caused Mill Creek to have more of its upland sediment load to be coming from mined land than Mineral Fork (Troeh et al., 2004; Renwick et al., 2005).

Future work. Additional studies are needed to improve this research. For example, more field data can be collected on fine sediment variability for in-channel and overbank floodplain deposits. Presently, it is not clear to what degree the texture of channel and floodplain deposits varies spatially downstream and among different landforms. Additionally, more studies on floodplain sedimentation rates are needed such as similar to those completed for other Ozark rivers including Big River (Owen and Pavlowsky, 2015; Pavlowsky et al., 2017; Jordan, 2019).

According to the sediment budget from 1995 to 2015, floodplain deposition was estimated to provide 33 to 40% of the annual upland storage contributions in the two watersheds. A more precise analysis can try to validate the stream loads derived from this sediment budget by monitoring or modeling discharge and suspended loads. Further, Cs-137 can be used to date floodplain soil cores and quantify recent sedimentation rates (Owen et al., 2011; Reminga, 2019).

Because these are mining disturbed watersheds, the sediment budget can also be applied to sediment contamination questions by adding a component of metal contributions to the overall suspended sediment load. More sampling can be completed to determine the geochemical analysis of Pb, Zn, or Ba concentrations in the Southeastern Missouri Barite District (Barr, 2016; Pavlowsky et al., 2010, 2017; Schumacher and Smith, 2018). A wider range of analyses would need to be completed on more sediment samples from uplands, floodplains, and in channel locations including banks, gravel bars, benches, and bed samples in disturbed and undisturbed mining locations. Using geochemical analysis, the spatial distribution of metal concentrations could also be determined at different locations in the channel network.

Additional studies could be completed using LiDAR exclusively to model flows and sediment transport and loads. More geomorphic studies are being completed to using LiDAR to support geomorphic fieldwork (Roering et al., 2013). Remote sensing with LiDAR can be used to study channel reaches in detail or watersheds to detect changes over time (Betts et al., 2003; De Rose and Basher, 2011). The LiDAR for this study was collected in 2011, future work may include repeat LiDAR collection over this area to detect changes in the DEM through hillslope erosion or channel morphology over 10 plus years (De Rose and Basher, 2011; Roering et al., 2013). In theory, Sequential LiDAR data could also be used to calculate vertical sedimentation rates (Notebaert et al., 2009; Höfle and Rutzinger, 2011).

Understanding Ozark streams. Based the range of other sediment yields determined in SW Missouri (9-87 $Mg/km^2/yr$), sediment yields for Mineral Fork and Mill Creek were slightly higher than the range of sediment yields for watersheds of similar sizes (Table 3). However, the other studies may not have included in-channel sources. Since there are few published studies on sediment budgets and channel erosion available for the Ozarks, this study filled the gaps in our understanding of the watershed trends in channel erosion and where management efforts are needed to reduce erosion inputs. Recently, Ozark watersheds have been experiencing a decrease in water quality due to runoff and soil disturbances from historical land-clearing, lead and barite mining, and cattle grazing agriculture (Jacobson and Primm, 1997; Mugel, 2017; Schumacher and Smith, 2018; USEPA, 2018a). There are on-going concerns about excess sedimentation in Ozark streams from bank, sheet, and rill erosion (MDNR, 2014, 2016, 2018). Eroding stream banks can be significant sources of fine sediment to streams supplying up to 80% of the total suspended sediment load at the watershed outlet (Harden et al., 2009; De Rose and Basher, 2011; Kessler et al., 2013; Fox et al., 2016; Spiekermann et al., 2017). Other studies have assessed disturbance in different reaches across watersheds. The findings of this study indicate the in-channel sediment sources including bank and bar erosion can supply 19-55% of the annual suspended sediment load to Ozark watersheds.

Table 11. Total length of stream network by stream order assessed in Mineral Fork.

Mineral Fork	Stream Order						
	1	2	3	4	5	6	Total
Total Watershed Area (490.5 km^2)							
Delineated stream length (km)	486.0	224.0	104.1	50.7	25.4	28.4	918.6
Delineated distribution (% by order)	53	24	11	6	3	3	100
Digitized stream length (km)	18.2	65.6	82.1	50.7	25.4	28.4	270.5
Digitized coverage (% of delineated)	4	29	79	100	100	100	29
Below Dam Area (428.3 km^2)							
Delineated stream length (km)	346.6	158.7	85.5	40.2	22.1	28.4	681.5
Delineated distribution (% by order)	51	23	13	6	3	4	100
Digitized stream length (km)	11.4	43.0	66.5	40.2	22.1	28.4	211.6
Digitized coverage (% of delineated)	3	27	78	100	100	100	31

Table 12. Total length of stream network by stream order assessed in Mill Creek.

Mill Creek	Stream Order					
	1	2	3	4	5	Total
Total Watershed Area (132.6 km^2)						
Delineated stream length (km)	138.5	70.1	30.9	23.5	5.4	268.4
Delineated distribution (% by order)	52	26	12	9	2	100
Digitized stream length (km)	0	3.8	22.5	23.5	5.4	55.2
Digitized coverage (% of delineated)	0	5	73	100	100	21
Below Dam Area (96.5 km^2)						
Delineated stream length (km)	104.1	45.9	24.6	23.5	5.4	203.4
Delineated distribution (% by order)	51	23	12	12	3	100
Digitized stream length (km)	0	2.4	18.3	23.5	5.4	49.6
Digitized coverage (% of delineated)	0	5	75	100	99	24

Table 13. Comparison of antecedent flood Conditions five years prior to aerial photograph dates.

WY	Big River at Richwoods (#7018100) $Q_{2.33}$ = 625.3 m3/s (70-year record)			Meramec River near Sullivan (#7014500) $Q_{2.33}$ = 718.1 m3/s (70-year record)		
	Date	Qpk (m^3/s)	$Qpk/Q_{2.33}$	Date	Qpk (m^3/s)	$Qpk/Q_{2.33}$
Aerial photography collected during March-April 1995						
1990	May 26, 1990	863	1.38	May 04, 1990	557.5	0.78
1991	Dec. 30, 1990	515	0.82	Dec. 30, 1990	653.7	0.91
1992	Apr. 20, 1992	388	0.62	Apr. 21, 1992	778.3	1.08
1993	Sep. 23, 1993	1692	2.71	Sep. 26, 1993	967.9	1.35
1994	Apr. 11, 1994	1429	2.29	Apr. 12, 1994	1596.1	2.22
Mean		977	1.56		911	1.27
Aerial photography collected during March-April 2015						
2010	Oct. 30, 2009	889	1.42	Oct. 31, 2009	852	1.19
2011	Apr. 28, 2011	753	1.20	Apr. 28, 2011	722	1.00
2012	Mar. 17, 2012	149	0.24	Mar. 16, 2012	447	0.62
2013	Apr. 19, 2013	914	1.46	Mar. 18, 2013	801	1.12
2014	Apr. 03, 2014	201	0.32	Apr. 03, 2014	196	0.27
Mean=		581	0.93		603	0.84

Table 14. Active channel width reach assessment.

Reach	Stream	Order	2015 Area (m^2)	2015 Length (m)	2015 Width (m)	1995 Area (m^2)	1995 Length (m)	1995 Width (m)	Difference (m)	Difference %
1	MF	6	16,544	499	33	17,463	499	35	-1.8	-5.3
2	MF	6	33,272	482	69	30,540	482	63	5.7	8.9
3	MC	5	10,193	489	21	10,766	489	22	-1.2	-5.3
4	MC	5	19,497	490	40	17,716	490	36	3.6	10.1
5	FR	5	22,744	496	46	14,062	496	28	17.5	61.7
6	MBC	5	17,572	487	36	22,967	487	47	-11.1	-23.5
7	SB	4	11,107	487	23	5,297	487	11	11.9	109.7
8	MC	4	14,461	496	29	17,072	496	34	-5.3	-15.3
9	OMC	4	5,553	500	11	6,636	500	13	-2.2	-16.3
10	MBC	4	8,785	500	18	8,797	500	18	0.0	-0.1
11	FFB	3	5,472	494	11	4,886	494	10	1.2	12.0
12	PC	3	4,944	473	10	3,447	473	7	3.2	43.4
13	NFFR	3	3,170	494	6	6,085	494	12	-5.9	-47.9
14	CC	3	2,684	508	5	2,977	508	6	-0.6	-9.9
	Mean		12, 571	492	26	12,051	492	25	1	9

Table 15. Height distribution per HUC-12 by stream order for bank erosion.

	Avg. Bank Erosion Height			
	3	4	5	6
MC#	1.96	2.45	2.59	N/A
Cv%*	37.3	24.0	25.6	
n	10	11	5	
MF	2.04	N/A	N/A	2.85
Cv%	51.8			27.3
n	5			13
CCMF	1.58	1.85	N/A	2.66
Cv%	23.4	9.6		39.6
n	12	3		14
OMC	1.13	2.14	N/A	N/A
Cv%		26.8		
n	1	7		
MBC	1.80	1.96	2.02	N/A
Cv%	23.7	40.6	24.0	
n	10	10	5	
FR	1.63	1.85	2.04	N/A
Cv%	41.3	22.3	28.2	
n	10	4	13	
SLFR	1.62	1.61	1.90	N/A
Cv%	40.1	29.6		
n	10	7	1	
All	1.68	1.90	2.03	2.75
Cv%	35.5	31.7	25.8	33.4
n	58	42	24	27

12-Digit HUC subwatershed descriptions in Table 4

* Coefficent of Variation (%) = 100 x (Standard Deviation ÷ Mean)

Table 16. Height distribution per HUC-12 by stream order for bank deposition.

	Avg. Bank Deposition Height			
	3	4	5	6
MC[#]	1.27	1.63	1.66	N/A
Cv%[*]	27.9	32.1	29.3	
n	10	11	5	
MF	1.23	N/A	N/A	2.06
Cv%	61.5			29.5
n	5			13
CCMF	1.08	1.24	N/A	2.05
Cv%	34.9	4.2		36.8
n	12	3		14
OMC	0.88	1.18	N/A	N/A
Cv%		32.1		
n	1	7		
MBC	1.16	1.31	1.55	N/A
Cv%	38.8	40.5	17.4	
n	10	10	5	
FR	0.99	1.17	1.31	N/A
Cv%	37.6	42.5	34.0	
n	10	4	13	
SLFR	1.03	1.22	1.39	N/A
Cv%	30.1	33.0		
n	10	7	1	
All	1.08	1.24	1.38	2.06
Cv%	38.6	34.0	29.1	32.8
n	58	42	24	27

[#] 12-Digit HUC subwatershed descriptions in Table 4

[*] Coefficent of Variation (%) = 100 x (Standard Deviation ÷ Mean)

Table 17. Height distribution per HUC-12 by stream order for bar erosion.

	Avg. Bar Erosion Height			
	3	4	5	6
MC[#]	1.29	1.62	1.80	N/A
Cv%[*]	30.4	39.8	34.9	
n	10	14	5	
MF	1.42	N/A	N/A	1.73
Cv%	54.2			41.4
n	3			14
CCMF	1.41	1.62	N/A	1.74
Cv%	46.8	5.5		31.5
n	13	4		12
OMC	N/A	1.66	N/A	N/A
Cv%		21.4		
n		6		
MBC	1.32	1.31	2.07	N/A
Cv%	26.3	44.7	22.0	
n	11	12	6	
FR	0.95	1.25	1.26	N/A
Cv%	26.3	35.0	40.0	
n	13	5	13	
SLFR	1.27	1.44	1.16	N/A
Cv%	24.1	13.5	28.2	
n	7	7	2	
All	1.24	1.43	1.48	1.73
Cv%	38.7	30.5	40.3	36.4
n	57	48	26	26

[#] 12-Digit HUC subwatershed descriptions in Table 4

[*] Coefficent of Variation (%) = 100 x (Standard Deviation ÷ Mean)

Table 18. Height distribution per HUC-12 by stream order for bar deposition.

	Avg. Bar Deposition Height			
	3	4	5	6
MC#	1.43	1.48	1.69	N/A
Cv%*	37.2	36.5	45.5	
n	10	14	5	
MF	1.42	N/A	N/A	1.82
Cv%	54.2			36.6
n	3			14
CCMF	1.31	1.38	N/A	1.73
Cv%	57.5	14.9		32.3
n	13	4		12
OMC	N/A	1.32	N/A	N/A
Cv%		40.3		
n		6		
MBC	0.97	1.22	1.83	N/A
Cv%	40.9	46.8	34.7	
n	11	12	6	
FR	0.95	1.05	1.37	N/A
Cv%	26.3	28.7	37.1	
n	13	5	13	
SLFR	1.09	1.25	0.87	N/A
Cv%	22.6	29.1	4.0	
n	7	7	2	
All	1.11	1.24	1.46	1.78
Cv%	46.3	36.1	39.3	34.2
n	57	48	26	26

12-Digit HUC subwatershed descriptions in Table 4

* Coefficent of Variation (%) = 100 x (Standard Deviation ÷ Mean)

Table 19. Average cell mass for bank erosion.

	Mass by stream order (Mg/yr)			
HUC	3	4	5	6
MC	53	122	107	N/A
n	32	43	10	
MF	55	N/A	N/A	821
n	14			26
CCMF	40	91	N/A	357
n	28	43		29
OMC	34	47	N/A	N/A
n	1	21		
MBC	30	96	236	N/A
n	27	30	11	
FR	31	51	97	N/A
n	22	43	10	
SLFR	24	58	10	N/A
n	24	21	2	
All	37	87	124	576
n	179	134	53	55

Table 20. Average cell mass for bank deposition.

	Mass by stream order (Mg/yr)			
HUC	3	4	5	6
MC	-14	-32	-52	N/A
n	28	36	10	
MF	-30	N/A	N/A	-328
n	13			26
CCMF	-21	-83	N/A	-198
n	34	9		28
OMC	-12	-52	N/A	N/A
n	1	21		
MBC	-40	-60	-151	N/A
n	29	31	10	
FR	-19	-28	-80	N/A
n	41	10	28	
SLFR	-11	-83	-117	N/A
n	19	23	1	
All	-22	-54	-90	-261
n	165	130	49	54

Table 21. In-Channel sediment budget.

12-Digit HUC Watersheds	Below Dam Ad (km^2)	Bank Erosion (Mg/yr)	Bank Deposition (Mg/yr)	E/D Ratio*	Bar Erosion (Mg/yr)	Bar Deposition (Mg/yr)	E/D Ratio*	In-Channel Load (Net) (Mg/yr)	Sediment Yield ($Mg/km^2/yr$)
Mill Creek	96.2	8,334	2,144	3.9	5,546	9,985	0.6	1,751	18.2
Mineral Fork	42.3	22,219	8,993	2.5	11,985	15,661	0.8	9,550	225.6
Clear Creek-Mineral Fork	75.6	12,573	7,011	1.8	14,054	12,985	1.1	6,630	87.8
Old Mines Creek	39.4	1,197	1,167	1.0	1,875	651	2.9	1,254	31.8
Mine a Breton Creek	105.4	6,604	4,971	1.3	10,833	9,553	1.1	2,913	27.6
Fourche a Renault	96.8	4,845	3,319	1.5	6,520	8,155	0.8	-110	-1.1
Sunnen Lake-Fourche a Renault	68.8	944	1,132	0.8	3,511	1,813	1.9	1,510	21.9
Mineral Fork (Whole)	428.6	48,382	26,593	1.8	48,777	48,818	1.0	21,748	50.7

*Ratio between Erosion and Deposition rates for banks and bars, respectively

Table 22. Average cell mass for bar erosion.

	Mass by stream order (Mg/yr)			
	3	4	5	6
MC	11	102	111	N/A
n	27	40	10	
MF	48	N/A	N/A	440
n	9			26
CCMF	33	207	N/A	401
n	23	8		29
OMC	N/A	88	N/A	N/A
n		19		
MBC	66	103	473	N/A
n	25	32	11	
FR	35	64	148	N/A
n	39	11	30	
SLFR	82	206	192	N/A
n	23	21	3	
All	44	120	210	420
n	146	131	54	55

Table 23. Average cell mass for bar deposition.

HUC	Mass by stream order (Mg/yr) 3	4	5	6
MC	-30	-180	-219	N/A
n	27	40	9	
MF	-26	N/A	N/A	-593
n	9			26
CCMF	-17	-123	N/A	-391
n	23	8		29
OMC	N/A	-34	N/A	N/A
n		19		
MBC	-26	-103	-487	N/A
n	25	32	11	
FR	-26	-47	-219	N/A
n	39	11	30	
SLFR	-30	-125	-68	N/A
n	23	21	3	
All	-25	-118	-266	-486
n	156	128	53	55

Table 24. Average cell mass for net in-channel supply.

	Mass by stream order (Mg/yr)			
HUC	3	4	5	6
MC	22	28	-32	N/A
n	33	43	10	
MF	71	N/A	N/A	1,526
n	14			26
CCMF	57	315	N/A	957
n	35	9		29
OMC	22	96	N/A	N/A
n	1	22		
MBC	69	237	1,058	N/A
n	184	32	11	
FR	65	132	389	N/A
n	47	11	30	
SLFR	119	299	227	N/A
n	25	21	3	
All	64	156	439	1,226
n	183	138	54	55

Table 25. Sediment load with above dam contributions.

12-Digit HUC Watersheds	Ad (km^2)	Upland Erosion	Floodplain Storage (Mg/yr)	Other Storage	Upland Load	Sediment Yield ($Mg/km^2/yr$)
Mill Creek	132.6	115,157	-25,000	-77,603	12,554	94.7
Mineral Fork	51.5	21,230	-17,879	-2,276	5,627	109.3
Clear Creek-Mineral Fork	98.8	30,672	-27,464	-856	4,064	41.1
Old Mines Creek	48.1	27,521	-7,939	-15,168	4,413	91.8
Mine a Breton Creek	123.6	116,466	-24,482	-77,457	14,528	117.5
Fourche a Renault	100.7	71,619	-31,777	-30,516	9,326	92.6
Sunnen Lake-Fourche a Renault	68.8	14,503	-17,331	-4,988	2,160	31.4
Mineral Fork (Whole)	490.5	292,522	-122,682	-145,708	24,132	49.2

Table 26. Sediment load below dams.

12-Digit HUC Watersheds	Ad (km^2)	Upland Erosion	Floodplain Storage (Mg/yr)	Other Storage	Upland Load	Sediment Yield ($Mg/km^2/yr$)	% Dam Sediment Reduction
Mill Creek	96.2	57,525	-23,269	-26,516	7,741	58.4	38.3
Mineral Fork	42.3	25,492	-16,027	-5,340	4,125	80.1	26.7
Clear Creek-Mineral Fork	75.6	24,509	-19,803	-962	3,467	35.1	14.7
Old Mines Creek	39.4	23,843	-6,948	-12,878	4,018	83.5	9.0
Mine a Breton Creek	105.4	110,394	-23,417	-72,646	14,331	115.9	1.4
Fourche a Renault	96.8	70,904	-31,340	-30,237	9,328	92.7	0.0
Sunnen Lake-Fourche a Renault	68.8	7,251	-4,232	-2,384	635	9.2	70.6
Mineral Fork (Whole)	428.6	198,538	-108,263	-72,490	17,785	36.3	26.3

Table 27. Sediment load budget for below dams.

12-Digit HUC Watersheds	Ad (km^2)	Upland Erosion	Upland Load	Floodplain Storage	Other Storage (Mg/yr)	Net Bank Erosion	Net Bar Erosion	Total Load	Sediment Yield ($Mg/km^2/yr$)
Mill Creek	96.2	57,525	7,741	-23,269	-26,516	6,190	-4,439	9,492	98.6
Mineral Fork	42.3	25,492	4,125	-16,027	-5,340	13,227	-3,676	13,675	323.0
Clear Creek-Mineral Fork	75.6	24,509	3,467	-19,803	-962	5,561	1,069	10,098	133.7
Old Mines Creek	39.4	23,843	4,018	-6,948	-12,878	30	1,224	5,272	133.7
Mine a Breton Creek	105.4	110,394	14,331	-23,417	-72,646	1,633	1,280	17,244	163.6
Fourche a Renault	96.8	70,904	9,328	-31,340	-30,237	1,525	-1,635	9,218	95.2
Sunnen Lake-Fourche a Renault	68.8	7,251	635	-4,232	-2,384	-188	1,698	2,146	31.2
Mineral Fork (Whole)	428.6	198,538	17,785	-108,263	-72,490	21,789	-41	39,533	92.2

Table 28. Suspended sediment loads below dams from upland erosion by land use.

Watershed	Ad (km^2)	TSS (Mg/yr) Urban	Cropland	Pastureland	Forest	Mined	Total
Mineral Fork	490.5	916	1,872	4,856	4,705	5,436	17,785
% of Load		5	11	27	26	31	100
% of total Area		6	0.3	10	82	3	100
Mill Creek	132.6	304	191	1,045	1,687	4,513	7,741
% of Load		4	2	14	22	58	100
% of total Area		7	0.2	7	78	8	100

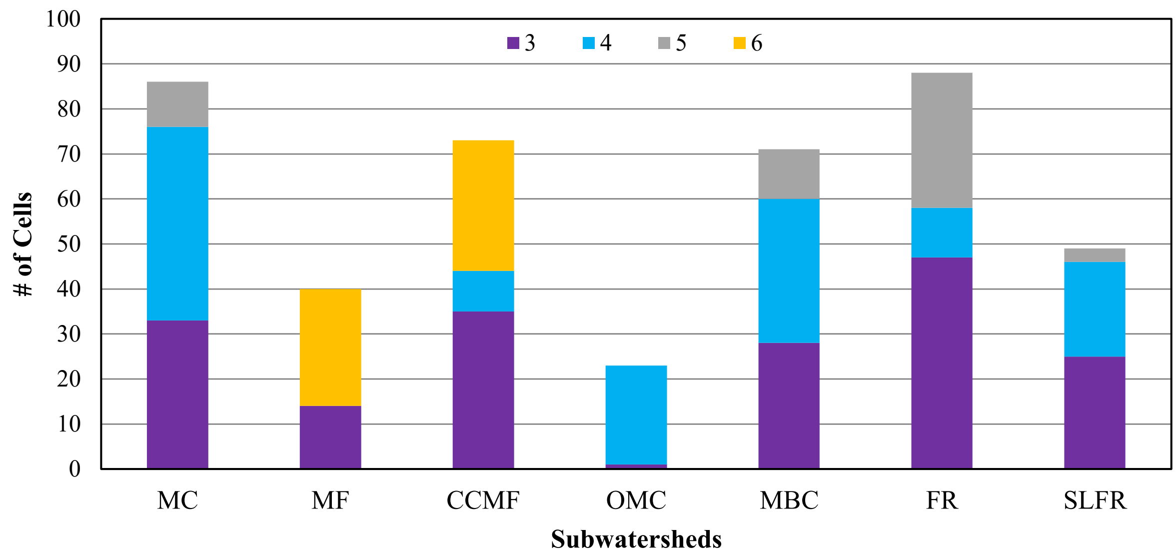

Figure 15. Number of cells in each subwatershed by stream order below dams.

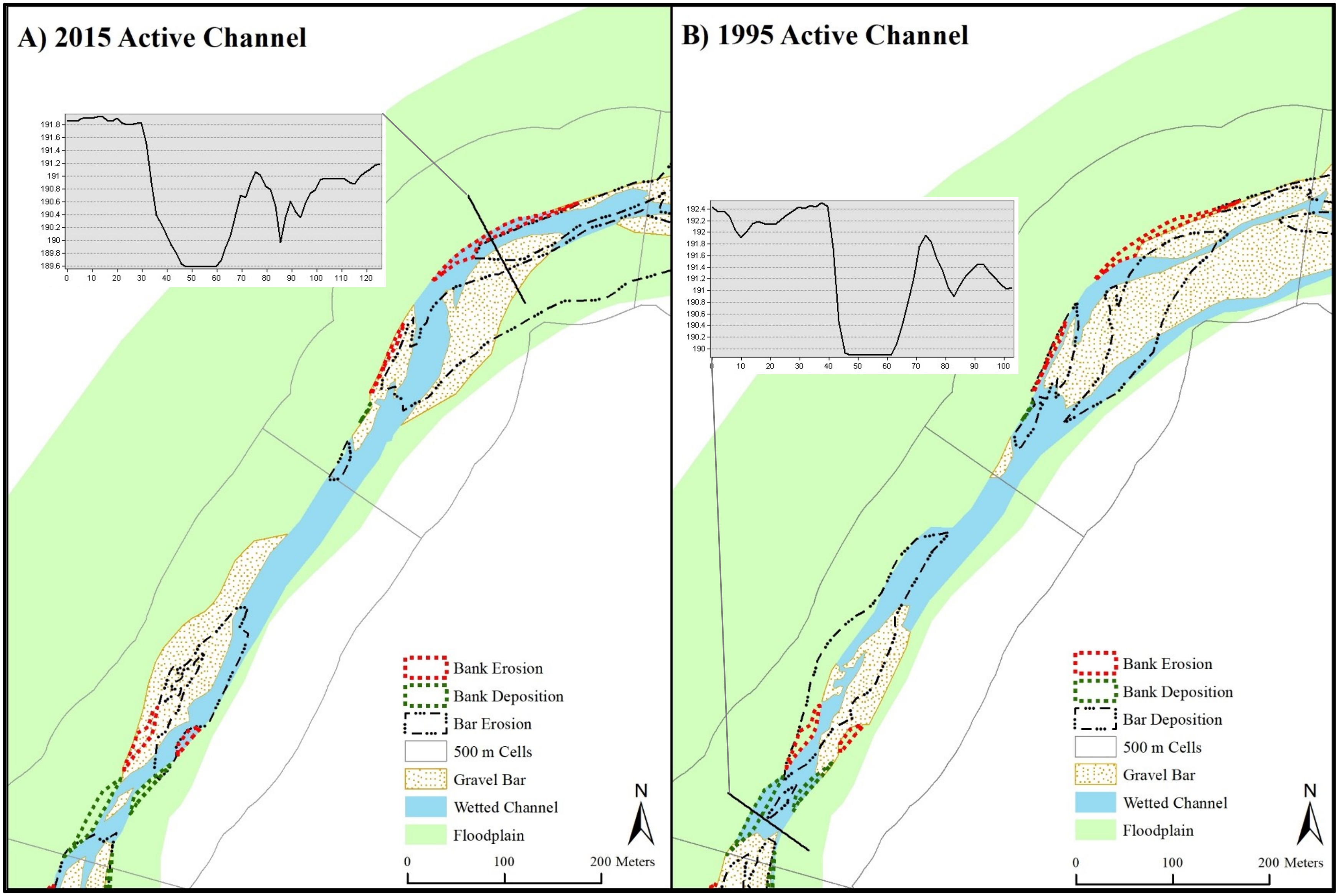

Figure 16. Planform analysis for Mineral Fork with bar and bank erosion and polygons.

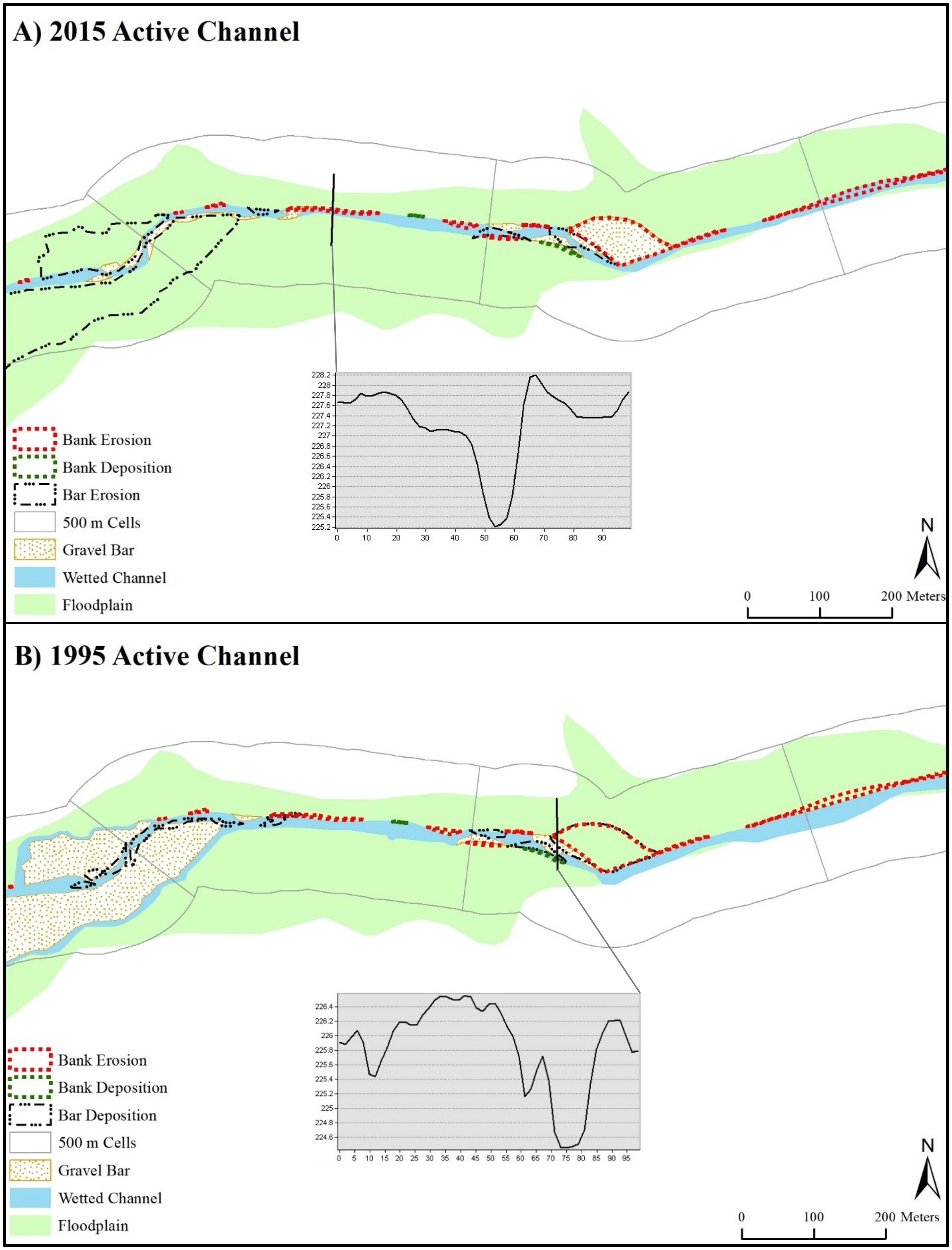

Figure 17. Planform analysis for Mill Creek with bar and bank erosion and polygons.

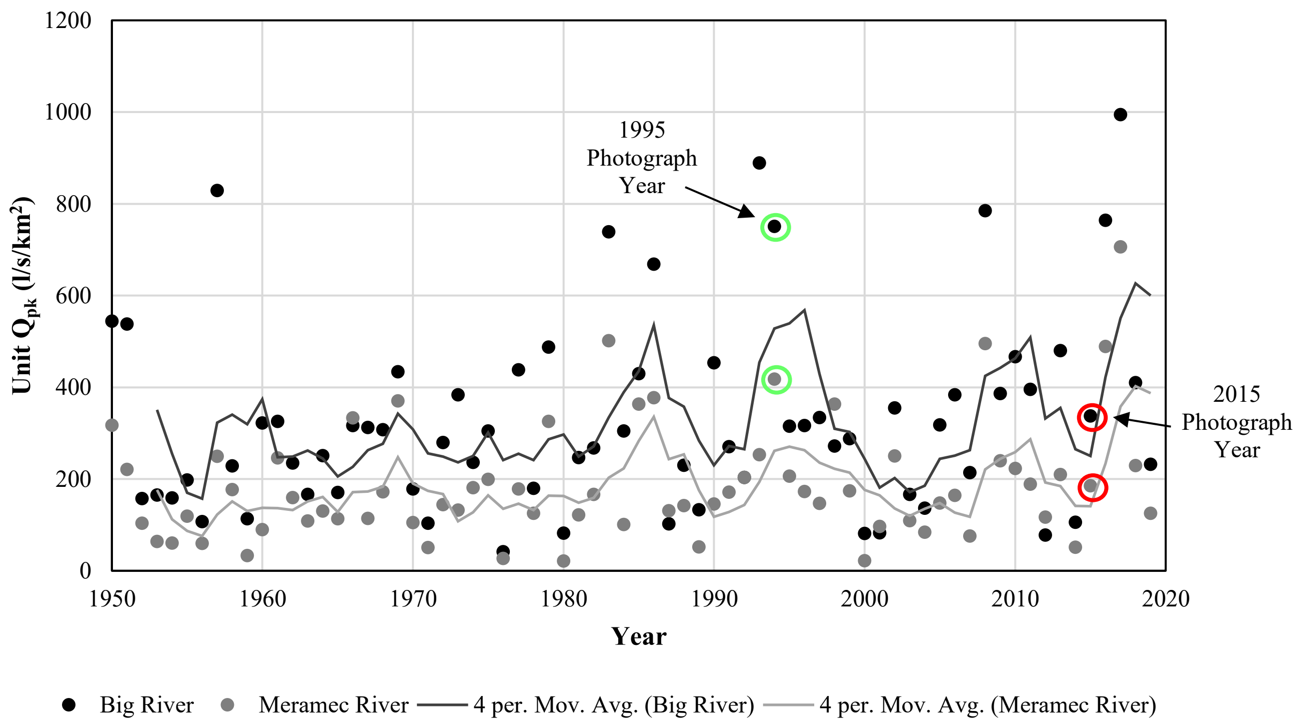

Figure 18. Annual peak flood record (1950-2019, 70 years).

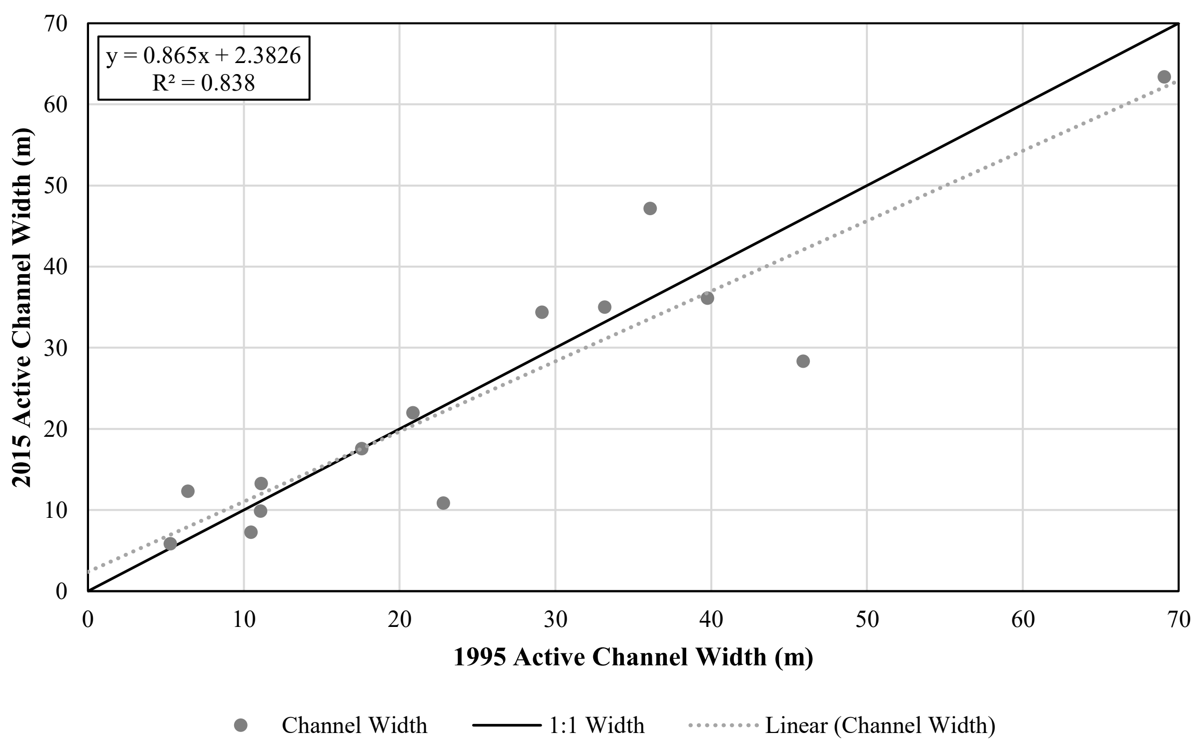

Figure 19. Active channel width reach assessment.

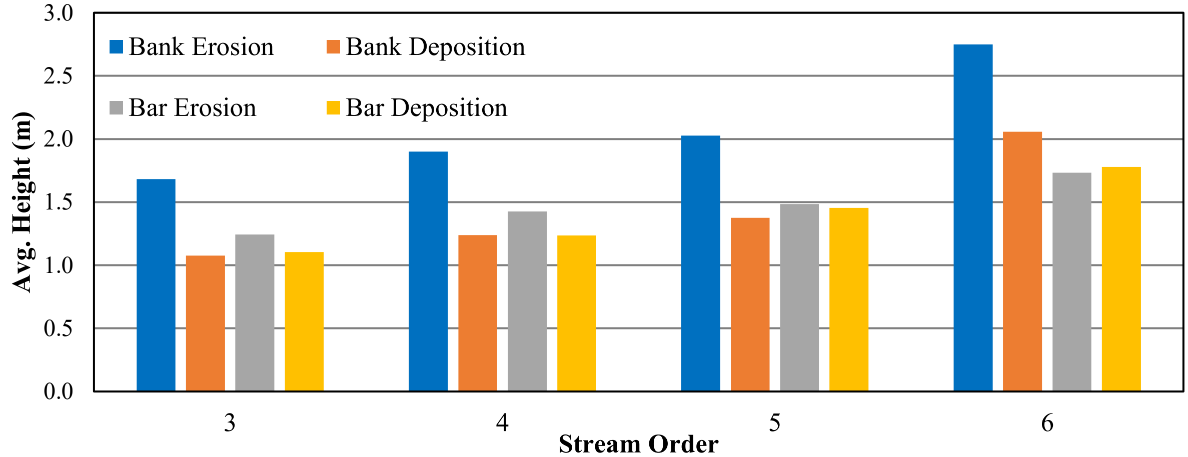

Figure 20. Average bank and bar heights.

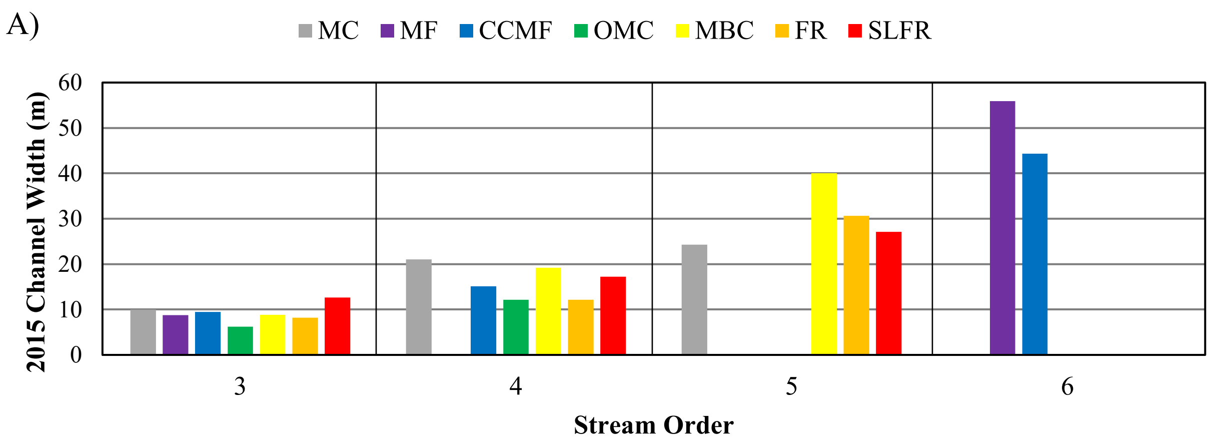

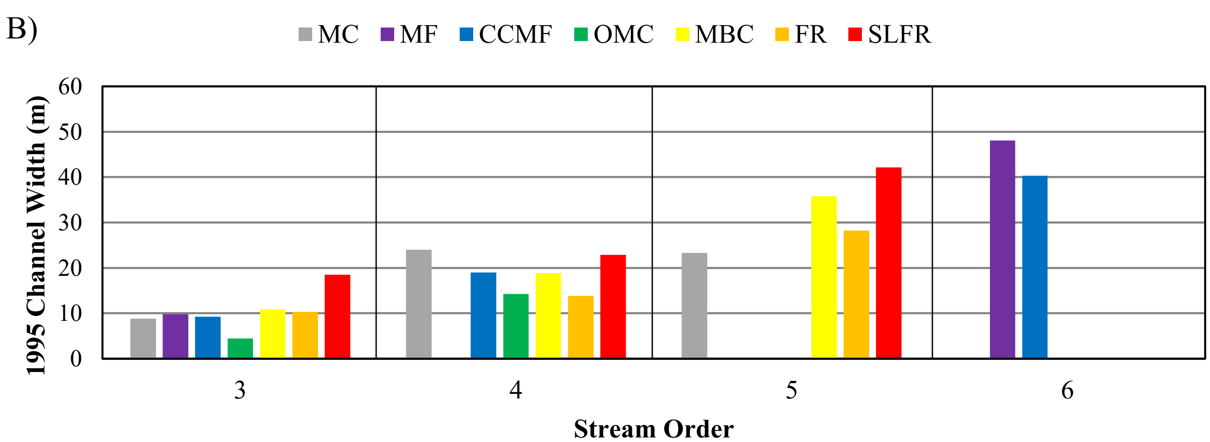

Figure 21. Average active channel width in 2015 (A) and 1995 (B).

A)

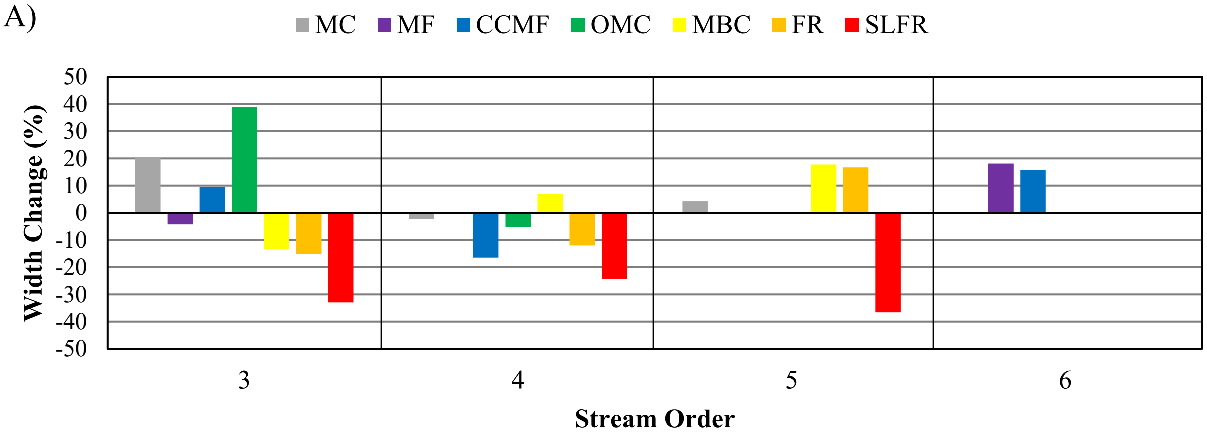

B)

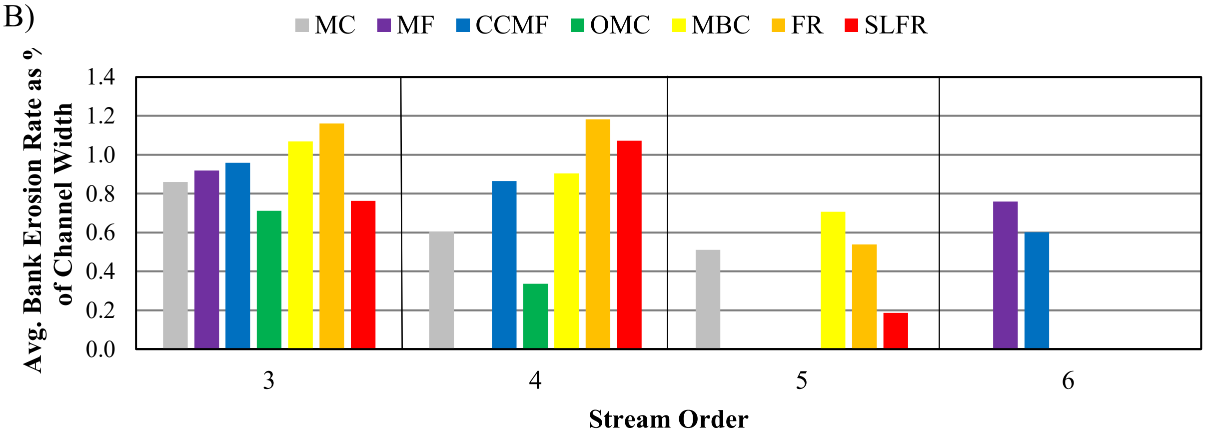

Figure 22. Active channel width change from 1995 to 2015. A) percent change in active width; and B) annual bank erosion rate as a percent of active channel width.

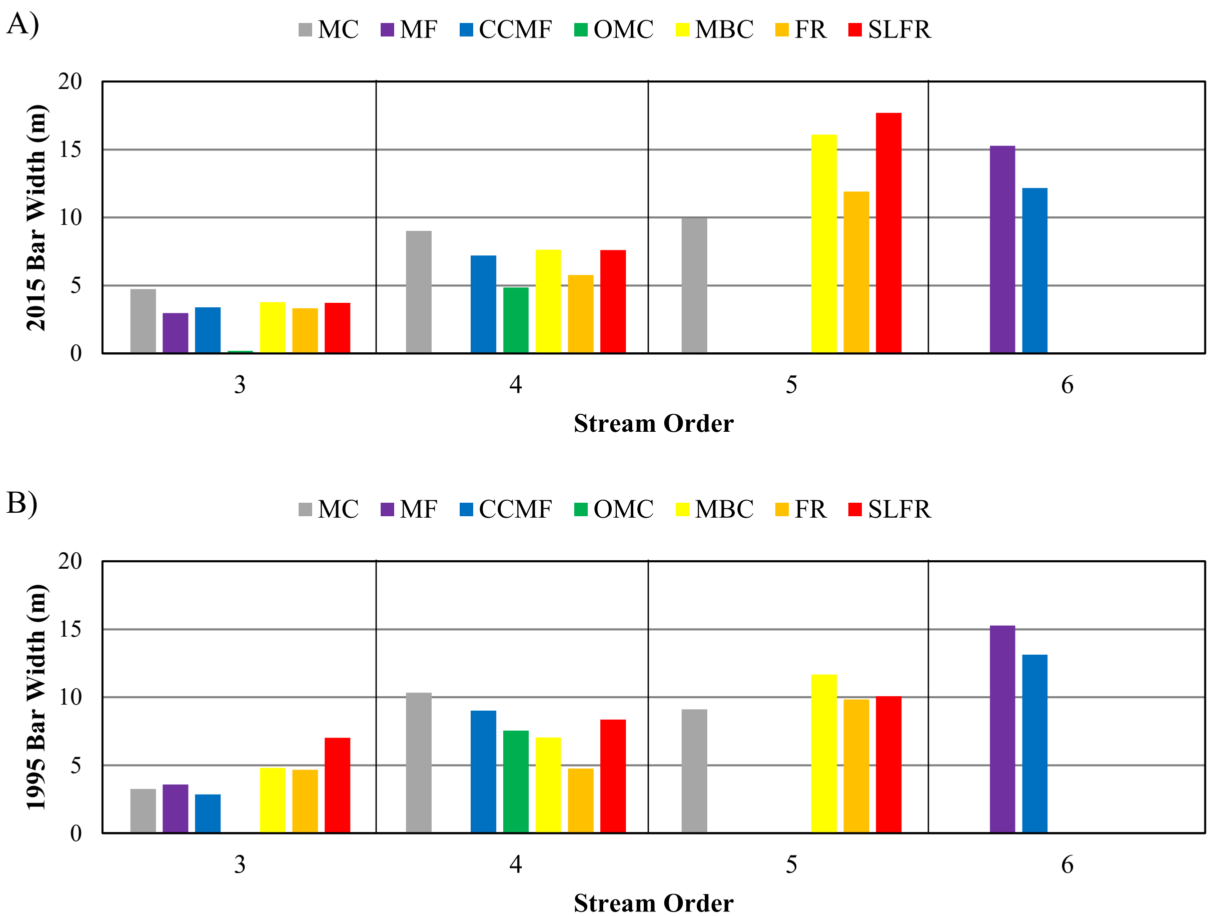

Figure 23. Average bar width in 2015 (A) and 1995 (B).

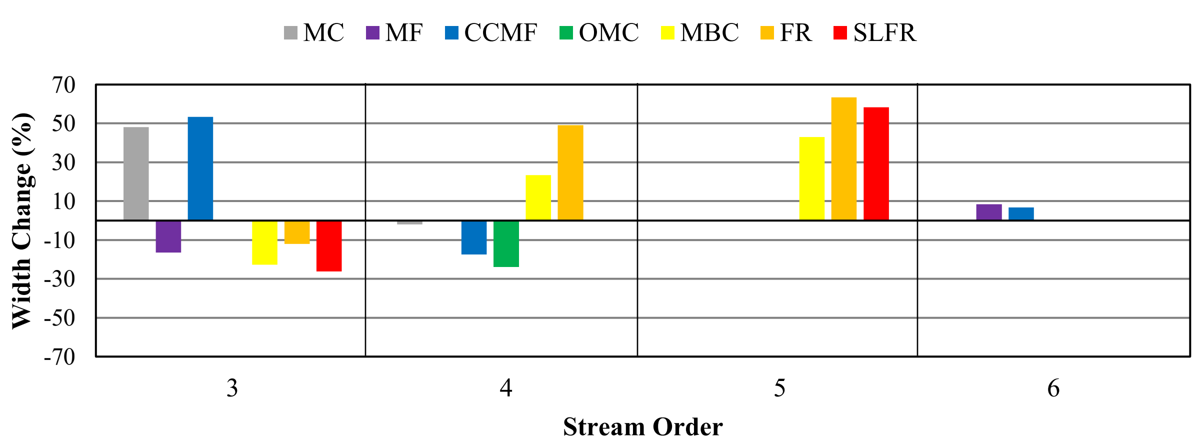

Figure 24. Percent bar width change from 1995 to 2015.

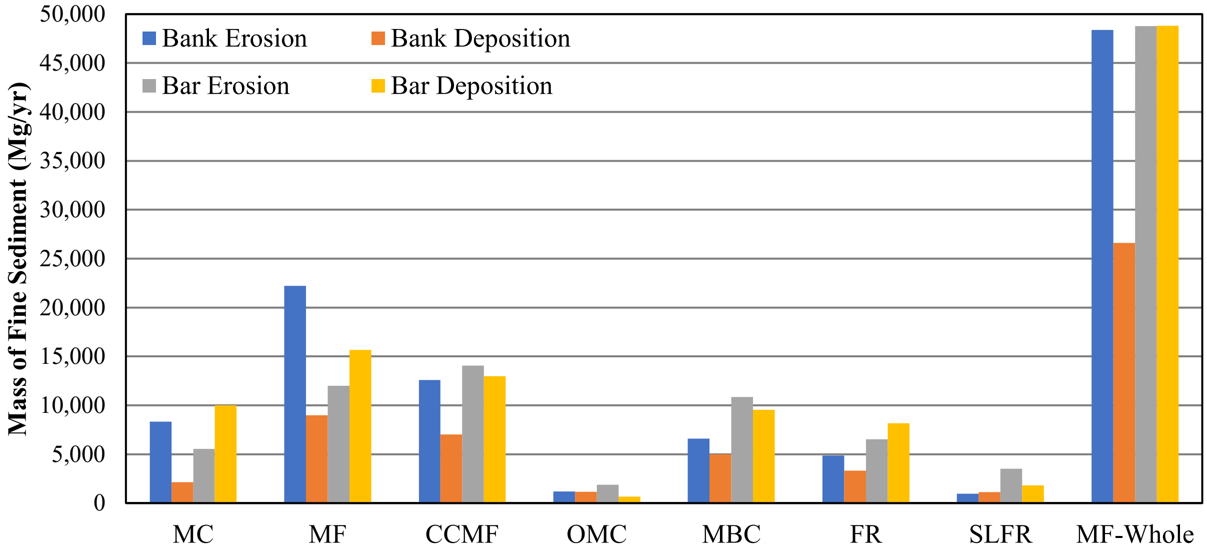

Figure 25. Mass of fine sediment from in-channel contributions.

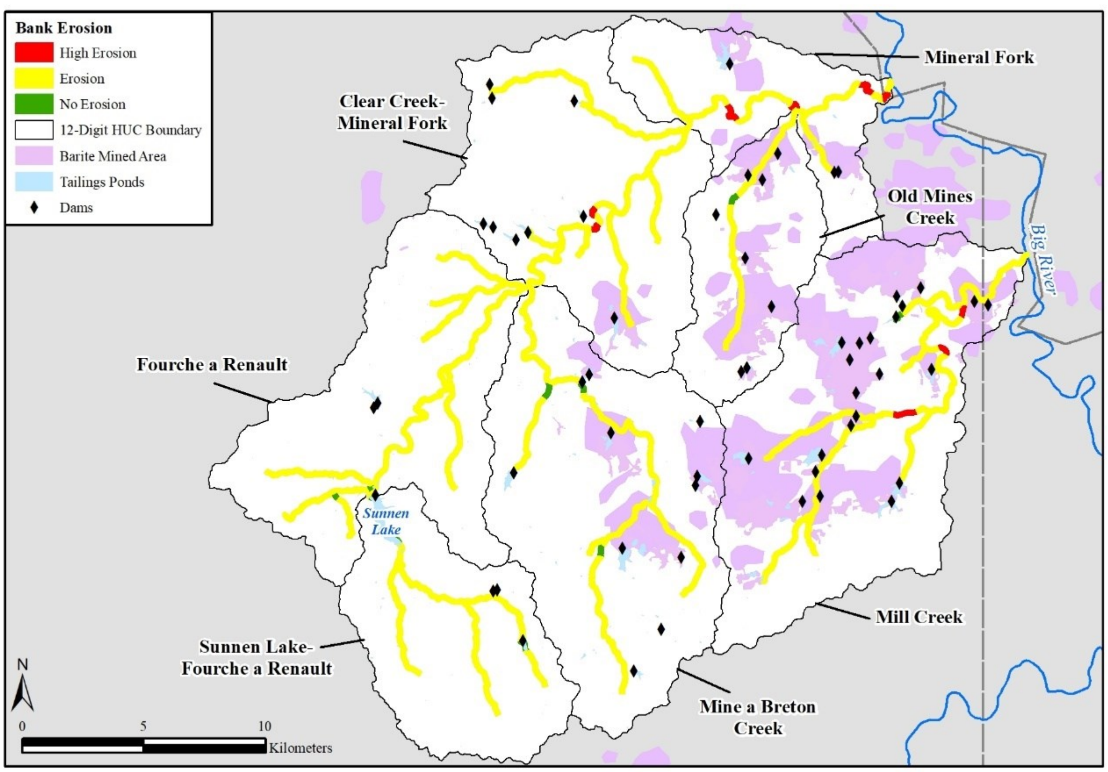

Figure 26. Cells highlighting no erosion, erosion, and high erosion cells that make up 25% of the bank erosion mass.

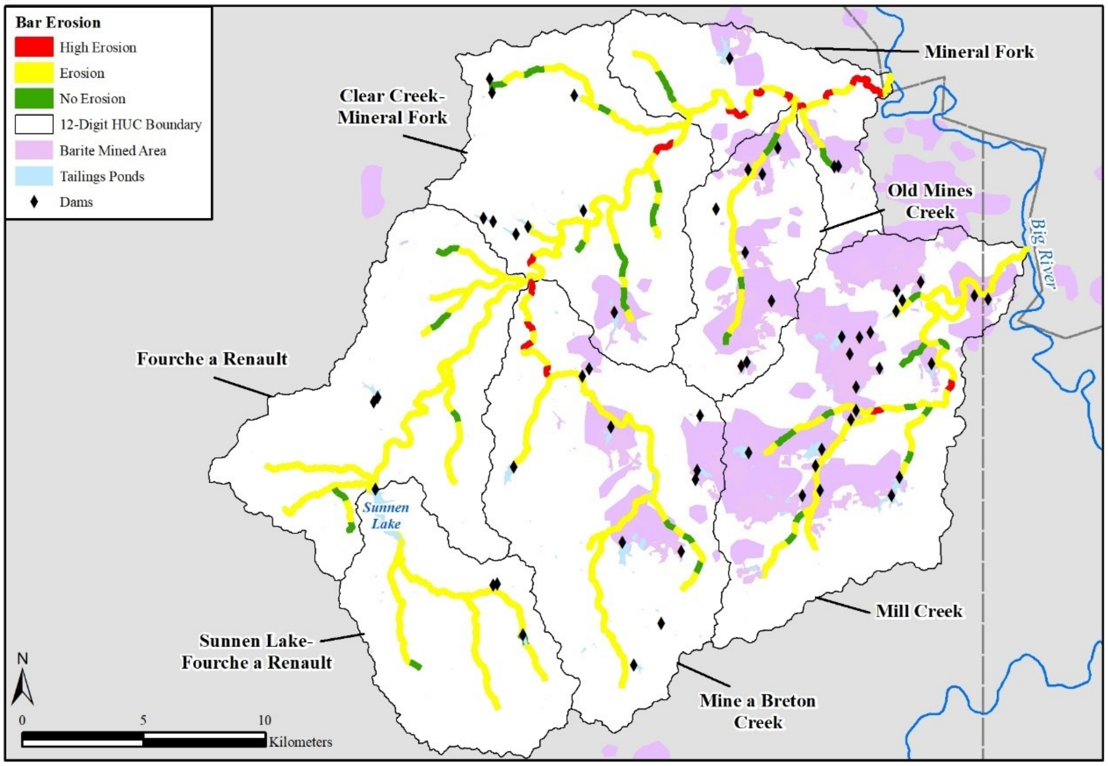

Figure 27. Cells highlighting no erosion, erosion, and high erosion cells that make up 25% of the bar erosion mass.

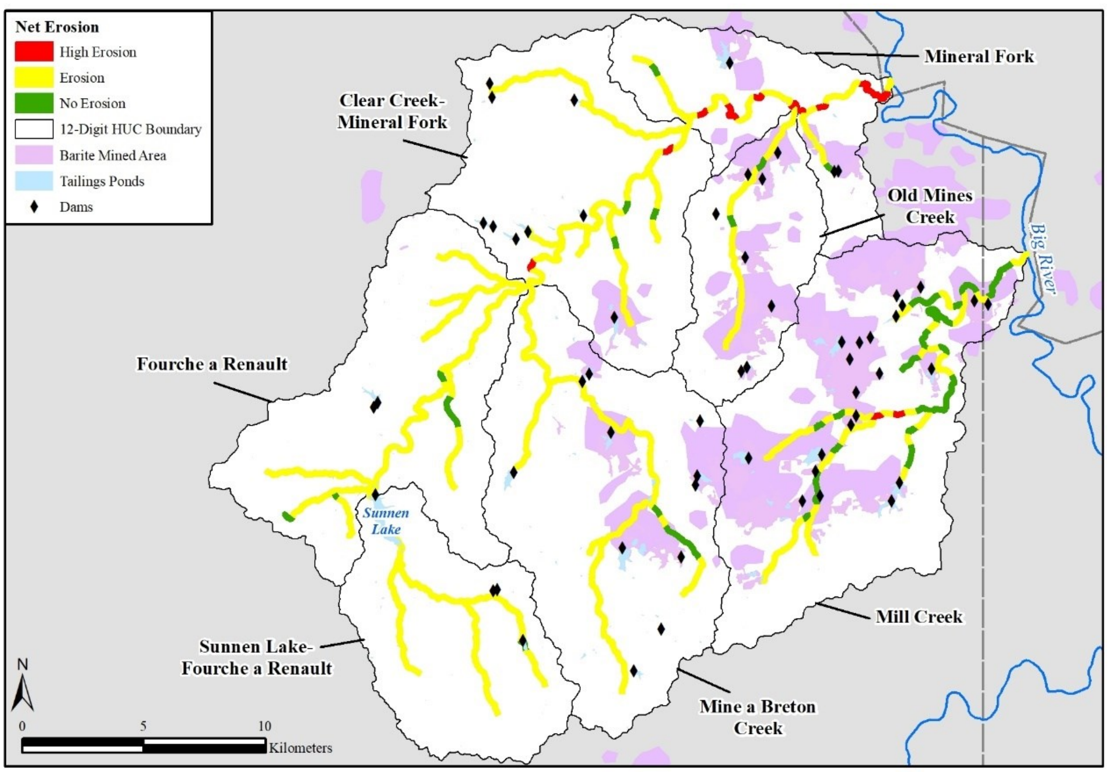

Figure 28. Cells highlighting deposition, erosion, and high erosion cells that make up 25% of the erosion mass.

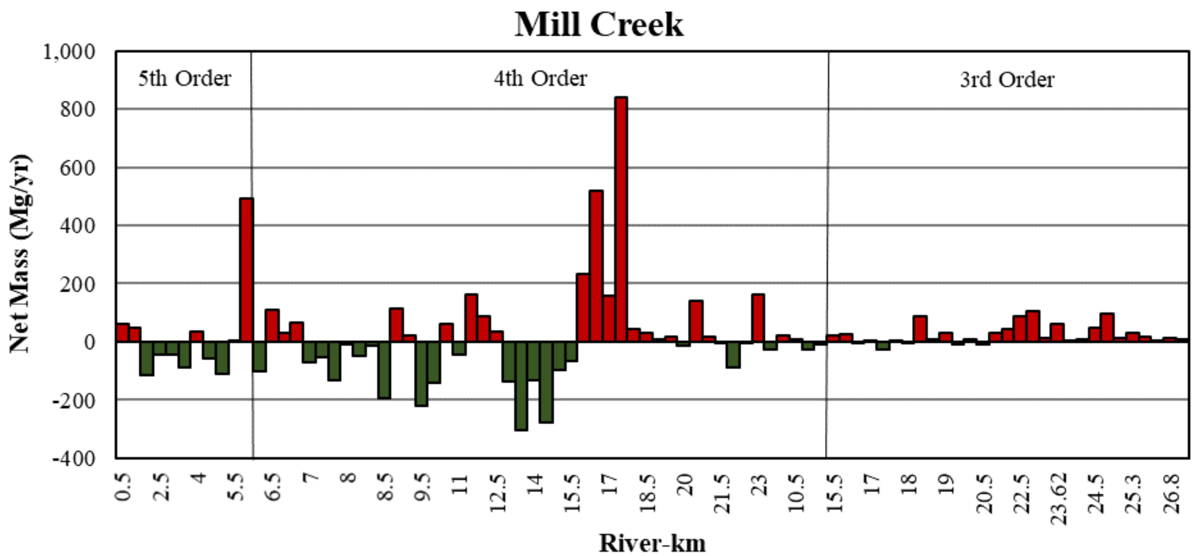

Figure 29. Alternating pattern of erosion and deposition upstream (27 km) to downstream (0 km) in the Mill Creek watershed.

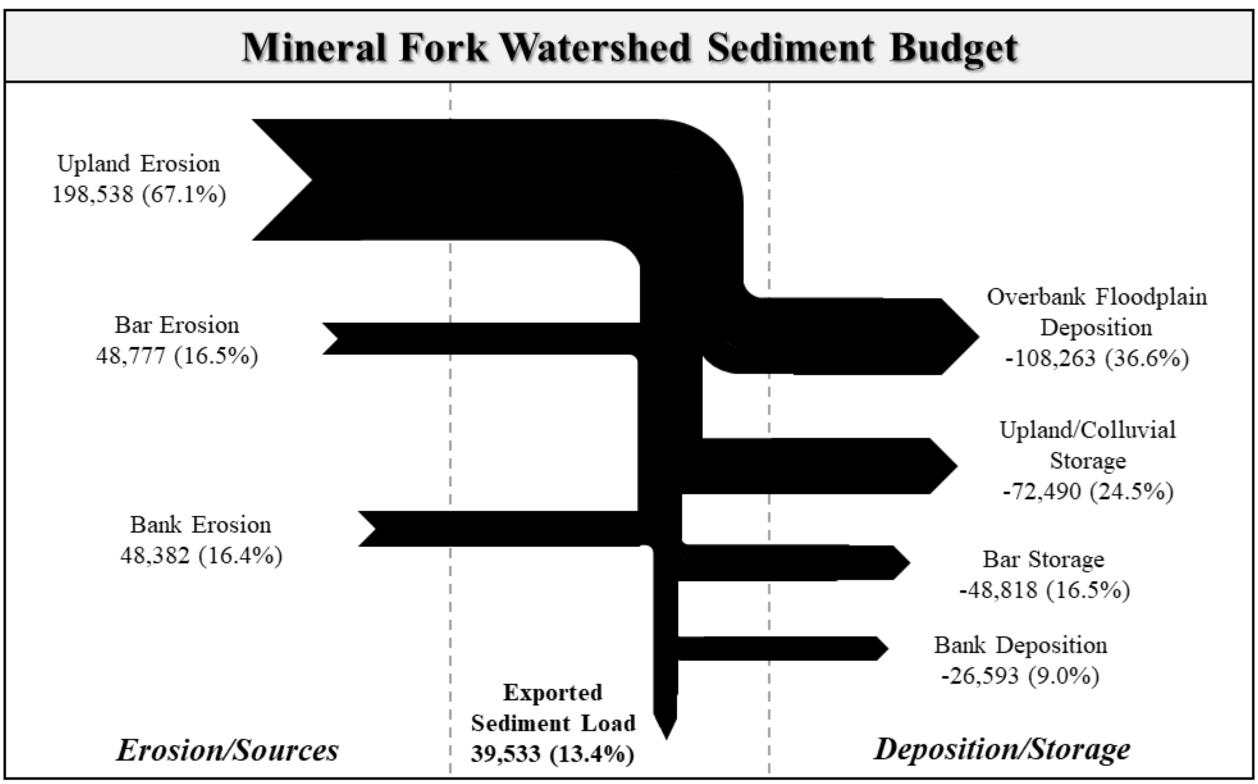

Figure 30. Mass sediment budget for Mineral Fork watershed (Mg/yr).

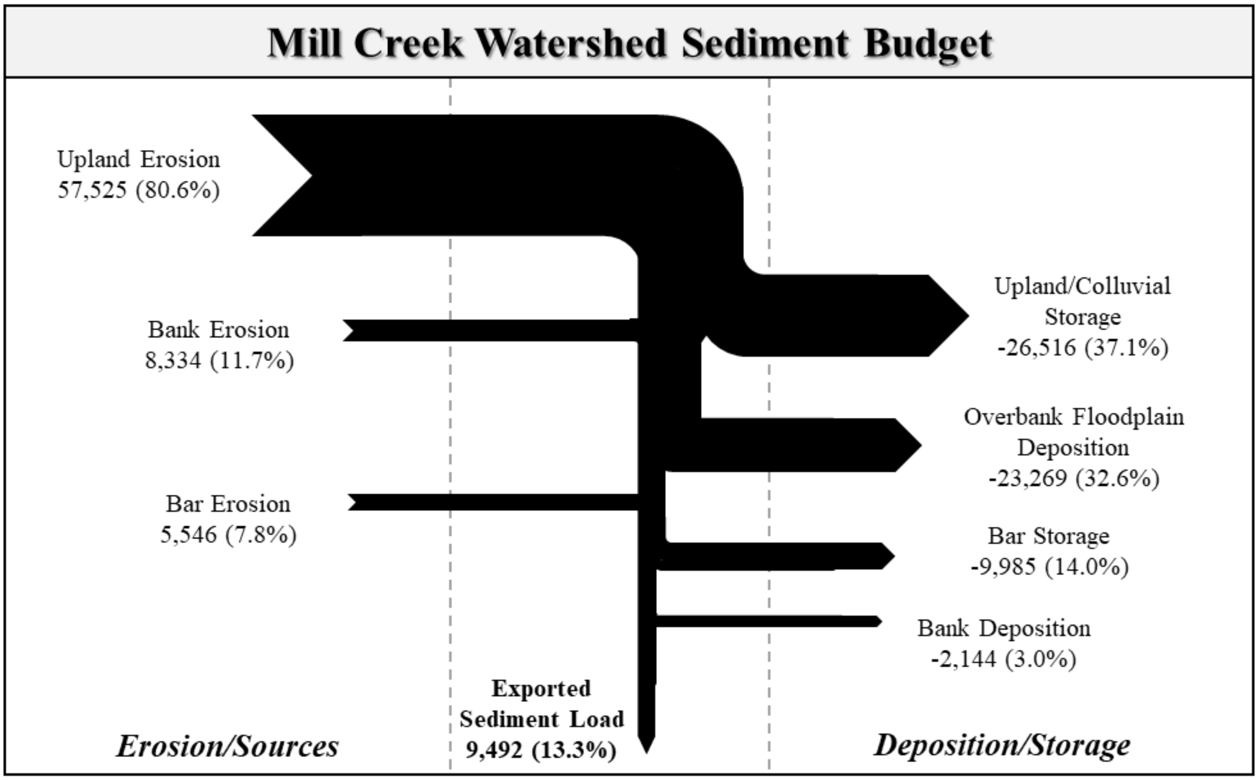

Figure 31. Mass sediment budget for Mill Creek watershed (Mg/yr).

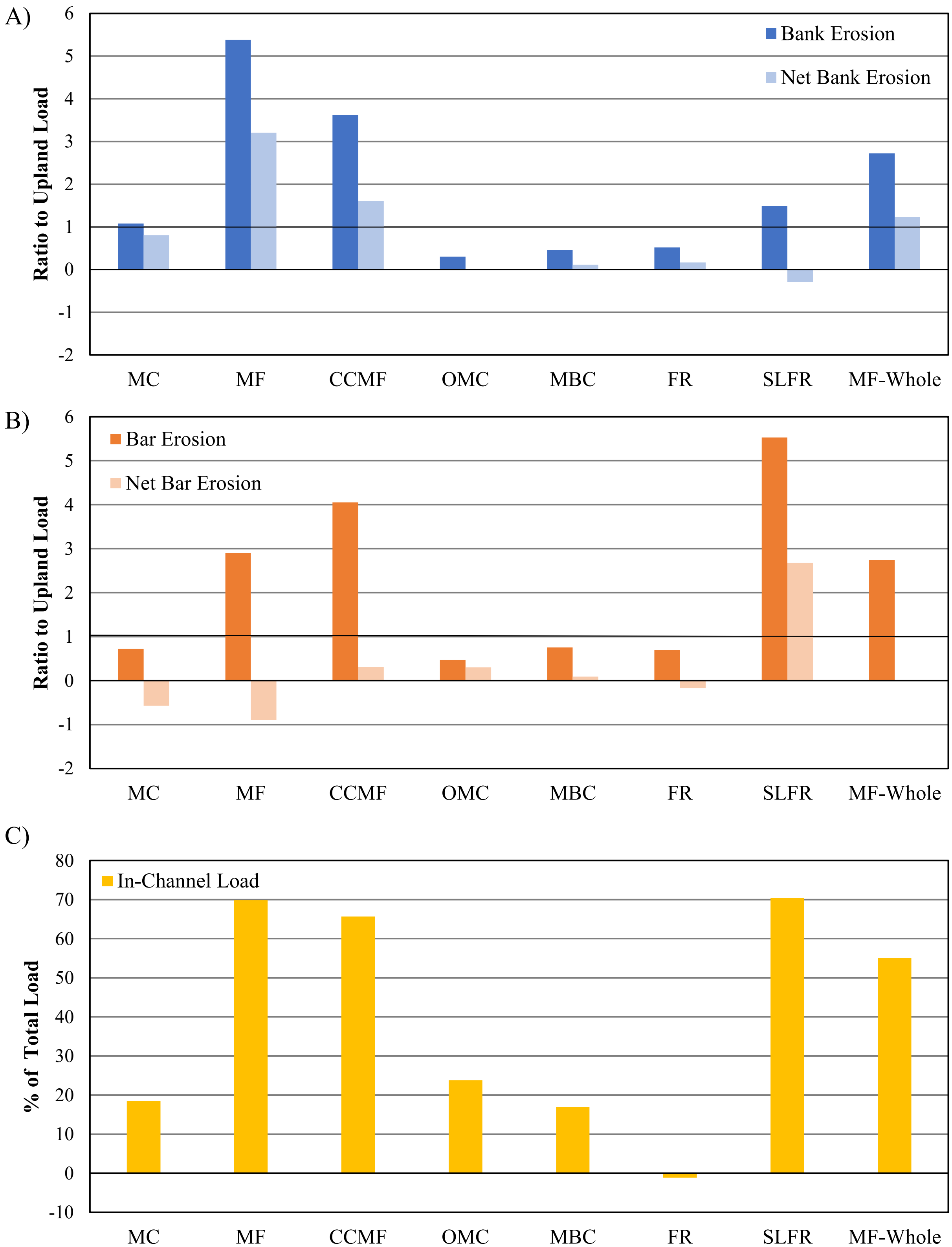

Figure 32. In-channel contributions to sediment loads. (A) Bank erosion compared to upland erosion loads; (B) Bar erosion compared to upland erosion loads; and (C) In-channel load contribution to total load.

CONCLUSIONS

The purpose of this study was to assess and evaluate the contributions of bank and bar erosion to annual sediment loads of the Mineral Fork and Mill Creek watersheds in the Ozark Highlands, Missouri. Since there were no published studies available for the Ozarks on this topic, this study filled a research gap and presented a methodology for understanding the watershed trends (i.e. by stream order and subwatersheds) in channel erosion which can be used to inform management efforts to reduce bank erosion impacts on sediment loads. Historical tailings dams were also assessed to evaluate the degree to which these legacy structures trapped upland sediment loads. Sediment budgets were created using the EPA's STEPL model to calculate suspended sediment loads and from in-channel erosion and deposition rates derived from this study. The land use and soil types were also assessed to understand their influence suspended sediment loads. Fine sediment can be deposited on the channel banks, beds, and bars and remain in storage for variable amounts of time before it is remobilized and transported downstream (Jacobson and Gran, 1999; Davis, 2009; Donovan et al., 2015; Groten et al., 2016). This is one of the first studies to directly assess the amounts and spatial distribution of bank and bar erosion and deposition at the watershed-scale in the Ozark Highlands. The findings indicated that channel processes are important controls on sediment yields in these watersheds and validates the use of historical aerial photography to assess channel morphology and sediment processes in a mining-disturbed watershed. The main conclusions of this study were:

1. Based the range of other sediment yields determined in Missouri, Mineral Fork and Mill Creek are slightly above the range of sediment yields for watersheds of similar size within the Ozark Highlands from 9 to 1,197 km^2. After establishing a sediment

budget, Mineral Fork was contributing a sediment yield of 92 $Mg/km^2/yr$ to Big River and Mill Creek was contributing a sediment yield of 99 $Mg/km^2/yr$ to Big River.

2. In-channel processes from bank and bar erosion and deposition contribute a significant amount of sediment to the overall sediment budget. Bank erosion contributes to 55% of the sediment load in Mineral Fork and 33% in Mill Creek. Additionally, the bars influenced the load by <1% in Mineral Fork and 24% in Mill Creek by reducing the overall sediment load to the outlet of the watershed. Eroding stream banks can supply <1% to 63% of the total suspended sediment load at the watershed outlet from the subwatersheds. Some subwatersheds had bar erosion supply 7% to 67% to the of the load, while other reduced the load from 13 to 24%. These results indicate that in-channel processes are important controls on sediment yields in these disturbed watersheds.
3. Remaining barite tailings ponds and dams trap significant amounts of eroded soil and stream sediment in these watersheds. These large dams retain 100% of the sediment delivered to them and almost all the flow. Contributing land areas draining to large tailings dams cover 27% of the land area in Mineral Fork and 28% in Mill Creek. A USLE-modeling approach (STEPL) suggests that about 26% of the annual sediment load is captured behind tailings dams in Mineral Fork and 38% in Mill Creek. This is equivalent to reducing sediment yields by 12.9 and 36.3 $Mg/km^2/yr$, respectively.
4. Upland soil erosion from mining disturbed lands and pastures provide the highest contributions to suspended sediment loads to the study watersheds. This study used LiDAR and aerial photography to develop an accurate delineation of lands disturbed by historical mining. Mining disturbed lands cover about 3% of Mineral Fork and

15% of Mill Creek watershed but contribute 31% and 58% of the sediment load from the uplands, respectively. Pastures cover about 10% of Mineral Fork and 6% of Mill Creek watershed but contribute 27% and 14% of the sediment load, respectively. More work is needed to further evaluate why mining areas were associated with high channel erosion and sediment load rates in this study.

Fluvial erosion of channel banks and gravel bars can provide significant contributions of fine sediment to stream loads in streams in the Ozark Highlands. This study found that in-channel erosion can provide 19-55% of the predicted annual sediment load from Mineral Fork and its subwatersheds and Mill Creek in Washington County, Missouri. Previous work has focused attention on the spatial distribution and causes of mobile gravel bar formation as an indicator of coarse sediment transport and storage in Ozark rivers. However, this study is the first to evaluate the role of bar erosion and deposition in the storage and supply of fine sediment in the channel. While bank erosion was a net source of fine sediment to the channel during the 1995 to 2015 study period, bar deposition involved relatively large masses of fine sediment indicating the potential to be an important net sink or source in the channel system if environmental conditions change. It is not clear about the long-term influence of bar storage on sediment loads in these watersheds.

Land use may also have played a role in controlling in-channel sources of fine sediment. Tailings ponds and dams left behind by historical barite mining activities presently trap about a third of the stream sediment loads in these watersheds. Further, mining disturbed lands tend to be associated with relatively high upland erosion rates and channel instability. This study provided evidence that in-channel fine sediment may play an important role in regulating suspended sediment loads, thus potentially linking geomorphic processes to NPS water quality conditions.

However, more research is needed to better understand fine-grained sediment storage and suspended sediment transport in Ozark streams. Nevertheless, the present study provided a framework to use the combination of stream channel and fine sediment assessments to better understand how fluvial processes and sediment transport operate over decadal timescales in watersheds.

REFERENCES

Adamski, J.C., Petersen, J.C., Freiwald, D.A., Davis, J. V, 1995. Environmental and hydrologic setting of the Ozark Plateaus study unit, Arkansas, Kansas, Missouri, and Oklahoma, U.S. Geological Survey Water-Resources Investigations Report.

Baartman, J.E.M., Masselink, R., Keesstra, S.D., Temme, A.J.A.M., 2013. Linking landscape morphological complexity and sediment connectivity. Earth Surf. Process. Landforms 38, 1457–1471. https://doi.org/10.1002/esp.3434

Barr, M.N., 2016. Surface-Water Quality and Suspended-Sediment Quantity and Quality within the Big River Basin, Southeastern Missouri, 2011–13. Scientific Investigations Report 2015 – 5171.

Beach, T., 1994. The Fate of Eroded Soil: Sediment Sinks and Sediment Budgets of Agrarian Landscapes in Southern Minnesota, 1851-1988. Ann. Assoc. Am. Geogr. 84, 5–28. https://doi.org/10.1111/j.1467-8306.1994.tb01726.x

Beck, W., Isenhart, T., Moore, P., Schilling, K., Schultz, R., Tomer, M., 2018. Streambank alluvial unit contributions to suspended sediment and total phosphorus loads, walnut Creek, Iowa, USA. Water (Switzerland) 10, 22. https://doi.org/10.3390/w10020111

Betts, H.D., Trustrum, N.A., De Rose, R.C., 2003. Geomorphic changes in a complex gully system measured from sequential digital elevation models, and implications for management. Earth Surf. Process. Landforms 28, 1043–1058.

Blanckaert, K., 2011. Hydrodynamic processes in sharp meander bends and their morphological implications. J. Geophys. Res. Earth Surf. 116, 1–22. https://doi.org/10.1029/2010JF001806

Bracken, L.J., Turnbull, L., Wainwright, J., Bogaart, P., 2015. Sediment connectivity: A framework for understanding sediment transfer at multiple scales. Earth Surf. Process. Landforms 40, 177–188. https://doi.org/10.1002/esp.3635

Brierley, G., Fryirs, K., Jain, V., 2006. Landscape connectivity: The geographic basis of geomorphic applications. R. Geogr. Soc. 38, 165–174. https://doi.org/10.1111/j.1475-4762.2006.00671.x

Brown, T.C., Froemke, P., 2012. Nationwide Assessment of Nonpoint Source Threats to Water Quality. Bioscience 62, 136–146. https://doi.org/10.1525/bio.2012.62.2.7

Brown, T.C., Froemke, P., 2010. Risk of impaired condition of watersheds containing National Forest lands. Fort Collins, CO.

Bunte, K., Abt, S.R., 2001. Sampling Surface and Subsurface Particle-Size Distributions in Wadable Gravel- and Cobble-Bed Streams for Analyses in Sediment Transport , Hydraulics , and Streambed Monitoring, General Technical Report RMRS-GTR-74. Rocky Mountain Research Station, Fort Collins, CO. https://doi.org/10.1017/CBO9781107415324.004

Carlson, J.L., 1999. Zinc mining contamination and sedimentation rates of historical overbank deposits, Honey Creek Watershed, southwest Missouri. Missouri State University.

Couper, P., Stott, T., Maddock, I., 2002. Insights into river bank erosion processes derived from analysis of negative erosion-pin recordings: Observations from three recent UK studies. Earth Surf. Process. Landforms 27, 59–79. https://doi.org/10.1002/esp.285

Davis, L., 2009. Sediment Entrainment Potential in Modified Alluvial Streams: Implications for Re-mobilization of Stored In-channel Sediment. Phys. Geogr. 30, 249–268.

De Rose, R.C., Basher, L.R., 2011. Geomorphology Measurement of river bank and cliff erosion from sequential LIDAR and historical aerial photography. Geomorphology 126, 132–147. https://doi.org/10.1016/j.geomorph.2010.10.037

Donovan, M., Miller, A., Baker, M., Gellis, A., 2015. Sediment contributions from floodplains and legacy sediments to Piedmont streams of Baltimore County, Maryland. Geomorphology 235, 88–105. https://doi.org/10.1016/j.geomorph.2015.01.025

Dunning, D., 2017. Void Ratio for Common Gravel & Sand [WWW Document]. Sciencing. URL https://sciencing.com/void-ratio-common-gravel-sand-7958152.html (accessed 4.2.20).

Emili, L.A., Greene, R.P., 2013. Modeling agricultural nonpoint source pollution using a geographic information system approach. Environ. Manage. 51, 70–95. https://doi.org/10.1007/s00267-012-9940-4

Ferguson, R.I., Parsons, D.R., Lane, S.N., Hardy, R.J., 2003. Flow in meander bends with recirculation at the inner bank. Water Resour. Res. 39. https://doi.org/10.1029/2003WR001965

Foucher, A., Salvador-Blanes, S., Vandromme, R., Cerdan, O., Desmet, M., 2017. Quantification of bank erosion in a drained agricultural lowland catchment. Hydrol. Process. 31. https://doi.org/10.1002/hyp.11117

Fox, G.A., Purvis, R.A., Penn, C.J., 2016. Streambanks: A net source of sediment and phosphorus to streams and rivers. J. Environ. Manage. 181, 602–614. https://doi.org/10.1016/j.jenvman.2016.06.071

Gillespie, J.L., Noe, G.B., Hupp, C.R., Gellis, A.C., Schenk, E.R., 2018. Floodplain trapping and cycling compared to streambank erosion of sediment and nutrients in an agricultural watershed. J. Am. Water Resour. Assoc. 54, 565–582.

Gran, K.B., Belmont, P., Day, S.S., Jennings, C., Johnson, A., Perg, L., Wilcock, P.R., 2009. Geomorphic evolution of the Le Sueur River, Minnesota, USA, and implications for current sediment loading. Spec. Pap. Geol. Soc. Am. 451, 119–130. https://doi.org/https://doi.org/10.1130/2009.2451(08)

Gregg, J.M., Shelton, K.L., 1989. Minor- and trace-element distributions in the Bonneterre Dolomite (Cambrian), southeast Missouri: Evidence for possible multiple-basin fluid sources and pathways during lead-zinc mineralization. Bull. Geol. Soc. Am. 101, 221–230. https://doi.org/10.1130/0016-7606(1989)101<0221:MATEDI>2.3.CO;2

Groten, J.T., Ellison, C.A., Hendrickson, J.S., 2016. Suspended-Sediment Concentrations, Bedload, Particle Sizes, Surrogate Measurements, and Annual Sediment Loads for Selected Sites in the Lower Minnesota River Basin, Water Years 2011 through 2016, U.S. Geological Survey Scientific Investigations Report 2016-5174.

Hagstrom, C.A., Leckie, D.A., Smith, M.G., 2018. Point bar sedimentation and erosion produced by an extreme flood in a sand and gravel-bed meandering river. Sediment. Geol. 377, 1–16.

Happ, S.C., 1944. Effect of sedimentation on floods in the Kickapoo Valley, Wisconsin. Geology 52, 53–68.

Harden, C.P., Foster, W., Morris, C., Chartrand, K.J., Henry, E., 2009. Rates and Processes of Streambank Erosion in Tributaries of the Little River, Tennessee. Phys. Geogr. 30, 1–16. https://doi.org/10.2747/0272-3646.30.1.1

Hart, E.A., Schurger, S.G., 2005. Sediment storage and yield in urbanized karst waters. Geomorphology 70, 85–96.

Hession, W.C., Pizzuto, J.E., Johnson, T.E., Horwitz, R.J., 2003. Influence of bank vegetation on channel morphology in rural and urban watersheds. Geol. Soc. Am. 31, 147–150.

Höfle, B., Rutzinger, M., 2011. Topographic airborne LiDAR in geomorphology: A technological perspective. Zeitschrift fur Geomorphol. 55, 1–29. https://doi.org/10.1127/0372-8854/2011/0055S2-0043

Huang, D., 2012. Quantifying Stream Bank Erosion and Deposition Rates in a Central U.S. Urban Watershed. University of Missouri-Columbia.

Hughes, M.L., McDowell, P.F., Marcus, W.A., 2006. Accuracy assessment of georectified aerial photographs: Implications for measuring lateral channel movement in a GIS. Geomorphology 74, 1–16. https://doi.org/10.1016/j.geomorph.2005.07.001

Hutchison, E.C.D., 2010. Mass transport of suspended sediment, dissolved solids, nutrients, and anions in the James River, SW Missouri. Missouri State University.

Jacobson, R.B., 1995. Spatial controls on patterns of land-use induced stream disturbance at the drainage-basin scale—An example from gravel-bed streams of the Ozark Plateaus, Missouri., AGU Geophy. ed. American Geophysical Union, Washington, DC.

Jacobson, R.B., Gran, K.B., 1999. Gravel sediment routing from widespread, low-intensity landscape disturbance, Current River basin, Missouri. Earth Surf. Process. Landforms 24, 897–917. https://doi.org/10.1002/(SICI)1096-9837(199909)24:10<897::AID-ESP18>3.0.CO;2-6

Jacobson, R.B., Primm, a T., 1997. Historical land-use changes and potential effects on stream disturbance in the Ozark Plateaus, Missouri, U. S. Geological Survey Water-Supply Paper 2484.

Jacobson, R.B., Pugh, A.L., 1997. Riparian-vegetation controls on the spatial pattern of stream-channel instability, Little Piney Creek, Missouri. Denver, CO.

James, L.A., 2013. Legacy sediment: Definitions and processes of episodically produced anthropogenic sediment. Anthropocene 2, 16–26. https://doi.org/10.1016/j.ancene.2013.04.001

Janes, V.J.J., Nicholas, A.P., Collins, A.L., Quine, T.A., 2017. Analysis of fundamental physical factors influencing channel bank erosion: results for contrasting catchments in England and Wales. Environ. Earth Sci. 76, 1–18. https://doi.org/10.1007/s12665-017-6593-x

Jordan, M.M., 2019. Historical Floodplain Sedimentation Rates Using Mining Contaminant Profiles, Cesium-137, and Sediment Source Indicators along the Lower Big River, Jefferson County, Missouri. Missouri State University.

Joyce, H.M., Hardy, R.J., Warburton, J., Large, A.R.G., 2018. Sediment continuity through the upland sediment cascade: geomorphic response of an upland river to an extreme flood event. Geomorphology 317, 45–61. https://doi.org/10.1016/j.geomorph.2018.05.002

Julian, J.P., Torres, R., 2006. Hydraulic erosion of cohesive riverbanks. Geomorphology 76, 193–206.

Keppel, A., Owen, M.R., Pavlowsky, R.T., 2015. Mining influence on lead profiles in historical floodplain deposits along the Big River, in: 49th Annual Meeting of the South Central Section of the Geological Society of America. Stillwater, OK, March 19-20.

Kessler, A.C., Gupta, S.C., Brown, M.K., 2013. Assessment of river bank erosion in Southern Minnesota rivers post European settlement. Geomorphology 201, 312–322. https://doi.org/10.1016/j.geomorph.2013.07.006

Kessler, A.C., Gupta, S.C., Dolliver, H.A.S., Thoma, D.P., 2012. Lidar Quantification of Bank Erosion in Blue Earth County, Minnesota. J. Environ. Qual. 41, 197. https://doi.org/10.2134/jeq2011.0181er

Knighton, D., 1998. Fluvial Forms & Processes: A New Perspective. Oxford University Press Inc., New York.

Knox, J.C., 2006. Floodplain sedimentation in the Upper Mississippi Valley: Natural versus human accelerated. Geomorphology 79, 286–244. https://doi.org/10.1016/j.geomorph.2006.06.031

Knox, J.C., 1987. Historical Valley Flood Sedimentation in the Upper Mississippi Valley. Ann. Assoc. Am. Geogr. 77, 224–244.

Knox, J.C., 1972. Valley alluviation in southwestern Wisconsin. Ann. Assoc. Am. Geogr. 62, 401–410.

Kondolf, G.M., 1997. Hungry water: Effects of dams and gravel mining on river channels. Environ. Manage. 21, 533–551. https://doi.org/10.1007/s002679900048

Lauer, J.W., Echterling, C., Lenhart, C., Belmont, P., Rausch, R., 2017. Air-photo based change in channel width in the Minnesota River basin: Modes of adjustment and implications for sediment budget. Geomorphology 297, 170–184. https://doi.org/10.1016/j.geomorph.2017.09.005

Lawler, D.M., 1993. The Measurement of River Bank Erosion and Lateral Channel Change: A Review. Earth Process. Landforms 18, 777–821.

Lecce, S.A., 1997. Spatial patterns of historical overbank sedimentation and floodplain evolution, Blue river, Wisconsin. Geomorphology 18, 265–277. https://doi.org/10.1016/s0169-555x(96)00030-x

Lecce, S.A., Pavlowsky, R.T., 2014. Geomorphology Floodplain storage of sediment contaminated by mercury and copper from historic gold mining at Gold Hill , North Carolina , USA. Geomorphology 206, 122–132. https://doi.org/10.1016/j.geomorph.2013.10.004

Leopold, L.B., 1973. River Channel Change with Time: An Example. Geol. Soc. Am. Bull. 84, 1845–1869.

Liu, Y., Li, S., Wallace, C.W., Chaubey, I., Flanagan, D.C., Theller, L.O., Engel, B.A., 2017. Comparison of Computer Models for Estimating Hydrology and Water Quality in an Agricultural Watershed. Water Resour. Manag. https://doi.org/10.1007/s11269-017-1691-9

Magilligan, F.J., 1985. Historical floodplain sedimentation in the Galena River Basin, Wisconsin and Illinois. Ann. Assoc. Am. Geogr. 75, 583–594.

Manger, G.E., 1963. Porosity and Bulk Density of Sedimentary Rocks: Contributions to Geochemistry. Washington, DC. https://doi.org/10.1111/nan.12452

Marron, D.C., 1992. Floodplain Strogae of Mine Tailings in the Belle Fourche River System: A Sediment Budget Approach. Earth Surf. Process. Landforms 17, 675–685.

Martin, D.J., Pavlowsky, R.T., 2011. Spatial Patterns of Channel Instability Along an Ozark River, Southwest Missouri. Phys. Geogr. 32, 445–468.

MDNR, 2018. 2018 Section 303(d) Listed Waters: TMDL Prioritization and Development Schedule [WWW Document]. URL https://dnr.mo.gov/env/wpp/tmdl/documents/tmdl-priorities-and-schedule-for-2018-303dlist.pdf (accessed 10.2.18).

MDNR, 2016. The State of Our Missouri Waters: Meramec River Watershed [WWW Document].

MDNR, 2014. The State of Our Missouri Waters: Big River Watershed [WWW Document]. Missouri Dep. Nat. Resour. URL https://dnr.mo.gov/omw/docs/omw-big-summary.pdf (accessed 10.3.18).

MDNR, 2008. Missouri Department of Natural Resources Water Protection Program Total Maximum Daily Load (TMDL) for Tributary to Pond Creek Washington County, Missouri.

MDNR, 2006. Biological Assessment Report Mill Creek Washington County , Missouri September 2005- March 2006.

Meade, R.H., 1982. Sources, Sinks, and Storage of River Sediment in the Atlantic Drainage of the United States. Geology 90, 235–252.

Michalkova, M., PieGay, H., Kondolf, G.M., Greco, S.E., 2011. Lateral erosion of the Sacramento River, California (1942-1999), and responses of channel and floodplain lake to human influences. Earth Surf. Process. Landforms 36, 257–272. https://doi.org/10.1002/esp.2106

Mount, N., Louis, J., 2005. Estimation and propagation of error in measurements of river channel movement from aerial imagery. Earth Surf. Process. Landforms 30, 635–643. https://doi.org/10.1002/esp.1172

MRCC, 2018. State and Climate Division Data - Monthly by Year [WWW Document]. URL https://mrcc.illinois.edu/CLIMATE/nClimDiv/STCD_monthly1.jsp (accessed 10.17.18).

MSDIS, 2019. MO 2019 Dams [WWW Document]. Missouri Spat. Data Inf. Serv.

MSDIS, 2017. Missouri County-Extent Digital Ortho Quarter Quads [WWW Document]. URL http://www.msdis.missouri.edu/data/imagery/index.html (accessed 10.18.18).

Mugel, D.N., 2017. Geology and Mining History of the Southeast Missouri Barite District and the Valles Mines, Washington, Jefferson, and St. Francois Counties, Missouri.

Nejadhashemi, A.P., Woznicki, S.A., Douglas-Mankin, K.R., 2011. Comparison of Four Models (STEPL, PLOAD, L-THIA, and SWAT) in Simulating Sediment, Nitrogen, and Phosphorus Loads and Pollutant Source Areas. Am. Soc. Agric. Biol. Eng. 54, 875–890.

Nigh, T.A., Schroeder, W.A., 2002. Atlas of Missouri Ecoregions.

Notebaert, B., Verstraeten, G., Govers, G., Poesen, J., 2009. Qualitative and quantitative applications of LiDAR imagery in fluvial geomorphology. Earth Surf. Process. Landforms 34, 217–231. https://doi.org/10.1002/esp

NRCS, 1983. National Engineering Handbook:, Part 630 Hydrology.

Odgaard, A.J., 1987. Streambank erosion along two rivers in Iowa. Water Resour. Res. 23.

Olson, L.M., 2017. Channel Bar Morphology, Distribution, and Mining-Related Geochemistry in the Big River, St. Francois County, Missouri: Implications for Geomorphic Recovery. Missouri State University.

Owen, M.R., Pavlowsky, R.T., 2015. Nonpoint Source Bank Erosion and Load Reduction Assessment for the Pearson Creek 319 Riparian Corridor Easement Site, 5377 E . Foxgrove Lane Greene County, Missouri.

Owen, M.R., Pavlowsky, R.T., Womble, P.J., 2011. Historical disturbance and contemporary floodplain development along an Ozark river, Southwest Missouri. Phys. Geogr. 32, 423–444.

Palmer, J.A., Schilling, K.E., Isenhart, T.M., Schultz, R.C., Tomer, M.D., 2014. Streambank erosion rates and loads within a single watershed: Bridging the gap between temporal and spatial scales. Geomorphology 209, 66–78. https://doi.org/10.1016/j.geomorph.2013.11.027

Panfil, M.S., Jacobson, R.B., 2001. Relations Among Geology, Physiography, Land Use, and Stream Habitat Conditions in the Buffalo and Current River Systems, Missouri and Arkansas [WWW Document]. Biol. Sci. Rep. USGS/BRD/BSR--2001-0005. URL https://www.cerc.usgs.gov/pubs/center/pdfdocs/BSR2001-0005.pdf (accessed 10.1.19).

Park, Y.S., Engel, B.A., Harbor, J., 2014. A web-based model to estimate the impact of best management practices. Water (Switzerland) 6, 455–471. https://doi.org/10.3390/w6030455

Park, Y.S., Engel, B.A., Kim, J., Theller, L., Chaubey, I., Merwade, V., Lim, K.J., 2015. A web tool for STORET/WQX water quality data retrieval and Best Management Practice scenario suggestion. J. Environ. Manage. 150, 21–27. https://doi.org/10.1016/j.jenvman.2014.11.006

Pavlowsky, R.T., 2013. Source allocation for lead-contaminated sediment in the Big River from two different mining sources in St. Francois and Washington Counties, Missouri.

Pavlowsky, R.T., Lecce, S.A., Owen, M.R., Martin, D.J., 2017. Legacy sediment, lead, and zinc storage in channel and floodplain deposits of the Big River, Old Lead Belt Mining District, Missouri, USA. Geomorphology 299, 54–75. https://doi.org/10.1016/j.geomorph.2017.08.042

Pavlowsky, R.T., Owen, M.R., 2015. Floodplain Core Sampling and Lead Contamination at St . Francois State Park and Washington State Park , Southeast Missouri.

Pavlowsky, R.T., Owen, M.R., Martin, D.J., OEWRI, 2010. Distribution, Geochemistry, and Storage of Mining Sediment in Channel and Floodplain Deposits of the Big River System in St . Francois, Washington, and Jefferson Counties, Missouri Field work completed Fall 2008 to Spring 2009.

Peel, M.C., Finlayson, B.L., McMahon, T.A., 2007. Updated world map of the Köppen-Geiger climate classification. Hydrol. Earth Systm. Sci. Discuss. 4, 439–473.

Phillips, J.D., 1991. Fluvial sediment budgets in the North Carolina Piedmont. Geomorphology 4, 231–241. https://doi.org/10.1016/0169-555X(91)90006-V

Podhoranyi, M., Fedorcak, D., 2014. Inaccuracy introduced by LiDAR-generated cross sections and its impact on 1D hydrodynamic simulations. Environ. Earth Sci. 73, 1–11. https://doi.org/10.1007/s12665-014-3390-7

Poole, G.C., 2002. Fluvial landscape ecology: Addressing uniqueness within the river discontinuum. Freshw. Biol. 47, 641–660. https://doi.org/https://doi.org/10.1046/j.1365-2427.2002.00922.x

Reminga, K.N., 2019. Historical Land Use Influence on Fine-Grained Sedimentation in Channel and Floodplain Deposits in a Forested Missouri Ozark Watershed. Missouri State University.

Renwick, W.H., Smith, S. V., Bartley, J.D., Buddemeier, R.W., 2005. The role of impoundments in the sediment budget of the conterminous United States. Geomorphology 71, 99–111. https://doi.org/10.1016/j.geomorph.2004.01.010

Rhoades, E.L., O'Neal, M.A., Pizzuto, J.E., 2009. Quantifying bank erosion on the South River from 1937 to 2005, and its importance in assessing Hg contamination. Appl. Geogr. 29, 125–134. https://doi.org/10.1016/j.apgeog.2008.08.005

Roering, J.J., Mackey, B.H., Marshall, J.A., Sweeney, K.E., Deligne, N.I., Booth, A.M., Handwerger, A.L., Cerovski-Darriau, C., 2013. "You are HERE": Connecting the dots with airborne lidar for geomorphic fieldwork. Geomorphology 200, 172–183. https://doi.org/10.1016/j.geomorph.2013.04.009

Rosgen, D.L., 1994. A classification of natural rivers. Catena 22, 169–199. https://doi.org/https://doi.org/10.1016/0341-8162(94)90001-9

Schenk, E.R., Hupp, C.R., 2009. Legacy effects of colonial millponds on floodplain sedimentation, bank erosion, and channel morphology, Mid-Atlantic, USA. J. Am. Water Resour. Assoc. 45, 596–606.

Schumacher, J.G., Smith, D.C., 2018. Distribution of Mining-Related Trace Elements in Streambed and Flood-Plain Sediment along the Middle Big River and Tributaries in the Southeast Missouri Barite District , 2012 – 15 Scientific Investigations Report 2018 – 5103.

Seeger, C., 2006. Old Mines Area Sample Area Mining History and Geology, Memorandum.

Sekely, A.C., Mulla, D.J., Bauer, D.W., 2002. Streambank slumping and its contributions to the phosphous and suspended sediment loads of the Blue Earth River, Minnesota. J. Soil Water Conserv. 57, 243–250.

Simon, A., Bingner, R.L., Langendoen, E.J., Alonso, C.V., 2002. Actual and reference sediment yields for the James Creek Watershed, Mississippi, Technical Report No. 31.

Simon, A., Hupp, C.R., 1986. Channel evolution in modified Tennessee channels. Proc. Fourth Interag. Sediment. Conf. 2, 71–82.

Simon, A., Langendoen, E.J., Bingner, R.L., Wells, R.R., Yuan, Y., Alonso, C.V., 2004. Suspended-sediment Transport and Bed-material Characteristics of Shades Creek, Alabama and Ecoregion 67: Developing Water-quality Criteria for Suspended and Bed-material Sediment, Technical Report No. 43.

Simon, A., Thomas, R.E., 2002. Processes and forms of an ustable alluvial stream with resistant cohesive streambeds. Earth Surf. Process. Landforms 27.

Skaer, D.M., Cook, M.A., 2005. Soil Survey of Washington County, Missouri.

Spiekermann, R., Betts, H., Dymond, J., Basher, L., 2017. Volumetric measurement of river bank erosion from sequential historical aerial photography. Geomorphology 296, 193–208. https://doi.org/10.1016/j.geomorph.2017.08.047

St. Louis District Corps of Engineers, 1970. Sunnen Lake Dam Inspection Report, US Army Engineer District. https://doi.org/10.1017/CBO9781107415324.004

StormTech, 2012. Porosity of Structural Backfill. Rocky Hill, CT.

Tetra Tech, I., 2018. USER ’ S GUIDE: Spreadsheet Tool for the Estimation of Pollutant Load (STEPL) Version 4.4. Fairfax, VA.

Thoma, D.P., Gupta, S.C., Bauer, M.E., Kirchoff, C.E., 2005. Airborne laser scanning for riverbank erosion assessment. Remote Sens. Environ. 95, 493–501. https://doi.org/. http://dx.doi.org/10.1016/j.rse.2005.01.012

Trimble, S.W., 2009. Geomorphology Fluvial processes , morphology and sediment budgets in the Coon Creek Basin , WI ,. Geomorphology 108, 8–23. https://doi.org/10.1016/j.geomorph.2006.11.015

Trimble, S.W., 1999. Decreased Rates of Alluvial Sediment Storage in the Coon Creek Basin, Wisconsin, 1975-93. Am. Assoc. Adv. Sci. 285, 1244–1246. https://doi.org/10.1126/science.285.5431.1244

Trimble, S.W., 1983. A sediment budget for Coon Creek Basin in the Driftless Area, Wisconsin. Am. J. Sci. 283, 454–474.

Trimble, S.W., Lund, S.W., 1982. Soil Conservation and the Reduction of Erosion and Sedimentation in the Coon Creek Basin, Wisconsin. Geol. Surv. Prof. Pap. 1234.

Troeh, F.R., Hobb, J.A., Donahue, R.L., 2004. Soil and Water Conservation for Productivity and Environmental Protection, Fourth Edi. ed. Pearson Education Inc., Upper Saddle River, New Jersey.

Turner, R.E., Rabalais, N.N., 2004. Suspended sediment, C, N, P, and Si yields from the Mississippi River Basin. Hydrobologia 511, 79–89.

US Census Bureau, 2017. American Community Survey 5-Year Estimates: Potosi [WWW Document]. US Census Bur. Am. FactFinder. URL https://factfinder.census.gov/faces/nav/jsf/pages/searchresults.xhtml?refresh=t (accessed 10.18.18).

USACE, 1983. Sacramento River and Tributaries Bank Protection and Erosion Control Investigation, California Sediment Transport Studies. Sacramento, CA.

USDA-NASS, 2018. CropScape and Cropland Data Layer [WWW Document]. URL https://www.nass.usda.gov/Research_and_Science/Cropland/SARS1a.php (accessed 10.9.18).

USDA-NRCS, 2017. Web Soil Survey [WWW Document]. URL https://websoilsurvey.sc.egov.usda.gov/App/WebSoilSurvey.aspx (accessed 10.26.18).

USDA-NRCS, 2006. Land Resource Regions and Major Land Resource Areas of the United States, the Caribbean, and the Pacific Basin.

USDA, 2017. 2017 Census of Agriculture: County Profile. Washington County, Missouri.

USEPA, 2019. Spreadsheet Tool for Estimating Pollutant Loads (STEPL) [WWW Document]. Polluted Runoff Nonpoint Source Pollut. URL https://www.epa.gov/nps/spreadsheet-tool-estimating-pollutant-loads-stepl#doc (accessed 1.31.19).

USEPA, 2018a. Land Reclamation Activities Improve Water Quality in the Upper. Missouri.

USEPA, 2018b. Basic Information about Nonpoint Source (NPS) Pollution [WWW Document]. United States Environ. Prot. Agency. URL https://www.epa.gov/nps/basic-information-about-nonpoint-source-nps-pollution (accessed 11.7.18).

USGS, 2018a. National Hydrology Dataset [WWW Document]. URL https://nhd.usgs.gov (accessed 9.6.18).

USGS, 2018b. USGS Current Water Data for Missouri [WWW Document]. URL https://waterdata.usgs.gov/mo/nwis/rt (accessed 9.19.18).

Walter, R.C., Merritts, D.J., 2008. Natural streams and the legacy of water-powered mills. Science (80-.). 219, 299–304.

Ward, A.D., Elliot, W.J., 1995. Environmental Hydrology. Lewis Publishers, Inc, Boca Raton.

Ward, A.D., Trimble, S.W., Burckhard, S.R., Lyon, J.G., 2016. Environmental Hydrology, Third Edit. ed. CRC Press, Taylor and Francis Group, Boca Raton.

WiDNR, 2014. The Spreadsheet Tool for Estimating Pollutant Loads (STEPL).

Wilkinson, B.H., McElroy B.J, 2007. The impact of humans on continental erosion and sedimentation. Geol. Soc. Am. Bull. 119, 140–156.

Xia, J., Li, T., Li, X., Zhang, X., Zong, Q., 2014. Daily bank erosion rates in the lower yellow river before and after dam construction. J. Am. Water Resour. Assoc. 50, 1325–1337. https://doi.org/10.1111/jawr.12192

Zaimes, G.N., Schultz, R.C., 2015. Riparian land-use impacts on bank erosion and deposition of an incised stream in north-central Iowa, USA. Catena 125. https://doi.org/10.1016/j.catena.2014.09.013

APPENDICES

Appendix A. Drainage area and discharge relationships for 32 USGS gaging stations near the study watershed.

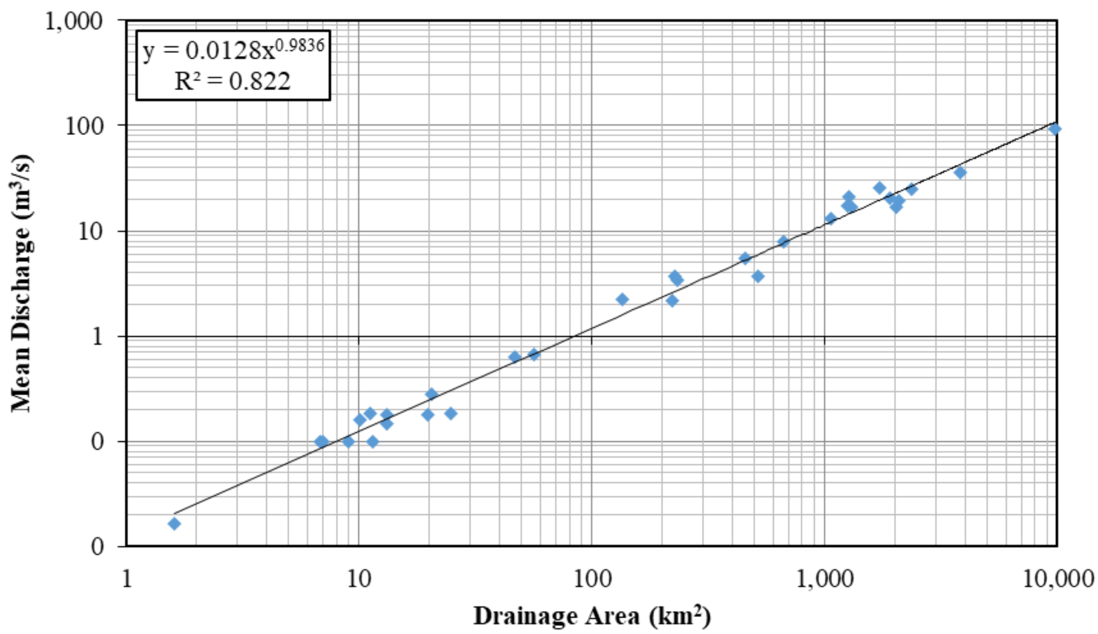

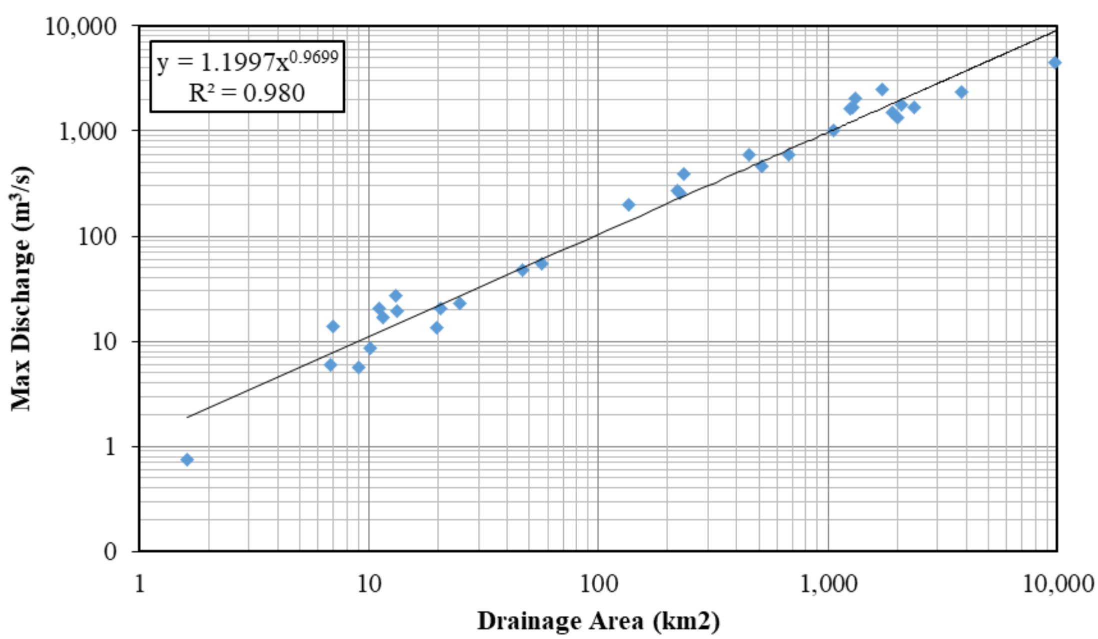

Appendix A-1. Mean and max discharge and drainage area relationships for USGS gaging stations near the study watershed.

Appendix A-2. USGS gaging stations near the watershed.

USGS				Years of			Flow Exceedence (m^3/s)				
Gage ID	Station Name	Stream	Start Year	Record	Ad (km^2)	Elevation (m)	90%	50%	10%	Max	Mean
06935755	Bonhomme Creek near Ellisville, MO	Bonhomme Creek	1997	21	11.4996	173.3	0.00	0.02	0.13	16.82	0.10
07010090	MacKenzie Creek near Shrewsbury, MO	MacKenzie Creek	1997	21	9.0391	129.4	0.00	0.02	0.19	5.66	0.10
07010094	Grammond Creek near Wilbur Park, MO	Grammond Creek	1997	21	1.6058	133.5	0.00	0.01	0.04	0.76	0.02
07010097	River Des Peres at St. Louis, MO	River Des Peres	2002	16	220.668	119.0	0.05	0.20	3.60	274.70	2.16
07010180	Gravois Creek near Mehlville, MO	Gravois Creek	1996	22	46.879	128.7	0.03	0.12	1.06	47.01	0.63
07010208	Martigney Creek near Arnold, MO	Martigney Creek	1997	21	6.8376	124.2	0.01	0.03	0.17	6.03	0.10
07010350	Meramec River at Cook Station, MO	Meramec River	1965	53	515.41	263.6	0.48	1.19	6.57	467.28	3.68
07013000	Meramec River near Steelville, MO	Meramec River	1922	96	2022.79	207.8	3.79	7.65	31.15	1353.70	17.05
07014000	Huzzah Creek near Steelville, MO	Huzzah Creek	2007	11	670.81	202.7	1.54	3.17	14.16	597.55	7.87
07014500	Meramec River near Sullivan, MO	Meramec River	1921	97	3820.25	177.3	7.56	17.22	68.25	2350.56	35.65
07016500	Bourbeuse River at Union, MO	Bourbeuse River	1921	97	2092.72	148.9	1.19	4.96	37.95	1784.16	19.50
07017200	Big River at Irondale, MO	Big River	1965	53	453.25	229.6	0.28	1.55	10.39	603.22	5.41
07017610	Big River below Bonne Terre, MO	Big River	2011	7	1059.31	191.4	1.32	3.82	22.68	1011.02	13.08
07018100	Big River near Richwoods, MO	Big River	1949	69	1903.65	159.4	2.92	8.16	37.67	1517.95	20.53
07018500	Big River at Byrnesville, MO	Big River	1922	96	2375.03	132.2	3.37	9.60	48.14	1687.87	24.75
07019000	Meramec River near Eureka, MO	Meramec River	1903	115	9810.92	123.2	15.26	40.50	195.46	4502.88	93.78
07019072	Kiefer Creek near Ballwin, MO	Kiefer Creek	1996	22	10.1269	133.8	0.03	0.07	0.31	8.55	0.16
07019090	Williams Creek near Peerless Park, MO	Williams Creek	1997	21	19.7358	126.6	0.02	0.07	0.38	13.45	0.18
07019120	Fishpot Creek at Valley Park, MO	Fishpot Creek	1996	22	24.8122	128.6	0.00	0.00	0.15	23.14	0.19
07019150	Grand Glaize Creek near Manchester, MO	Grand Glaize Creek	1997	21	13.1831	137.8	0.00	0.02	0.27	19.26	0.15
07019175	Sugar Creek at Kirkwood, MO	Sugar Creek	1997	21	13.1572	128.3	0.01	0.03	0.22	27.44	0.18
07019185	Grand Glaize Creek near Valley Park, MO	Grand Glaize Creek	1997	21	56.462	127.1	0.04	0.15	1.07	55.22	0.68
07019195	Yarnell Creek at Fenton, MO	Yarnell Creek	1997	21	7.0189	123.3	0.01	0.02	0.16	13.91	0.10
07019220	Fenton Creek near Fenton, MO	Fenton Creek	1997	21	11.1111	126.8	0.01	0.03	0.27	20.25	0.18
07019317	Mattese Creek near Mattese, MO	Mattese Creek	1996	22	20.4092	128.6	0.00	0.04	0.48	20.48	0.28
07035000	Little St. Francis River at Fredericktown, MO	Little St. Francis River	1939	79	234.395	206.8	0.08	0.93	7.00	390.82	3.44
07035800	St. Francis River near Mill Creek, MO	St. Francis River	1987	31	1307.95	169.6	0.42	4.90	32.57	2039.04	16.72
07036100	St. Francis River near Saco, MO	St. Francis River	1983	35	1719.76	143.9	0.88	7.28	51.83	2509.15	25.91
07061270	East Fork Black River near Lesterville, MO	East Fork Black River	2001	17	135.198	251.5	0.11	0.57	3.79	197.11	2.25
07061290	East Fork Black River below Lower Taum Sauk Reservoir, MO	East Fork Black River	2008	10	226.107	221.0	0.16	1.01	7.84	254.03	3.73
07061500	Black River near Annapolis, MO	Black River	1939	79	1253.56	173.7	3.48	7.93	32.57	1622.74	17.17
07061600	Black River below Annapolis, MO	Black River	2006	12	1276.87	169.3	4.81	9.49	37.10	1690.70	21.03

Appendix B. Field assessments.

	Location		Major	Stream	Date
Site #	Easting	Northing	Watershed	Order	Assessed
1	697,486.96	4,218,825.81	Mineral Fork	5	6/20/2019
2	694,756.23	4,218,145.52	Mineral Fork	2	12/17/2018
3	693,524.85	4,217,365.72	Mineral Fork	3	12/17/2018
4	689,491.40	4,212,240.43	Mineral Fork	5	12/17/2018
5	698,326.50	4,216,875.00	Mineral Fork	1	6/20/2019
6	698,326.50	4,216,701.39	Mineral Fork	3	6/20/2019
7.1	696,905.74	4,211,905.84	Mineral Fork	3	6/20/2019
7.2	696,903.51	4,211,838.80	Mineral Fork	1	6/20/2019
8	696,655.55	4,209,189.72	Mineral Fork	2	6/20/2019
9	686,393.90	4,211,894.93	Mineral Fork	2	6/20/2019
10	683,497.01	4,210,422.94	Mineral Fork	1	6/20/2019
11	682,491.74	4,204,138.61	Mineral Fork	4	6/20/2019
12	685,772.92	4,198,062.38	Mineral Fork	3	6/20/2019
13	692,734.66	4,201,718.25	Mineral Fork	3	6/20/2019
14	692,287.55	4,210,532.79	Mineral Fork	2	11/6/2019
15	686,339.11	4,209,358.10	Mineral Fork	4	11/6/2019
16	688,132.67	4,207,244.61	Mineral Fork	2	11/6/2019
17	688,948.30	4,206,544.35	Mineral Fork	3	11/6/2019
18	693,665.41	4,201,932.80	Mineral Fork	2	11/6/2019
19	681,870.98	4,203,061.68	Mineral Fork	2	11/6/2019
20.1	682,993.53	4,198,052.15	Mineral Fork	2	11/6/2019
20.2	683,009.91	4,198,032.45	Mineral Fork	2	11/6/2019
1	705,661.09	4,210,520.83	Mill Creek	3	6/20/2019
2	706,207.39	4,210,219.38	Mill Creek	3	12/17/2018
3	705,337.67	4,207,763.60	Mill Creek	3	12/17/2018
4	705,031.98	4,206,075.55	Mill Creek	3	12/17/2018
5	699,590.48	4,205,176.99	Mill Creek	2	6/20/2019
6	703,742.55	4,203,250.33	Mill Creek	2	6/20/2019
7	699,928.02	4,202,673.17	Mill Creek	1	6/20/2019
8	700,191.36	4,202,047.74	Mill Creek	3	6/20/2019

Appendix B. Field assessments (Continued).

Site #	Major Watershed	Bank Height (m) Field	Bank Height (m) LiDAR	Coarse Unit Thickness (CUT) (m) Upper Unit	Coarse Unit Thickness (CUT) (m) Lower Unit	CUT (% of bank Height)	Channel Width (m)	Water depth (m)
1	Mineral Fork	2.9	2.75	0.6	2.3	79	33	0.4
2	Mineral Fork	1.2	1.5	0.4	0.8	67	10	0.3
3	Mineral Fork	1.3	1.3	1	0.3	23	8	0.4
4	Mineral Fork	1.3	1.3	0.8	0.5	38	23	0.15
5	Mineral Fork	1.2	0.9	0.75	0.5	38	8	0.2
6	Mineral Fork	0.8	0.85	0.4	0.4	50	14	0.1
7.1	Mineral Fork	2.6	2.75	1.1	1.5	58	7	0.08
7.2	Mineral Fork	1.1	0.8	0.3	0.8	73	6	0.1
8	Mineral Fork	1.6	1.5	0.5	1.1	69	6	0.07
9	Mineral Fork	2.5	2.25	0.7	1.1	44	14	0.1
10	Mineral Fork	1.1	0.95	0.2	0.9	82	5	0.1
11	Mineral Fork	1.4	1.2	0.3	1.1	79	25	0.3
12	Mineral Fork	2	1.5	0.7	1.3	65	10	0.3
13	Mineral Fork	1.3	1.3	0.7	0.6	46	13	0.4
14	Mineral Fork	0.9	0.9	0.2	0.7	78	8.1	0.1
15	Mineral Fork	1.8	1.75	0.2	1.1	61	18.5	0.4
16	Mineral Fork	1.2	1	0.2	0.7	58	4.2	0.35
17	Mineral Fork	0.85	0.9	0.4	0.5	53	13.7	0.25
18	Mineral Fork	0.6	0.8	0.2	0.4	67	7.2	0.3
19	Mineral Fork	1	0.95	0.55	0.5	45	6.6	dry
20.1	Mineral Fork	1.5	1.3	0.2	0.6	40	10.7	0.4
20.2	Mineral Fork	1.9	1.5	1	0.9	47	10.7	0.4
1	Mill Creek	1.4	1.5	0.9	0.5	35.7	11	0.04
2	Mill Creek	2.9	2.75	2.3	0.4	13.8	9	0.22
3	Mill Creek	1.45	1.45	1.0	0.5	31.0	7	0.25
4	Mill Creek	2.1	1.6	0.4	1.7	81.0	22	0.5
5	Mill Creek	1.5	1.4	0.3	1.2	80.0	5	0.3
6	Mill Creek	0.8	0.8	0.5	0.3	34.3	4	0.1
7	Mill Creek	1.4	1.3	0.9	0.5	34.5	8	0.1
8	Mill Creek	0.9	1	0.2	0.7	77.8	6	0.3

Appendix B. Field assessments (Continued).

Site #	Major Watershed	Stream Order	Soil Characteristics (NRCS) Series	Texture-Upper	Slope (%)	Flood Frequency
1	Mineral Fork	5	Haymond	silt loam	0-3	Frequently
2	Mineral Fork	2	Cedargap	gravelly silt loam	0-2	Frequently
3	Mineral Fork	3	Cedargap	gravelly silt loam	0-2	Frequently
4	Mineral Fork	5	Cedargap	gravelly silt loam	0-2	Frequently
5	Mineral Fork	1	Cedargap	gravelly silt loam	0-2	Frequently
6	Mineral Fork	3	Cedargap	gravelly silt loam	0-2	Frequently
7.1	Mineral Fork	3	Cedargap	gravelly silt loam	0-2	Frequently
7.2	Mineral Fork	1	Cedargap	gravelly silt loam	0-2	Frequently
8	Mineral Fork	2	Cedargap	gravelly silt loam	0-2	Frequently
9	Mineral Fork	2	Cedargap	gravelly silt loam	1-3	Frequently
10	Mineral Fork	1	Cedargap	gravelly silt loam	1-3	Frequently
11	Mineral Fork	4	Cedargap	gravelly silt loam	0-2	Frequently
12	Mineral Fork	3	Cedargap	gravelly silt loam	0-2	Frequently
13	Mineral Fork	3	Cedargap	gravelly silt loam	0-2	Frequently
14	Mineral Fork	2	Cedargap	gravelly silt loam	1-3	Frequently
15	Mineral Fork	4	Cedargap	gravelly silt loam	0-2	Frequently
16	Mineral Fork	2	Cedargap	gravelly silt loam	1-3	Frequently
17	Mineral Fork	3	Cedargap	gravelly silt loam	0-2	Frequently
18	Mineral Fork	2	Cedargap	gravelly silt loam	0-2	Frequently
19	Mineral Fork	2	Cedargap	gravelly silt loam	0-2	Frequently
20.1	Mineral Fork	2	Cedargap	gravelly silt loam	0-2	Frequently
20.2	Mineral Fork	2	Cedargap	gravelly silt loam	0-2	Frequently
1	Mill Creek	3	Cedargap	gravelly silt loam	0-2	Frequently
2	Mill Creek	3	Racket	loam	0-3	Frequently
3	Mill Creek	3	Cedargap	gravelly silt loam	0-2	Frequently
4	Mill Creek	3	Cedargap	gravelly silt loam	0-2	Frequently
5	Mill Creek	2	Cedargap	gravelly silt loam	1-3	Frequently
6	Mill Creek	2	Cedargap	gravelly silt loam	1-3	Frequently
7	Mill Creek	1	Cedargap	gravelly silt loam	1-3	Frequently
8	Mill Creek	3	Cedargap	gravelly silt loam	0-2	Frequently

Appendix C. Sediment sample information.

Site #	Sample ID	Lab Name	Lab ID	Watershed	Sample Mass (Mg) < 2mm to 250 µm	Sample Mass (Mg) Total	% Fines
14	MF 14-1	KC	65	Mineral Fork	110	154	71.4
14	MF 14-2	KC	66	Mineral Fork	183	633	28.9
15	MF 15-1	KC	69	Mineral Fork	225	373	60.3
15	MF 15-2	KC	70	Mineral Fork	117	743	15.7
15	MF 15-3	KC	71	Mineral Fork	93	271	34.3
16	MF 16-1	KC	74	Mineral Fork	139	288	48.3
16	MF 16-2	KC	75	Mineral Fork	90	209	43.1
16	MF 16-3	KC	76	Mineral Fork	137	371	36.9
17	MF 17-1	KC	79	Mineral Fork	148	262	56.5
17	MF 17-2	KC	80	Mineral Fork	226	799	28.3
18	MF 18-1	KC	83	Mineral Fork	215	326	66.0
18	MF 18-2	KC	84	Mineral Fork	141	522	27.0
19	MF 19-1	KC	91	Mineral Fork	363	545	66.6
19	MF 19-2	KC	92	Mineral Fork	143	1,225	11.7
20	MF 20-1	KC	87	Mineral Fork	84	280	30.0
20	MF 20-2	KC	88	Mineral Fork	191	513	37.2

Appendix D. Cell location information in Mineral Fork.

Cell ID	Stream Order	Location Easting	Northing	12-Digit HUC Watershed	Cell Land Use
66	6	694,922.58	4,217,711.55	Clear Creek-Mineral Fork	Forest
69	6	694,752.87	4,217,254.00	Clear Creek-Mineral Fork	Forest
73	6	694,478.82	4,216,899.30	Clear Creek-Mineral Fork	Forest
77	6	694,091.88	4,216,761.71	Clear Creek-Mineral Fork	Forest
81	6	693,688.40	4,216,619.50	Clear Creek-Mineral Fork	Forest
85	6	693,425.75	4,216,236.31	Clear Creek-Mineral Fork	Forest
89	6	693,176.31	4,215,827.90	Clear Creek-Mineral Fork	Forest
94	6	692,794.38	4,215,677.15	Clear Creek-Mineral Fork	Forest
98	6	692,497.63	4,215,356.56	Clear Creek-Mineral Fork	Forest
102	6	692,421.56	4,214,902.78	Clear Creek-Mineral Fork	Forest
106	6	692,393.09	4,214,435.52	Clear Creek-Mineral Fork	Forest
111	6	692,059.81	4,214,225.10	Clear Creek-Mineral Fork	Forest
116	6	691,744.89	4,214,509.87	Clear Creek-Mineral Fork	Road Crossing
121	6	691,305.17	4,214,564.70	Clear Creek-Mineral Fork	Forest
126	6	691,017.42	4,214,248.70	Clear Creek-Mineral Fork	Forest
131	6	691,259.61	4,213,947.74	Clear Creek-Mineral Fork	Forest
136	6	691,115.57	4,213,602.10	Clear Creek-Mineral Fork	Forest
141	6	690,697.49	4,213,610.91	Clear Creek-Mineral Fork	Forest
147	6	690,232.56	4,213,665.51	Clear Creek-Mineral Fork	Forest
153	6	689,767.25	4,213,559.20	Clear Creek-Mineral Fork	Forest
159	6	689,718.07	4,213,172.04	Clear Creek-Mineral Fork	Forest
164	6	689,663.39	4,212,718.51	Clear Creek-Mineral Fork	Forest
170	6	689,539.99	4,212,342.07	Clear Creek-Mineral Fork	Road Crossing
174	6	689,226.84	4,212,326.56	Clear Creek-Mineral Fork	Forest
181	6	688,491.69	4,212,046.29	Clear Creek-Mineral Fork	Forest
185	6	688,712.93	4,211,763.74	Clear Creek-Mineral Fork	Forest
188	6	688,853.08	4,211,436.65	Clear Creek-Mineral Fork	Forest
191	6	688,465.50	4,211,368.50	Clear Creek-Mineral Fork	Forest
177	6	688,819.94	4,212,339.58	Clear Creek-Mineral Fork	Road Crossing
70	4	694,535.79	4,217,607.14	Clear Creek-Mineral Fork	Forest
74	4	694,035.66	4,217,503.61	Clear Creek-Mineral Fork	Forest
78	4	693,581.45	4,217,377.47	Clear Creek-Mineral Fork	Road Crossing
82	4	693,148.75	4,217,384.08	Clear Creek-Mineral Fork	Forest
86	4	692,667.53	4,217,510.40	Clear Creek-Mineral Fork	Forest
90	4	692,208.08	4,217,761.83	Clear Creek-Mineral Fork	Forest
95	4	691,855.12	4,218,022.31	Clear Creek-Mineral Fork	Forest
99	4	691,467.32	4,218,268.13	Clear Creek-Mineral Fork	Forest
103	4	691,035.72	4,218,426.74	Clear Creek-Mineral Fork	Forest
162	3	687,060.52	4,219,254.77	Clear Creek-Mineral Fork	Forest
107	3	690,912.47	4,218,846.02	Clear Creek-Mineral Fork	Forest
112	3	690,743.93	4,219,296.43	Clear Creek-Mineral Fork	Road Crossing
117	3	690,431.24	4,219,626.47	Clear Creek-Mineral Fork	Forest
122	3	690,038.55	4,219,813.51	Clear Creek-Mineral Fork	Forest

Appendix D. Cell location information in Mineral Fork (Continued).

Cell ID	Stream Order	Location Easting	Location Northing	12-Digit HUC Watershed	Cell Land Use
127	3	689,650.22	4,220,012.88	Clear Creek-Mineral Fork	Road Crossing
132	3	689,218.36	4,219,944.34	Clear Creek-Mineral Fork	Forest
137	3	688,766.61	4,219,904.44	Clear Creek-Mineral Fork	Forest
142	3	688,351.07	4,219,758.18	Clear Creek-Mineral Fork	Forest
148	3	687,939.56	4,219,700.22	Clear Creek-Mineral Fork	Forest
154	3	687,546.49	4,219,546.58	Clear Creek-Mineral Fork	Forest
108	3	690,682.41	4,218,667.88	Clear Creek-Mineral Fork	Forest
96	3	693,485.08	4,215,625.79	Clear Creek-Mineral Fork	Forest
100	3	693,695.13	4,215,061.79	Clear Creek-Mineral Fork	Forest
104	3	693,688.20	4,214,588.50	Clear Creek-Mineral Fork	Forest
109	3	693,549.45	4,214,133.73	Clear Creek-Mineral Fork	Forest
114	3	693,483.74	4,213,656.52	Clear Creek-Mineral Fork	Forest
119	3	693,653.79	4,213,209.71	Clear Creek-Mineral Fork	Forest
120	3	691,715.01	4,213,952.77	Clear Creek-Mineral Fork	Forest
125	3	691,780.12	4,213,395.63	Clear Creek-Mineral Fork	Forest
130	3	691,936.68	4,212,944.06	Clear Creek-Mineral Fork	Forest
135	3	692,076.17	4,212,466.91	Clear Creek-Mineral Fork	Forest
140	3	692,300.14	4,212,041.76	Clear Creek-Mineral Fork	Forest
145	3	692,235.55	4,211,576.45	Clear Creek-Mineral Fork	Road Crossing
151	3	692,288.60	4,211,122.85	Clear Creek-Mineral Fork	Road Crossing
157	3	692,287.99	4,210,654.69	Clear Creek-Mineral Fork	Road Crossing
161	3	692,319.39	4,210,178.04	Clear Creek-Mineral Fork	Forest
166	3	692,512.85	4,209,758.40	Clear Creek-Mineral Fork	Road Crossing
152	3	690,740.33	4,212,980.68	Clear Creek-Mineral Fork	Forest
158	3	690,505.21	4,212,614.30	Clear Creek-Mineral Fork	Forest
146	3	690,773.03	4,213,346.70	Clear Creek-Mineral Fork	Forest
167	3	689,519.29	4,212,902.39	Clear Creek-Mineral Fork	Forest
172	3	689,117.55	4,212,914.63	Clear Creek-Mineral Fork	Road Crossing
175	3	688,696.56	4,213,128.79	Clear Creek-Mineral Fork	Forest
178	3	688,394.48	4,213,404.61	Clear Creek-Mineral Fork	Forest
194	5	688,152.01	4,211,095.02	Fourche a Renault	Forest
199	5	687,745.64	4,210,931.76	Fourche a Renault	Forest
204	5	687,331.54	4,210,789.08	Fourche a Renault	Forest
210	5	687,045.24	4,210,431.95	Fourche a Renault	Road Crossing
215	5	686,701.46	4,210,160.75	Fourche a Renault	Road Crossing
220	5	686,668.88	4,209,710.98	Fourche a Renault	Road Crossing
224	5	686,372.88	4,209,354.85	Fourche a Renault	Road Crossing
229	5	686,111.18	4,209,007.30	Fourche a Renault	Forest
234	5	685,984.55	4,208,568.48	Fourche a Renault	Forest
239	5	685,680.58	4,208,236.55	Fourche a Renault	Forest
249	5	684,900.88	4,207,780.83	Fourche a Renault	Road Crossing
244	5	685,296.25	4,207,979.37	Fourche a Renault	Road Crossing
254	5	684,793.57	4,207,433.46	Fourche a Renault	Forest

Appendix D. Cell location information in Mineral Fork (Continued).

Cell ID	Stream Order	Location Easting	Location Northing	12-Digit HUC Watershed	Cell Land Use
261	5	684,947.21	4,207,024.89	Fourche a Renault	Forest
265	5	684,707.78	4,206,763.56	Fourche a Renault	Road Crossing
269	5	684,344.68	4,206,553.10	Fourche a Renault	Road Crossing
274	5	683,963.12	4,206,466.14	Fourche a Renault	Forest
279	5	683,773.53	4,206,133.18	Fourche a Renault	Road Crossing
284	5	684,062.47	4,205,901.90	Fourche a Renault	Road Crossing
289	5	683,809.22	4,205,725.12	Fourche a Renault	Forest
293	5	683,434.90	4,205,594.29	Fourche a Renault	Road Crossing
296	5	683,257.72	4,205,194.01	Fourche a Renault	Pasture
301	5	683,468.55	4,204,784.08	Fourche a Renault	Pasture
306	5	683,301.58	4,204,423.43	Fourche a Renault	Forest
311	5	682,876.96	4,204,551.56	Fourche a Renault	Forest
316	5	682,531.25	4,204,317.30	Fourche a Renault	Road Crossing
321	5	682,476.43	4,203,847.79	Fourche a Renault	Pasture
326	5	682,229.61	4,203,458.19	Fourche a Renault	Forest
330	5	682,071.78	4,203,042.73	Fourche a Renault	Forest
335	5	681,864.51	4,202,652.09	Fourche a Renault	Forest
196	4	687,983.62	4,211,239.64	Fourche a Renault	Forest
201	4	687,572.52	4,211,284.95	Fourche a Renault	Forest
207	4	687,143.58	4,211,155.18	Fourche a Renault	Forest
213	4	686,734.73	4,210,980.89	Fourche a Renault	Forest
218	4	686,280.00	4,211,073.91	Fourche a Renault	Road Crossing
222	4	685,909.62	4,210,828.26	Fourche a Renault	Forest
333	4	681,842.64	4,202,883.86	Fourche a Renault	Road Crossing
338	4	681,532.68	4,202,795.49	Fourche a Renault	Road Crossing
343	4	681,166.64	4,202,789.22	Fourche a Renault	Forest
347	4	680,741.15	4,202,764.03	Fourche a Renault	Pasture
352	4	680,290.20	4,202,692.31	Fourche a Renault	Road Crossing
384	3	678,463.84	4,201,668.28	Fourche a Renault	Forest
226	3	685,473.53	4,210,739.24	Fourche a Renault	Road Crossing
231	3	685,030.07	4,210,604.05	Fourche a Renault	Road Crossing
236	3	684,568.21	4,210,477.74	Fourche a Renault	Road Crossing
358	3	679,876.96	4,202,457.12	Fourche a Renault	Forest
365	3	679,481.13	4,202,344.33	Fourche a Renault	Forest
371	3	679,103.80	4,202,154.54	Fourche a Renault	Forest
377	3	678,791.00	4,201,869.22	Fourche a Renault	Forest
206	3	687,200.68	4,211,468.74	Fourche a Renault	Forest
212	3	686,802.20	4,211,600.62	Fourche a Renault	Forest
217	3	686,409.03	4,211,873.43	Fourche a Renault	Road Crossing
221	3	686,072.23	4,212,215.55	Fourche a Renault	Forest
225	3	685,665.85	4,212,421.84	Fourche a Renault	Road Crossing
230	3	685,233.46	4,212,507.23	Fourche a Renault	Pasture
235	3	684,818.88	4,212,357.98	Fourche a Renault	Pasture

Appendix D. Cell location information in Mineral Fork (Continued).

Cell ID	Stream Order	Location Easting	Location Northing	12-Digit HUC Watershed	Cell Land Use
227	3	685,670.56	4,210,387.61	Fourche a Renault	Forest
232	3	685,231.36	4,210,015.14	Fourche a Renault	Road Crossing
237	3	684,899.48	4,209,685.61	Fourche a Renault	Forest
242	3	684,549.09	4,209,354.11	Fourche a Renault	Road Crossing
247	3	684,157.92	4,209,101.16	Fourche a Renault	Road Crossing
257	3	685,105.40	4,207,401.48	Fourche a Renault	Road Crossing
263	3	685,205.39	4,206,830.60	Fourche a Renault	Road Crossing
267	3	685,026.20	4,206,416.68	Fourche a Renault	Road Crossing
271	3	685,097.63	4,205,994.51	Fourche a Renault	Forest
276	3	685,378.11	4,205,597.57	Fourche a Renault	Forest
281	3	685,491.23	4,205,125.76	Fourche a Renault	Road Crossing
286	3	685,500.80	4,204,651.43	Fourche a Renault	Pasture
291	3	685,273.32	4,204,246.62	Fourche a Renault	Pasture
294	3	685,056.99	4,203,857.95	Fourche a Renault	Forest
297	3	685,081.08	4,203,428.43	Fourche a Renault	Forest
303	3	685,217.85	4,203,014.92	Fourche a Renault	Forest
334	3	681,743.13	4,203,126.93	Fourche a Renault	Road Crossing
340	3	681,380.08	4,203,327.21	Fourche a Renault	Forest
345	3	681,002.08	4,203,486.89	Fourche a Renault	Forest
349	3	680,621.09	4,203,382.13	Fourche a Renault	Forest
355	3	680,228.22	4,203,449.64	Fourche a Renault	Pasture
361	3	679,784.53	4,203,468.26	Fourche a Renault	Forest
368	3	679,339.07	4,203,422.01	Fourche a Renault	Forest
374	3	678,967.30	4,203,564.22	Fourche a Renault	Forest
380	3	678,562.82	4,203,537.24	Fourche a Renault	Forest
387	3	678,123.94	4,203,478.68	Fourche a Renault	Forest
394	3	677,710.69	4,203,474.83	Fourche a Renault	Forest
350	3	680,437.67	4,202,506.73	Fourche a Renault	Pasture
356	3	680,716.25	4,202,290.37	Fourche a Renault	Forest
362	3	680,934.06	4,201,894.82	Fourche a Renault	Forest
369	3	681,006.70	4,201,443.27	Fourche a Renault	Forest
375	3	681,037.67	4,201,007.04	Fourche a Renault	Forest
198	5	688,490.54	4,210,907.44	Mine a Breton Creek	Forest
203	5	688,269.89	4,210,444.80	Mine a Breton Creek	Forest
209	5	688,167.36	4,210,081.98	Mine a Breton Creek	Forest
214	5	688,340.20	4,209,690.12	Mine a Breton Creek	Forest
219	5	688,428.90	4,209,306.40	Mine a Breton Creek	Forest
223	5	688,560.39	4,208,869.90	Mine a Breton Creek	Forest
228	5	688,284.89	4,208,520.20	Mine a Breton Creek	Road Crossing
233	5	688,277.72	4,208,241.11	Mine a Breton Creek	Road Crossing
238	5	688,703.97	4,208,204.55	Mine a Breton Creek	Forest
243	5	689,052.45	4,207,873.68	Mine a Breton Creek	Forest
248	5	689,119.24	4,207,450.62	Mine a Breton Creek	Forest

Appendix D. Cell location information in Mineral Fork (Continued).

Cell ID	Stream Order	Location Easting	Location Northing	12-Digit HUC Watershed	Cell Land Use
253	4	689,407.57	4,207,259.36	Mine a Breton Creek	Road Crossing
260	4	689,838.45	4,207,337.86	Mine a Breton Creek	Forest
264	4	690,298.19	4,207,344.99	Mine a Breton Creek	Forest
268	4	690,599.39	4,207,005.21	Mine a Breton Creek	Forest
272	4	690,723.51	4,206,609.73	Mine a Breton Creek	Forest
277	4	691,022.94	4,206,366.78	Mine a Breton Creek	Forest
282	4	691,268.59	4,205,960.25	Mine a Breton Creek	Forest
287	4	691,605.32	4,205,658.74	Mine a Breton Creek	Forest
292	4	691,992.59	4,205,357.25	Mine a Breton Creek	Forest
295	4	692,329.96	4,205,376.16	Mine a Breton Creek	Forest
300	4	692,571.68	4,205,472.29	Mine a Breton Creek	Forest
305	4	692,889.77	4,205,135.43	Mine a Breton Creek	Forest
310	4	693,308.95	4,205,010.62	Mine a Breton Creek	Road Crossing
315	4	693,395.51	4,204,560.02	Mine a Breton Creek	Forest
320	4	693,365.64	4,204,074.28	Mine a Breton Creek	Pasture
325	4	693,407.01	4,203,594.06	Mine a Breton Creek	Forest
339	4	693,616.57	4,203,192.04	Mine a Breton Creek	Forest
344	4	693,595.34	4,202,713.36	Mine a Breton Creek	Forest
348	4	693,489.73	4,202,272.91	Mine a Breton Creek	Road Crossing
256	4	689,149.06	4,206,860.17	Mine a Breton Creek	Road Crossing
262	4	688,845.19	4,206,396.04	Mine a Breton Creek	Road Crossing
266	4	688,681.13	4,205,934.68	Mine a Breton Creek	Forest
270	4	688,523.31	4,205,492.79	Mine a Breton Creek	Road Crossing
275	4	688,323.17	4,205,075.06	Mine a Breton Creek	Pasture
280	4	688,262.80	4,204,600.37	Mine a Breton Creek	Pasture
285	4	688,262.91	4,204,168.08	Mine a Breton Creek	Road Crossing
354	4	693,109.22	4,202,190.99	Mine a Breton Creek	Road Crossing
360	4	692,752.14	4,201,908.22	Mine a Breton Creek	Road Crossing
367	4	692,577.08	4,201,507.43	Mine a Breton Creek	Forest
373	4	692,215.68	4,201,199.83	Mine a Breton Creek	Forest
379	4	691,863.78	4,200,927.34	Mine a Breton Creek	Forest
386	4	691,508.02	4,200,682.32	Mine a Breton Creek	Forest
353	3	693,669.93	4,201,903.95	Mine a Breton Creek	Road Crossing
359	3	693,917.26	4,201,493.63	Mine a Breton Creek	Road Crossing
366	3	694,175.65	4,201,108.91	Mine a Breton Creek	Road Crossing
372	3	694,578.86	4,200,833.20	Mine a Breton Creek	Road Crossing
378	3	694,974.99	4,200,546.29	Mine a Breton Creek	Road Crossing
385	3	695,260.77	4,200,161.34	Mine a Breton Creek	Road Crossing
392	3	695,505.41	4,199,774.57	Mine a Breton Creek	Road Crossing
398	3	695,359.17	4,199,355.67	Mine a Breton Creek	Road Crossing
404	3	695,155.74	4,198,920.00	Mine a Breton Creek	Pasture
410	3	694,839.81	4,198,603.20	Mine a Breton Creek	Road Crossing
290	3	687,989.73	4,203,815.64	Mine a Breton Creek	Pasture

Appendix D. Cell location information in Mineral Fork (Continued).

Cell ID	Stream Order	Location Easting	Location Northing	12-Digit HUC Watershed	Cell Land Use
393	3	691,335.18	4,200,277.46	Mine a Breton Creek	Forest
399	3	691,194.47	4,199,861.88	Mine a Breton Creek	Forest
405	3	690,993.26	4,199,431.43	Mine a Breton Creek	Forest
411	3	690,984.36	4,198,973.75	Mine a Breton Creek	Forest
417	3	691,195.10	4,198,566.45	Mine a Breton Creek	Road Crossing
423	3	691,278.45	4,198,130.60	Mine a Breton Creek	Forest
429	3	691,292.85	4,197,720.35	Mine a Breton Creek	Road Crossing
434	3	691,498.51	4,197,328.35	Mine a Breton Creek	Forest
439	3	691,461.84	4,196,891.28	Mine a Breton Creek	Road Crossing
391	3	691,185.62	4,200,637.60	Mine a Breton Creek	Forest
397	3	690,923.60	4,200,310.98	Mine a Breton Creek	Forest
445	3	691,718.10	4,196,593.06	Mine a Breton Creek	Road Crossing
451	3	691,889.56	4,196,251.06	Mine a Breton Creek	Forest
457	3	692,103.99	4,195,889.32	Mine a Breton Creek	Forest
462	3	692,297.85	4,195,505.68	Mine a Breton Creek	Forest
466	3	692,335.20	4,195,047.68	Mine a Breton Creek	Forest
470	3	692,233.84	4,194,618.28	Mine a Breton Creek	Forest
1	6	703,227.27	4,219,464.35	Mineral Fork	Forest
2	6	703,073.82	4,219,020.11	Mineral Fork	Forest
3	6	702,721.92	4,219,013.83	Mineral Fork	Forest
4	6	702,271.25	4,219,387.11	Mineral Fork	Forest
5	6	701,810.44	4,219,463.65	Mineral Fork	Forest
6	6	701,529.44	4,219,094.38	Mineral Fork	Forest
7	6	701,098.16	4,218,992.83	Mineral Fork	Forest
8	6	700,681.67	4,218,866.69	Mineral Fork	Forest
9	6	700,443.29	4,218,552.06	Mineral Fork	Forest
10	6	700,002.19	4,218,425.64	Mineral Fork	Forest
11	6	699,587.71	4,218,414.68	Mineral Fork	Forest
13	6	699,302.52	4,218,639.09	Mineral Fork	Forest
16	6	699,066.48	4,218,825.25	Mineral Fork	Forest
19	6	698,692.44	4,219,024.76	Mineral Fork	Forest
22	6	698,222.00	4,219,135.33	Mineral Fork	Forest
25	6	697,839.36	4,218,958.41	Mineral Fork	Forest
29	6	697,475.89	4,218,784.08	Mineral Fork	Road Crossing
33	6	697,428.46	4,218,336.16	Mineral Fork	Road Crossing
38	6	697,128.17	4,218,033.40	Mineral Fork	Forest
43	6	696,749.54	4,218,184.28	Mineral Fork	Forest
48	6	696,652.67	4,218,494.33	Mineral Fork	Forest
52	6	696,403.87	4,218,887.13	Mineral Fork	Forest
55	6	696,052.32	4,218,873.81	Mineral Fork	Forest
58	6	695,918.20	4,218,503.50	Mineral Fork	Forest
61	6	695,517.76	4,218,286.53	Mineral Fork	Forest
64	6	695,097.50	4,218,134.30	Mineral Fork	Forest

Appendix D. Cell location information in Mineral Fork (Continued).

Cell ID	Stream Order	Location Easting	Location Northing	12-Digit HUC Watershed	Cell Land Use
91	3	693,248.14	4,220,424.70	Mineral Fork	Forest
12	3	699,691.44	4,218,084.67	Mineral Fork	Forest
14	3	699,824.49	4,217,638.59	Mineral Fork	Forest
17	3	700,077.06	4,217,245.02	Mineral Fork	Forest
20	3	700,354.29	4,216,859.50	Mineral Fork	Road Crossing
23	3	700,518.09	4,216,415.83	Mineral Fork	Forest
26	3	700,790.53	4,216,030.88	Mineral Fork	Forest
67	3	694,800.29	4,218,170.93	Mineral Fork	Road Crossing
71	3	694,482.09	4,218,405.82	Mineral Fork	Forest
75	3	694,242.94	4,218,795.23	Mineral Fork	Forest
79	3	694,056.81	4,219,227.18	Mineral Fork	Forest
83	3	693,817.16	4,219,653.63	Mineral Fork	Forest
87	3	693,574.71	4,220,081.70	Mineral Fork	Forest
93	3	692,838.11	4,220,544.81	Mineral Fork	Forest
15	4	699,291.49	4,218,205.02	Old Mines Creek	Forest
18	4	699,023.56	4,217,805.36	Old Mines Creek	Forest
21	4	698,758.50	4,217,445.08	Old Mines Creek	Forest
24	4	698,497.48	4,217,025.33	Old Mines Creek	Forest
27	4	698,244.77	4,216,606.11	Old Mines Creek	Road Crossing
35	4	697,681.25	4,215,835.76	Old Mines Creek	Road Crossing
31	4	697,970.85	4,216,199.65	Old Mines Creek	Road Crossing
40	4	697,458.59	4,215,448.38	Old Mines Creek	Forest
45	4	697,139.10	4,215,111.71	Old Mines Creek	Forest
50	4	696,793.46	4,214,776.64	Old Mines Creek	Forest
53	4	696,662.42	4,214,318.60	Old Mines Creek	Forest
56	4	696,741.96	4,213,838.39	Old Mines Creek	Forest
59	4	696,796.70	4,213,366.31	Old Mines Creek	Forest
63	4	696,752.40	4,212,885.57	Old Mines Creek	Road Crossing
65	4	696,782.99	4,212,425.36	Old Mines Creek	Road Crossing
68	4	696,869.58	4,211,982.22	Old Mines Creek	Road Crossing
72	4	697,041.08	4,211,560.90	Old Mines Creek	Road Crossing
76	4	697,127.13	4,211,083.49	Old Mines Creek	Road Crossing
80	4	697,126.59	4,210,594.02	Old Mines Creek	Forest
84	4	697,052.22	4,210,116.55	Old Mines Creek	Road Crossing
88	4	696,976.87	4,209,630.49	Old Mines Creek	Road Crossing
92	4	696,739.01	4,209,220.41	Old Mines Creek	Road Crossing
97	3	696,512.69	4,208,813.29	Old Mines Creek	Road Crossing
364	5	682,369.64	4,201,511.46	Sunnen Lake-Fourche a Renault	Dam/Pond
370	5	683,100.48	4,200,398.82	Sunnen Lake-Fourche a Renault	Road Crossing
376	5	683,085.04	4,199,956.51	Sunnen Lake-Fourche a Renault	Forest
383	4	683,137.64	4,199,532.25	Sunnen Lake-Fourche a Renault	Road Crossing
390	4	683,332.21	4,199,132.74	Sunnen Lake-Fourche a Renault	Forest
396	4	683,628.30	4,198,902.23	Sunnen Lake-Fourche a Renault	Forest

Appendix D. Cell location information in Mineral Fork (Continued).

Cell ID	Stream Order	Location Easting	Northing	12-Digit HUC Watershed	Cell Land Use
402	4	683,977.52	4,198,770.07	Sunnen Lake-Fourche a Renault	Pasture
408	4	684,315.86	4,198,524.13	Sunnen Lake-Fourche a Renault	Road Crossing
414	4	684,682.49	4,198,350.35	Sunnen Lake-Fourche a Renault	Road Crossing
420	4	685,081.33	4,198,284.46	Sunnen Lake-Fourche a Renault	Pasture
426	4	685,500.41	4,198,189.81	Sunnen Lake-Fourche a Renault	Road Crossing
381	4	682,923.22	4,199,707.72	Sunnen Lake-Fourche a Renault	Forest
388	4	682,756.71	4,199,303.42	Sunnen Lake-Fourche a Renault	Road Crossing
395	4	682,709.86	4,198,866.38	Sunnen Lake-Fourche a Renault	Pasture
431	4	685,827.73	4,198,012.72	Sunnen Lake-Fourche a Renault	Road Crossing
436	4	686,043.41	4,197,735.57	Sunnen Lake-Fourche a Renault	Pasture
441	4	686,176.65	4,197,362.96	Sunnen Lake-Fourche a Renault	Road Crossing
448	4	686,205.36	4,196,934.04	Sunnen Lake-Fourche a Renault	Forest
454	4	686,208.10	4,196,534.41	Sunnen Lake-Fourche a Renault	Forest
460	4	686,151.84	4,196,113.43	Sunnen Lake-Fourche a Renault	Pasture
464	4	686,205.78	4,195,694.49	Sunnen Lake-Fourche a Renault	Pasture
468	4	686,428.43	4,195,338.83	Sunnen Lake-Fourche a Renault	Pasture
471	4	686,616.23	4,194,959.50	Sunnen Lake-Fourche a Renault	Road Crossing
474	4	686,635.35	4,194,544.83	Sunnen Lake-Fourche a Renault	Road Crossing
401	3	682,852.95	4,198,459.68	Sunnen Lake-Fourche a Renault	Road Crossing
407	3	683,024.57	4,198,088.95	Sunnen Lake-Fourche a Renault	Road Crossing
413	3	683,132.68	4,197,737.61	Sunnen Lake-Fourche a Renault	Forest
419	3	683,030.32	4,197,322.09	Sunnen Lake-Fourche a Renault	Forest
425	3	683,052.11	4,196,891.96	Sunnen Lake-Fourche a Renault	Forest
430	3	683,126.65	4,196,446.13	Sunnen Lake-Fourche a Renault	Road Crossing
435	3	683,200.82	4,196,027.51	Sunnen Lake-Fourche a Renault	Road Crossing
440	3	683,347.14	4,195,592.59	Sunnen Lake-Fourche a Renault	Forest
447	3	683,713.39	4,195,331.98	Sunnen Lake-Fourche a Renault	Forest
477	3	686,805.01	4,194,112.41	Sunnen Lake-Fourche a Renault	Forest
480	3	687,027.86	4,193,730.42	Sunnen Lake-Fourche a Renault	Forest
432	3	685,949.86	4,198,201.53	Sunnen Lake-Fourche a Renault	Road Crossing
437	3	686,340.28	4,198,297.23	Sunnen Lake-Fourche a Renault	Road Crossing
442	3	686,739.60	4,198,377.28	Sunnen Lake-Fourche a Renault	Road Crossing
449	3	687,147.91	4,198,303.94	Sunnen Lake-Fourche a Renault	Forest
455	3	687,474.76	4,198,043.29	Sunnen Lake-Fourche a Renault	Forest
461	3	687,768.96	4,197,814.48	Sunnen Lake-Fourche a Renault	Road Crossing
465	3	687,996.60	4,197,523.19	Sunnen Lake-Fourche a Renault	Forest
469	3	688,083.38	4,197,107.14	Sunnen Lake-Fourche a Renault	Forest
472	3	688,089.18	4,196,702.83	Sunnen Lake-Fourche a Renault	Forest
475	3	688,194.91	4,196,368.18	Sunnen Lake-Fourche a Renault	Dam/Pond
478	3	688,415.49	4,195,986.49	Sunnen Lake-Fourche a Renault	Road Crossing
481	3	688,605.60	4,195,624.03	Sunnen Lake-Fourche a Renault	Pasture
483	3	688,712.67	4,195,255.80	Sunnen Lake-Fourche a Renault	Forest
485	3	688,966.97	4,194,910.29	Sunnen Lake-Fourche a Renault	Forest

Appendix E. Cell location information in Mill Creek.

Cell ID	Stream Order	Location Easting	Location Northing	12-Digit HUC Watershed	Cell Land Use
1	5	708,792.15	4,212,394.39	Mill Creek	Forest
2	5	708,470.21	4,212,151.70	Mill Creek	Forest
3	5	708,076.71	4,211,976.26	Mill Creek	Forest
4	5	707,767.00	4,211,672.92	Mill Creek	Forest
5	5	707,547.55	4,211,275.29	Mill Creek	Forest
6	5	707,426.78	4,210,872.91	Mill Creek	Forest
7	5	707,008.85	4,210,716.32	Mill Creek	Forest
8	5	706,643.30	4,211,145.77	Mill Creek	Forest
9	5	706,274.94	4,211,069.78	Mill Creek	Forest
10	5	706,326.97	4,210,645.06	Mill Creek	Forest
85	4	700,147.10	4,201,977.28	Mill Creek	Road Crossing
11	4	706,242.52	4,210,160.37	Mill Creek	Road Crossing
13	4	706,020.20	4,209,739.00	Mill Creek	Forest
15	4	705,605.64	4,209,745.17	Mill Creek	Forest
17	4	705,268.78	4,210,032.35	Mill Creek	Forest
19	4	704,926.66	4,210,185.38	Mill Creek	Forest
21	4	705,099.00	4,209,899.72	Mill Creek	Forest
23	4	705,021.99	4,209,517.73	Mill Creek	Forest
25	4	704,702.48	4,209,169.36	Mill Creek	Forest
27	4	704,650.25	4,208,773.04	Mill Creek	Forest
29	4	705,055.63	4,208,602.03	Mill Creek	Forest
32	4	705,495.41	4,208,576.48	Mill Creek	Forest
35	4	705,378.09	4,208,232.86	Mill Creek	Forest
38	4	705,260.05	4,207,830.20	Mill Creek	Road Crossing
41	4	705,636.71	4,207,660.03	Mill Creek	Forest
43	4	705,858.07	4,207,275.24	Mill Creek	Forest
44	4	705,748.02	4,206,860.03	Mill Creek	Forest
45	4	705,573.17	4,206,443.24	Mill Creek	Forest
46	4	705,408.37	4,206,095.92	Mill Creek	Forest
47	4	704,970.34	4,206,073.51	Mill Creek	Road Crossing
48	4	704,535.49	4,206,110.44	Mill Creek	Forest
50	4	704,076.22	4,205,986.96	Mill Creek	Forest
52	4	703,601.44	4,205,899.83	Mill Creek	Forest
54	4	703,123.63	4,205,938.89	Mill Creek	Forest
56	4	702,701.47	4,205,808.13	Mill Creek	Forest
58	4	702,444.56	4,205,502.47	Mill Creek	Forest
61	4	702,002.30	4,205,388.74	Mill Creek	Forest
64	4	701,579.02	4,205,236.17	Mill Creek	Forest
67	4	701,318.62	4,204,880.27	Mill Creek	Road Crossing
70	4	701,036.34	4,204,484.59	Mill Creek	Forest
73	4	700,757.29	4,204,090.92	Mill Creek	Forest
76	4	700,427.76	4,203,745.40	Mill Creek	Forest
80	4	700,220.59	4,203,302.41	Mill Creek	Forest

Appendix E. Cell location information in Mill Creek (Continued).

Cell ID	Stream Order	Location Easting	Location Northing	12-Digit HUC Watershed	Cell Land Use
82	4	700,258.40	4,202,833.73	Mill Creek	Forest
83	4	700,229.28	4,202,412.88	Mill Creek	Forest
12	4	706,026.38	4,210,380.73	Mill Creek	Road Crossing
14	4	705,692.25	4,210,430.76	Mill Creek	Road Crossing
16	4	705,483.53	4,210,820.43	Mill Creek	Road Crossing
18	4	705,087.70	4,210,693.38	Mill Creek	Forest
20	4	704,701.02	4,210,511.85	Mill Creek	Road Crossing
22	4	704,268.47	4,210,522.95	Mill Creek	Road Crossing
24	4	703,912.92	4,210,197.82	Mill Creek	Forest
89	4	699,807.25	4,201,676.31	Mill Creek	Forest
88	3	698,347.43	4,204,243.03	Mill Creek	Road Crossing
101	3	698,087.77	4,199,194.03	Mill Creek	Road Crossing
26	3	703,571.58	4,209,929.94	Mill Creek	Forest
31	3	704,567.06	4,208,421.51	Mill Creek	Forest
34	3	704,241.92	4,208,159.82	Mill Creek	Forest
37	3	703,899.65	4,207,849.34	Mill Creek	Road Crossing
60	3	702,330.60	4,205,781.34	Mill Creek	Forest
63	3	701,955.01	4,205,847.45	Mill Creek	Forest
66	3	701,563.25	4,205,993.52	Mill Creek	Road Crossing
69	3	701,142.64	4,205,863.00	Mill Creek	Forest
72	3	700,694.01	4,205,688.32	Mill Creek	Forest
75	3	700,308.58	4,205,414.54	Mill Creek	Forest
78	3	699,898.74	4,205,220.88	Mill Creek	Forest
81	3	699,488.00	4,205,118.43	Mill Creek	Road Crossing
84	3	699,112.77	4,204,839.81	Mill Creek	Forest
86	3	698,751.09	4,204,574.14	Mill Creek	Forest
49	3	704,771.83	4,205,800.00	Mill Creek	Forest
51	3	704,485.47	4,205,467.35	Mill Creek	Forest
53	3	704,115.14	4,205,228.40	Mill Creek	Forest
55	3	704,016.21	4,204,842.76	Mill Creek	Forest
57	3	704,136.86	4,204,379.38	Mill Creek	Forest
59	3	704,030.08	4,203,899.47	Mill Creek	Forest
62	3	703,823.53	4,203,455.27	Mill Creek	Road Crossing
87	3	699,955.01	4,201,498.08	Mill Creek	Road Crossing
90	3	699,867.66	4,201,084.91	Mill Creek	Road Crossing
92	3	699,930.06	4,200,678.54	Mill Creek	Road Crossing
94	3	700,116.49	4,200,299.15	Mill Creek	Forest
91	3	699,490.54	4,201,418.90	Mill Creek	Road Crossing
93	3	699,340.97	4,200,970.53	Mill Creek	Forest
95	3	699,157.60	4,200,542.37	Mill Creek	Forest
97	3	698,779.83	4,200,262.37	Mill Creek	Forest
99	3	698,498.93	4,199,935.82	Mill Creek	Road Crossing
100	3	698,323.77	4,199,555.06	Mill Creek	Forest

Appendix F. STEPL inputs.

	Load	A_d			Land use (%)				# of Animals		Septic Systems		
Watershed	Type	(km^2)	HSG	Urban	Crop	Pasture	Forest	Mined	Cattle	Chicken	# of Septic	Pop. per System	%
Mill Creek	Total Load	132.6	D	7.0	0.2	6.2	71.8	14.9	884	130	884	3	0.39
Mill Creek	Below Dams	96.2	D	7.1	0.2	6.5	78.4	7.9	615	130	884	3	0.39
Mineral Fork	Total Load	51.5	D	2.9	0.7	2.6	90.1	3.8	216	30	189	3	0.39
Mineral Fork	Below Dams	42.3	D	2.5	0.7	2.1	92.5	2.2	87	30	189	3	0.39
Clear Creek-Mineral Fork	Total Load	98.8	D	2.8	0.2	3.8	91.6	1.7	376	52	37	3	0.39
Clear Creek-Mineral Fork	Below Dams	75.6	D	2.6	0.2	4.4	91.5	1.3	324	52	37	3	0.39
Old Mines Creek	Total Load	48.1	D	7.5	0.2	6.3	75.1	11.0	339	47	454	3	0.39
Old Mines Creek	Below Dams	39.4	D	8.6	0.2	7.4	73.7	10.2	286	47	454	3	0.39
Mine a Breton Creek	Total Load	124	D	8.2	0.5	14.1	73.4	3.8	1,429	197	2,075	3	0.39
Mine a Breton Creek	Below Dams	105	D	8.4	0.5	16.2	73.1	1.7	1,687	197	2,075	3	0.39
Fourche a Renault	Total Load	101	D	3.7	0.1	16.4	79.6	0.2	1,314	181	106	3	0.39
Fourche a Renault	Below Dams	96.8	D	3.8	0.1	17.0	79.1	0.1	1,618	181	106	3	0.39
Sunnen Lake-Fourche a Renault	Total Load	68.8	C	4.1	0.0	6.5	88.1	1.3	411	56	204	3	0.39
Sunnen Lake-Fourche a Renault	Below Dams	68.6	C	4.1	0.0	6.5	88.1	1.3	220	56	204	3	0.39
Mineral Fork-Whole	Total Load	490.5	D	5.0	0.3	9.5	82.2	3.0	4,701	563	3,065	3	0.39
Mineral Fork-Whole	Below Dams	428.6	D	5.2	0.3	10.9	81.5	2.1	4,228	563	3,065	3	0.39

Appendix G. USLE inputs for STEPL.

Watershed	Load Type	A_d (km^2)	Crop K	Crop LS	Pasture K	Pasture LS	Forest K	Forest LS	Mined K	Mined LS	Mined C
Mill Creek	Total Load	132.6	0.476	1.194	0.480	1.231	0.407	2.436	0.300	1.530	0.170
Mill Creek	Below Dams	96.2	0.488	1.145	0.490	1.184	0.399	2.576	0.309	1.493	0.178
Mineral Fork	Total Load	51.5	0.453	1.045	0.409	3.304	0.285	4.301	0.276	3.344	0.215
Mineral Fork	Below Dams	42.3	0.453	0.505	0.400	2.812	0.278	4.585	0.256	3.669	0.299
Clear Creek-Mineral Fork	Total Load	98.8	0.457	1.831	0.438	2.497	0.266	3.438	0.268	1.575	0.157
Clear Creek-Mineral Fork	Below Dams	75.6	0.461	1.856	0.444	2.262	0.269	3.449	0.271	1.694	0.194
Old Mines Creek	Total Load	48.1	0.447	2.021	0.467	1.967	0.344	2.991	0.304	1.426	0.112
Old Mines Creek	Below Dams	39.4	0.450	2.110	0.470	1.996	0.358	2.996	0.308	1.425	0.119
Mine a Breton Creek	Total Load	124	0.483	6.149	0.458	4.231	0.310	3.385	0.305	2.245	0.033
Mine a Breton Creek	Below Dams	105	0.484	6.146	0.461	4.257	0.316	3.398	0.294	1.927	0.045
Fourche a Renault	Total Load	101	0.415	1.732	0.436	3.545	0.299	3.357	0.345	2.335	0.032
Fourche a Renault	Below Dams	96.8	0.417	1.737	0.437	3.556	0.297	3.361	0.344	2.180	0.114
Sunnen Lake-Fourche a Renault	Total Load	68.8	0.262	1.524	0.312	1.455	0.258	3.771	0.311	2.819	0.000
Sunnen Lake-Fourche a Renault	Below Dams	68.6	0.262	1.524	0.312	1.455	0.258	3.771	0.311	2.819	0.000
Mineral Fork-Whole	Total Load	490.5	0.461	3.521	0.434	3.407	0.291	3.516	0.296	1.948	0.097
Mineral Fork-Whole	Below Dams	428.6	0.464	3.487	0.333	1.788	0.399	2.576	0.295	3.540	0.133

Appendix H. Large dams in Mineral Fork and Mill Creek watersheds.

Appendix H-1. Large dams characteristics identified in Mineral Fork and Mill Creek watersheds.

ID#	Year Completed	Regulation	HUC12	Stream	Dam Height (m)	A_d (m^2)
MO31006	1965	Wet	Clear Creek-Mineral Fork	Sycamore Creek	6.1	6,291,875
MO31986	1991	Wet	Mineral Fork	Trib. Mineral Fork	6.1	1,121,645
MO30744	1947	Wet	Old Mines Creek	Trib. Old Mines Creek	6.4	1,015,205
MO30996	1965	Wet	Mine a Breton Creek	Mine a Breton Creek	4.9	1,948,590
MO30722	1972	Wet	Clear Creek-Mineral Fork	Simpson Branch	9.4	6,861,948
MO31123	1975	Wet	Mill Creek	Trib. Shibboleth Branch	9.4	2,470,149
MO30708	1959	Dry	Mill Creek	Trib. Mill Creek	30.2	220,254
MO30715	1978	Dry	Mill Creek	Trib. Mill Creek	29.6	277,201
MO31158	1963	Dry	Mill Creek	Trib. Mill Creek	27.1	143,573
MO30476	1962	Filled/Wet	Mine a Breton Creek	Trib. Mine a Breton Creek	25.9	3,286,917
MO30728	1967	Wet	Mineral Fork	Trib. Mineral Fork	25.9	1,755,412
MO31825	1980	Wet	Mill Creek	Pond Creek	24.4	9,131,134
MO31155	1973	Dry	Old Mines Creek	Trib. Old Mines Creek	24.1	355,241
MO30475	1953	Dry	Old Mines Creek	Trib. Old Mines Creek	23.8	91,681
MO30386	1979	Filled/Wet	Mill Creek	Fountain Farm Branch	23.5	836,326
MO30705	1968	Dry	Mill Creek	Trib. Mill Creek	21.9	1,129,036
MO31154	1943	Dry	Mill Creek	Trib. Mill Creek	21.3	1,067,055
MO30479	1971	Filled/Wet	Mine a Breton Creek	Trib. Mine a Breton Creek	20.7	668,043
MO30688	1965	Wet	Mine a Breton Creek	Trib. Bates Creek	20.7	2,498,095
MO30112	1971	Wet	Fourche a Renault	Ashly Branch	20.4	3,768,750
MO31124	1977	Filled/Wet	Mill Creek	Trib. Shibboleth Branch	18.9	740,778
MO30706	1980	Dry	Old Mines Creek	Mud Town Creek	18.6	1,754,851
MO31005	1957	Dry	Old Mines Creek	Trib. Old Mines Creek	17.1	399,823
MO30111	1948	Wet	Sunnen Lake-Fourche a Renault	Fourche a Renault	15.5	68,748,769
MO30101	1960	Wet	Mine a Breton Creek	Swan Branch	15.2	3,833,738
MO30903	1957	Wet	Mill Creek	Trib. Mill Creek	15.2	1,445,524
MO31118	1979	Dry	Mill Creek	Trib. Cadet Creek	14.6	480,594
MO30716	1970	Wet	Clear Creek-Mineral Fork	Trib. Arnault Branch	14.0	2,167,054
MO30731	1941	Wet	Mineral Fork	Trib. Mineral Fork	13.7	6,310,471
MO30124	1972	Dry	Mill Creek	Fountain Farm Branch	9.1	50,457
MO31117	1968	Dry	Mill Creek	Trib. Mill Creek	9.1	7,110,537
MO31122		Dry	Old Mines Creek	Salt Pine Creek	9.1	4,586,143
MO31949	1991	Wet	Old Mines Creek	Rubidoux Branch	9.1	1,301,740
MO30723	1967	Wet	Clear Creek-Mineral Fork	Trib. Mineral Fork	10.4	1,684,346
MO30480	1950	Wet	Mine a Breton Creek	Trib. Mine a Breton Creek	10.1	636,485
MO30746	1935	Wet	Mine a Breton Creek	Trib. Mine a Breton Creek	12.5	1,508,306
MO31147	1950	Dry	Mill Creek	Mill Creek	10.5	117,909
MO30749	1964	Wet	Mill Creek	Shibboleth Branch	8.5	11,635,162
MO30994	1968	Wet	Mine a Breton Creek	Trib. Bates Creek	8.5	3,034,165
MO30993	1952	Wet	Mine a Breton Creek	Trib. Mine a Breton Creek	3.7	834,759
MO30720	1974	Wet	Clear Creek-Mineral Fork	Rogue Creek	8.2	3,720,890
MO31396	1977	Wet	Clear Creek-Mineral Fork	Trib. Clear Creek	7.6	1,172,961
MO31397	1979	Filled/Wet	Clear Creek-Mineral Fork	Clear Creek	7.6	1,394,923

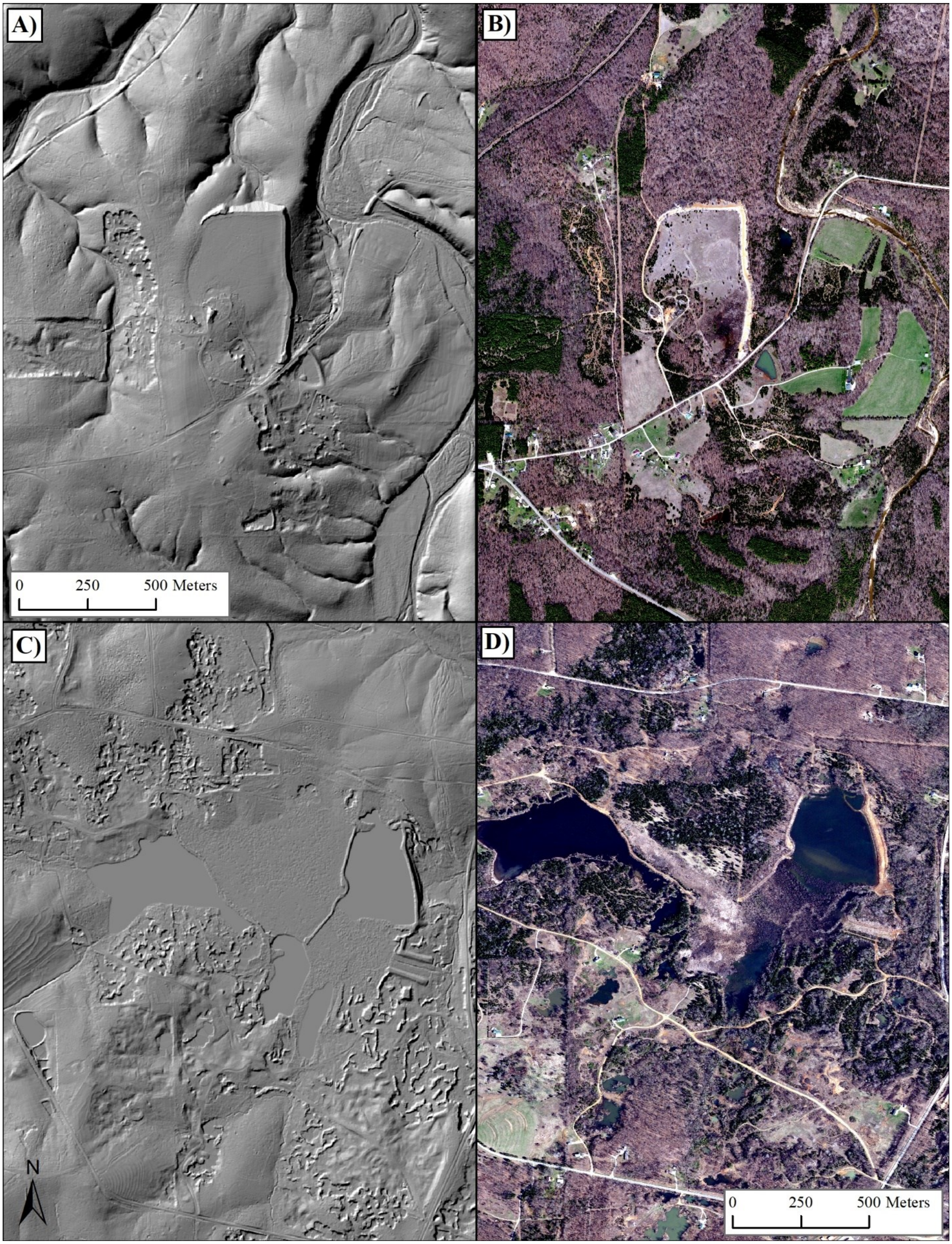

Appendix H-2. Topography and land use of historical mine tailings ponds and dams in Mill Creek (A & B) and Mineral Fork (C & D) watersheds.

Appendix H-3. Ground view of A) and B), the Cadet Mine Tailings Dam (#MO30715) within the Mill Creek watershed (Photo taken December 18, 2018).